CHAPTER IV

RESULTS AND DISCUSSION

4.1 Identification of intermediates from the degradation of acenaphthylene by *Rhizobium* sp. CU-A1 and its transposon mutants

4.1.1 Utilization of acenaphthylene

Poonthrigpun (2002) reported that eighteen transposon mutants of *Rhizobium* sp. CU-A1 defective in acenaphthylene degradation could be classified into 6 groups by the growth and intermediate profiles when grown in the presence of acenaphthylene as a sole carbon source. In the present work, mutants A53, E11, B1 were selected for further purification of acenaphthylene intermediates partially accumulated comparing with those of the wild type. Utilization of acenaphthylene as a sole source of carbon and energy by these three mutants was confirmed by growing in the mineral medium supplemented with acenaphthylene. Growth on acenaphthylene was measured by demonstrating a decrease in acenaphthylene concentration concomitant with an increase in bacterial cell number as described in 3.2.1.

The results shown in Fig. 4.1 indicated that a wild type *Rhizobium* sp. CU-A1 grown on acenaphthylene for 3 days completely degraded this compound with a corresponding increase in bacterial cell number. In contrast, after the first 3 days of incubation, acenaphthylene was reduced to 56.3, 63.0 and 54.6% by *Rhizobium* sp. A53, E11 and B1, respectively. Then, the concentration of acenaphthylene recovered from cultures decreased dramatically to non-detectable level over the next 8-9 days. Whereas, bacterial cell number of strain E11 and B1 was slightly decreased during the incubation period.

Determination of intermediates produced from the degradation of acenaphthylene after 12 days of incubation by TLC and HPLC as presented in Fig. 4.2 and 4.3, respecetively, revealed that transposon mutants transformed acenaphthylene to various accumulated intermediates different from those found in the wild type strain.

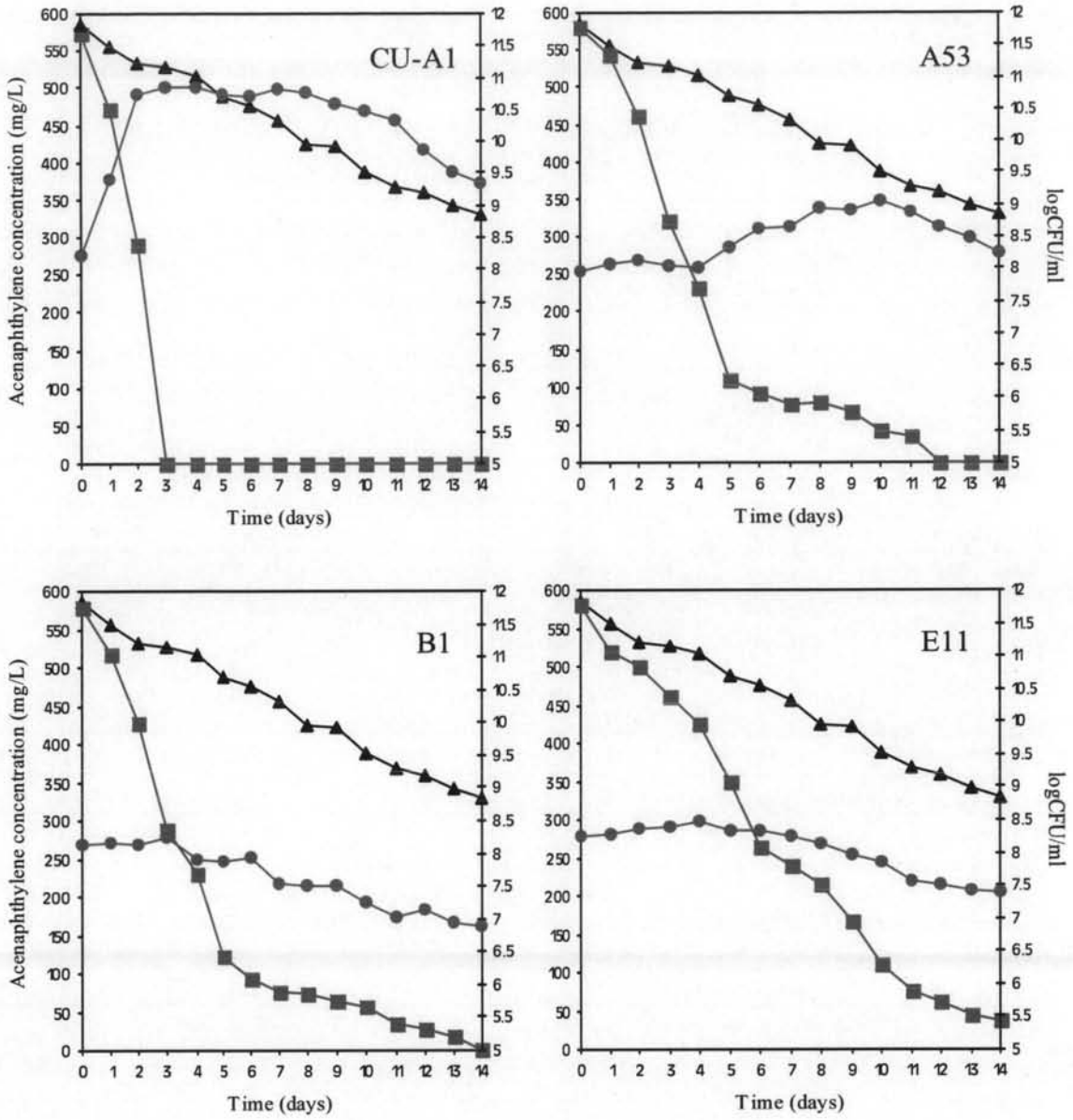

Fig. 4.1 Growth and acenaphthylene utilization of mutants A53, B1 and E11 in mineral medium containing 600 mg/L acenaphthylene comparing with *Rhizobium* sp. CU-A1

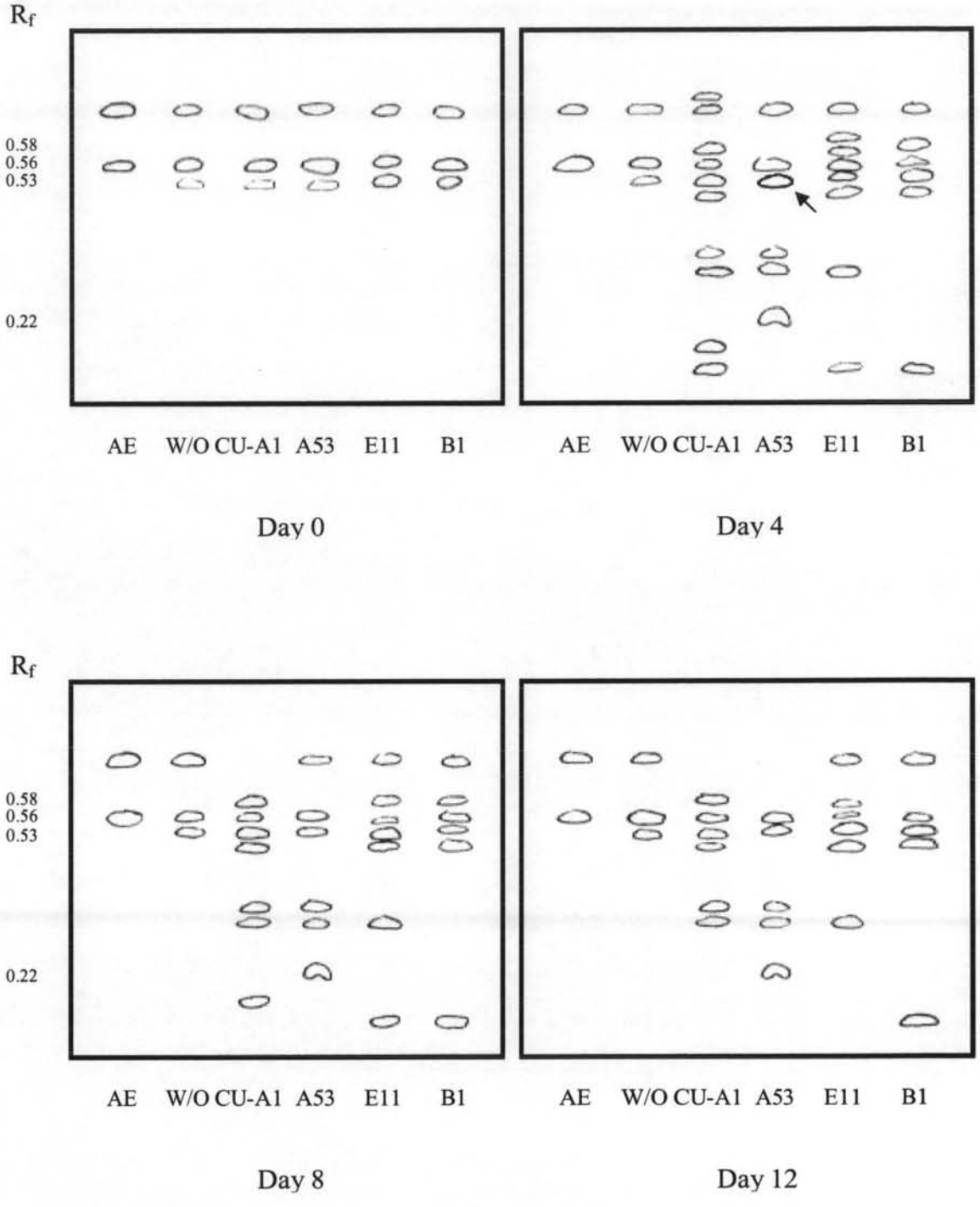

Fig. 4.2 TLC chromatograms of the culture extracts showing intermediates produced from the degradation of acenaphthylene in day 0, 4, 8 and 12 by mutants A53, B1 and E11grown in mineral medium containing 600 mg/L acenaphthylene comparing with *Rhizobium* sp. CU-A1. (AE, acenaphthylene; w/o, medium without bacteria). The arrow indicates the intermediate with R_f value 0.53 giving strong UV intensity on Day 4 in mutant A53.

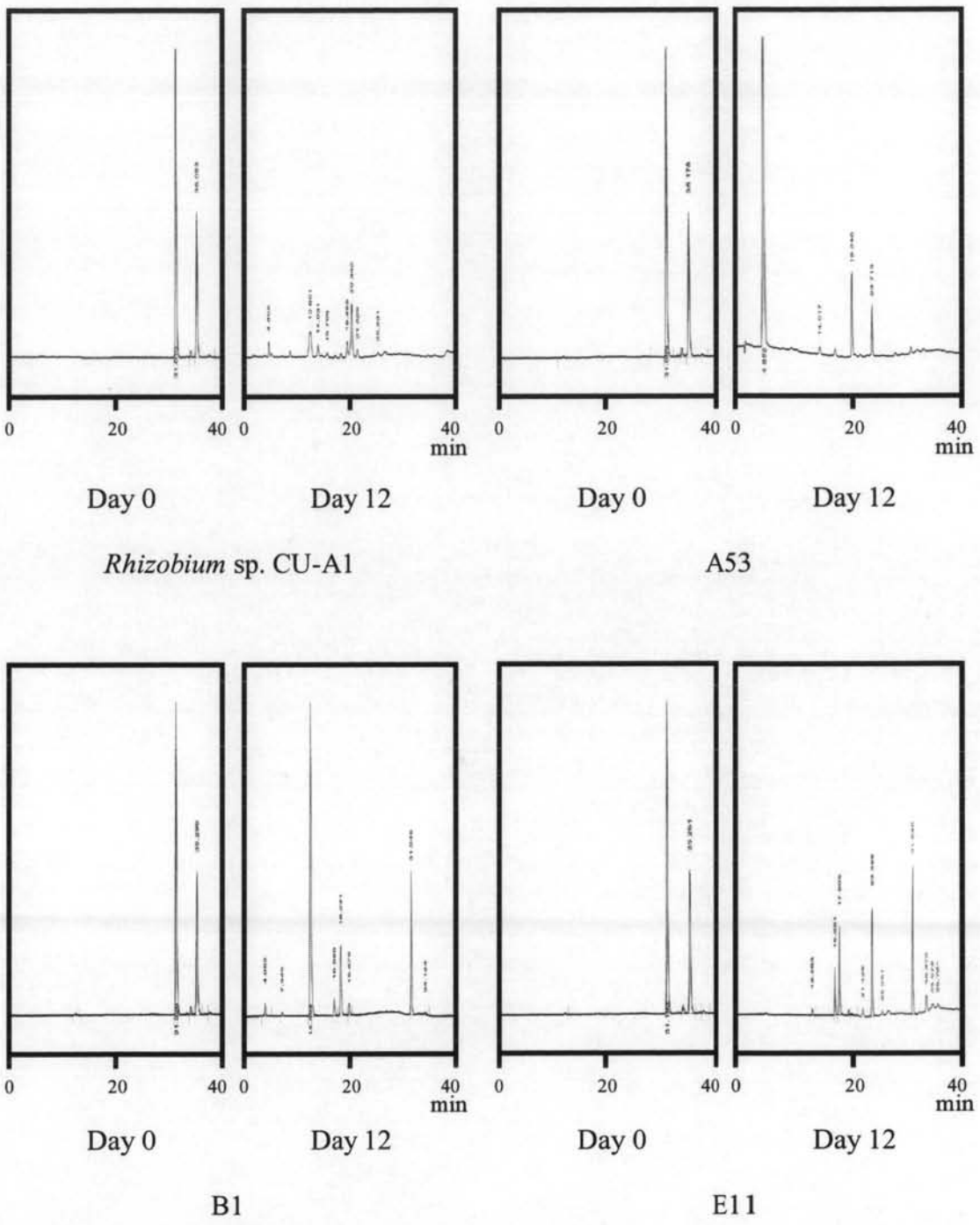

Fig. 4.3 HPLC chromatograms of the culture extracts showing intermediates produced from the degradation of acenaphthylene in day 0 and 12 by mutants A53, B1 and E11 grown in mineral medium containing 600 mg/L acenaphthylene comparing with *Rhizobium* sp. CU-A1

4.1.2 Identification of acenaphthylene intermediate from A53

From the previous study (Poonthrigpun, 2002), gentisic acid (2,5-dihydroxybenzoic acid) with the R_f value of 0.22 in Fig. 4.2 was proved to be an accumulated intermediate from the degradation of acenaphthylene in mutant A53. The present work also found that A53 could accumulate another intermediate with the R_f value of 0.53 when analyzed by TLC, described in 3.2.4. After 4 day of incubation, this intermediate gave a high intensity spot on TLC plate when illuminated with UV light (Fig. 4.2). The result indicated that this intermediate was present in relatively high concentration in the culture extract. Therefore, it was preliminary purified by preparative TLC using hexane : ethyl acetate : acetic acid (10:10:1, v/v/v) as a developing solvent. The resulting intermediate from preparative TLC step was subsequently purified by silica gel column chromatography using 0-100% ethyl acetate in hexane with 10% increment for each step as an eluting solvent. Then, its purity was determined by TLC (Fig. 4.4) and HPLC (Fig. 4.5).

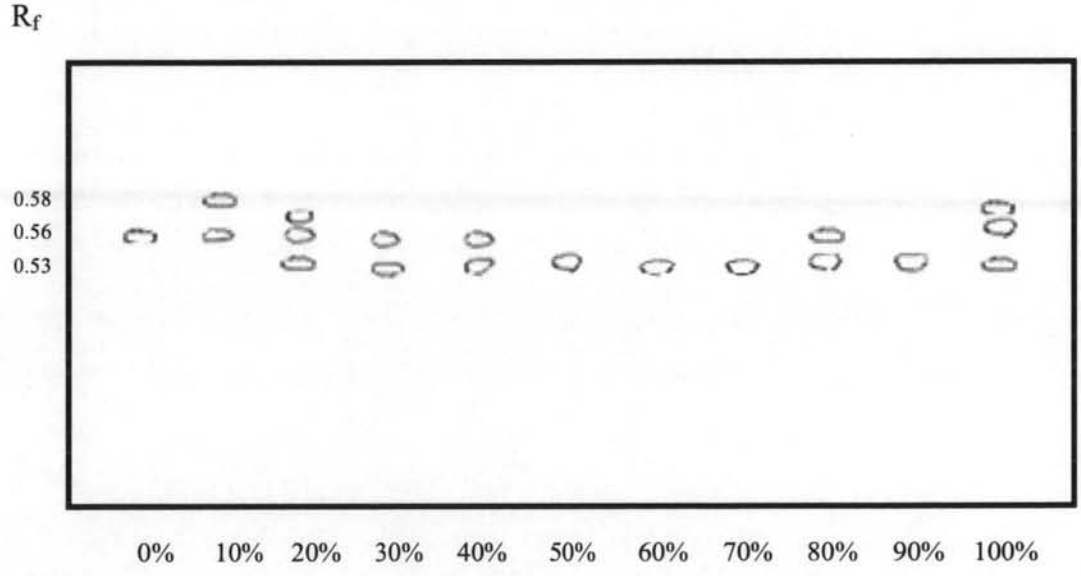

Fig. 4.4 TLC chromatogram of each fraction of acenaphthylene degrading intermediates from preliminary purified A53-culture extract eluted from silica gel column chromatography with 0-100% ethyl acetate in hexane

TLC analysis of the 50, 60 and 70% ethyl acetate fractions showed a single spot of intermediate. However, HPLC chromatogram of the 50% ethyl acetate fraction showed only one peak of purified intermediate with the highest concentration at the retention time of 3.58 min comparing with those of 60% and 70% ethyl acetate fractions. Therefore, this fraction was selected for further identification of the intermediate and designated as intermediate I.

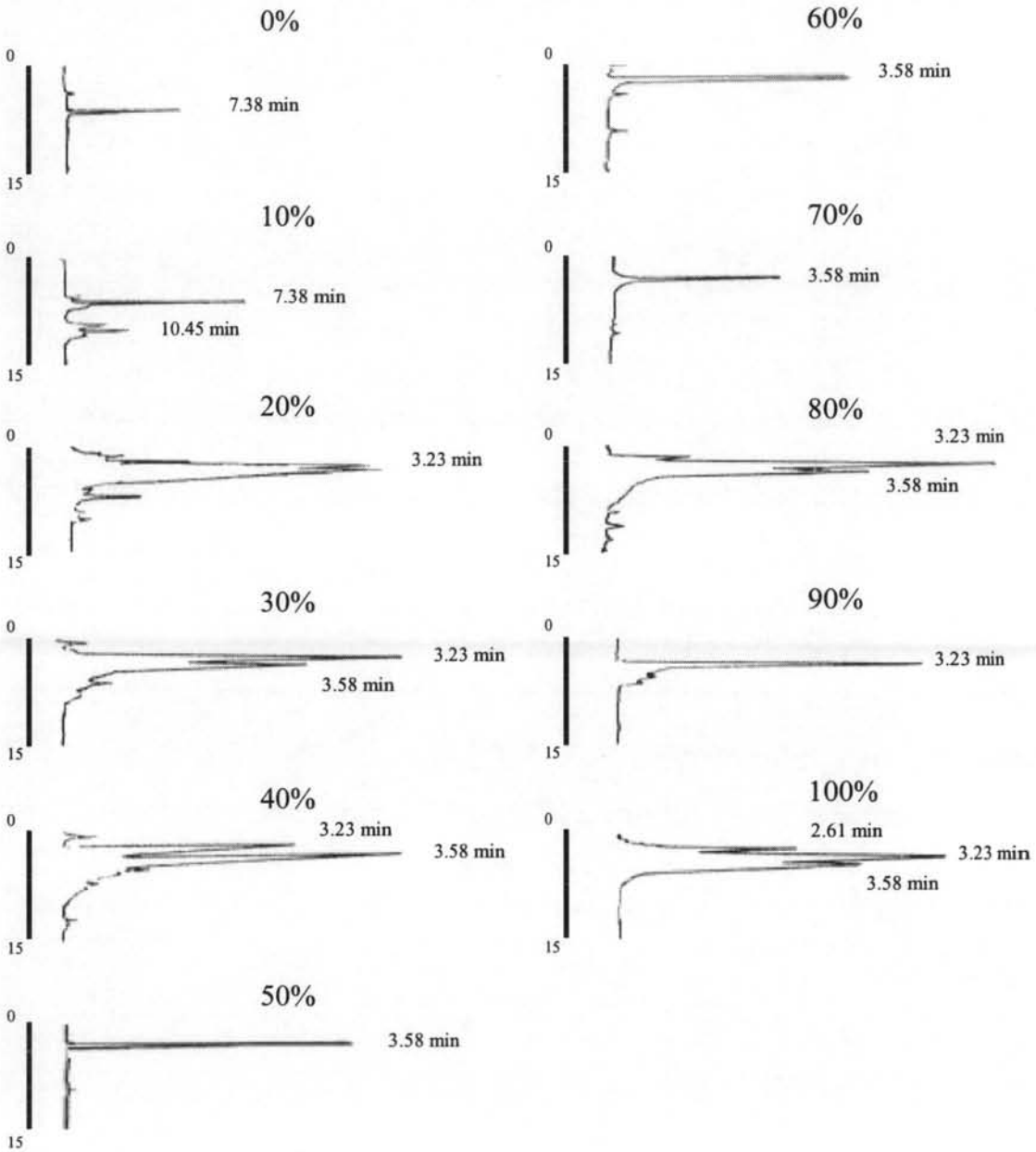

Fig. 4.5 HPLC chromatogram of each fraction of acenaphthylene degrading intermediates from preliminary purified A53-culture extract eluted from silica gel column chromatography with 0-100% ethyl acetate in hexane

HPLC analysis of the intermediate I showed a single peak with a retention time of 3.58 min as shown in Fig. 4.5. The electron impact mass spectrum of this compound, shown in Fig. 4.6 A, contained a base peak at an m/z value of 172, the molecular ion [M^+] and fragment ions at m/z values of 156 [M^+- OH] and 127 [M^+- OH - COOH]. The mass spectrum of this intermediate was identical to those of the authentic 1-naphthoic acid (Fig. 4.6 B). So, intermediate I was identified to be 1-naphthoic acid which had a molecular structure as shown in Fig. 4.7.

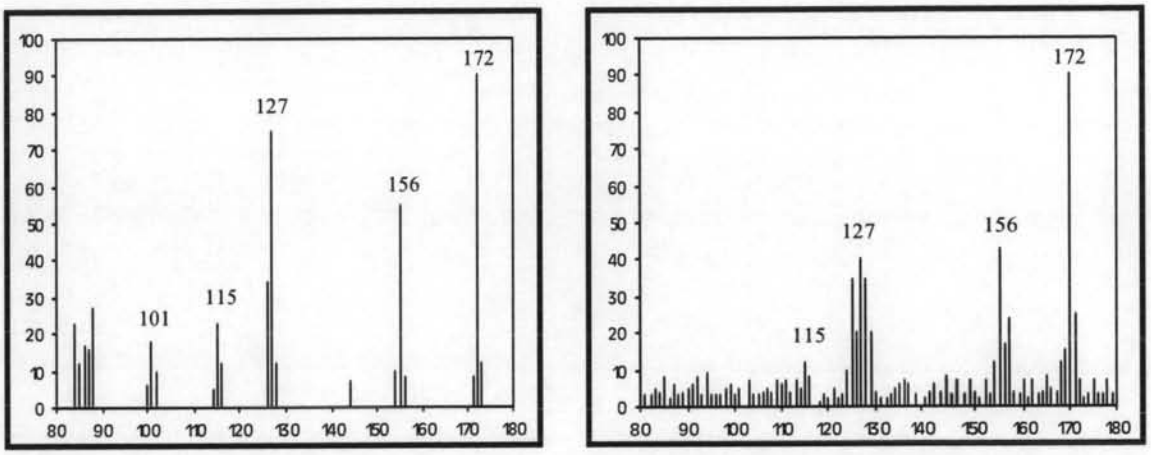

Fig. 4.6 Mass spectrum of intermediate I from A53 [A] compared with authentic standard 1-naphthoic acid [B]

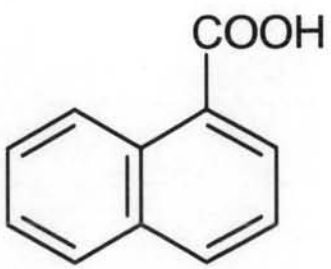

Fig. 4.7 Molecular structure of 1-naphthoic acid

4.1.3 Identification of acenaphthylene intermediate from E11

When mutant strain E11 was incubated for 6 days with acenaphthylene, it transformed acenaphthylene into a predominant product with a retention time of 23.5 min when analyzed by reversed phase HPLC using linear gradient of 40-80% methanol in water as a mobile phase. This product, designated as intermediate II was still remained in relatively high concentration until 14 days of incubation, shown in Fig. 4.8. On the basis of this result, a large scale experiment was set up and incubation for 6 days. After that, the culture extract was subjected to HPLC, equipped with ODS column using the condition described in 3.3.4. The intermediate II, eluted from the column at 23.5 min, was collected and re-checked for its purity by HPLC (Fig. 4.9) and then subjected to GC-MS analysis as described in 3.4.

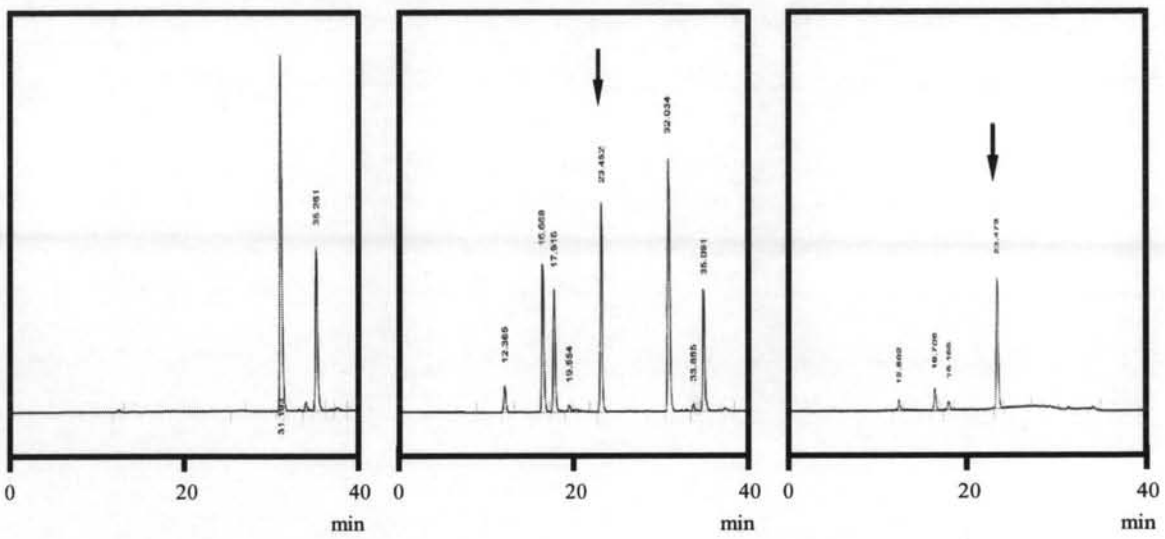

Fig. 4.8 HPLC chromatograms of E11-culture extracts showing intermediates produced from the degradation of acenaphthylene in day 0, 6 and 14 of incubation. The arrows indicate a predominant intermediate with retention time of 23.5 min to be identified.

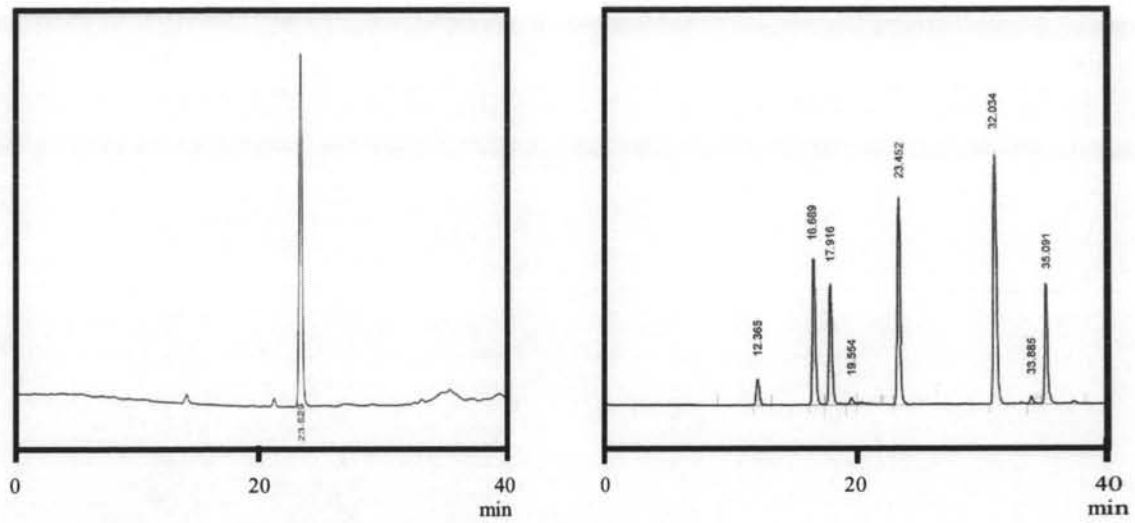

Fig. 4.9 HPLC chromatograms of the partially purified intermediate II (A) compared with the culture extract of E11 (B)

HPLC analysis of the purified intermediate II showed a major single peak with a retention time of 23.5 min. The intermediate II gave a mass spectrum, shown in Fig. 4.10, containing a molecular peak at an m/z value of 160 and fragment ions at m/z values of 131 and 114, identical to those of the authentic 1,2-dihydroxynaphthalene (Fig. 4.10 B). Moreover, HPLC retention time of the intermediate II was similar to those of 1,2-dihydroxynaphthalene. From the results, intermediate II was identified as 1,2-dihydroxynaphthalene with a molecular structure shown in Fig. 4.11.

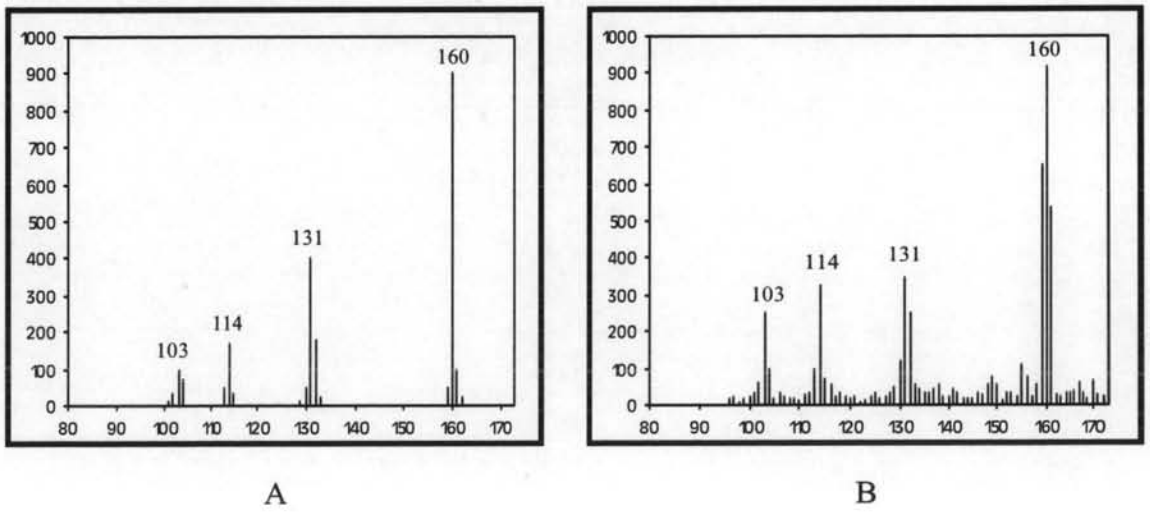

Fig. 4.10 Mass spectrum of intermediate II from E11 [A] compared with authentic standard 1,2-dihydroxynaphthalene [B]

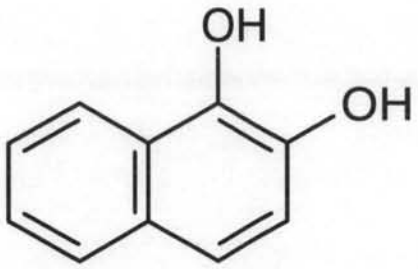

Fig. 4.11 Molecular structure of 1,2-dihydroxynaphthalene

4.1.4 Identification of acenaphthylene intermediate from B1

Due to the success in isolation and identification of 1-naphthoic acid from the degradation of acenaphthylene by A53, a gentisic acid accumulated mutant. B1, an acenaphthylene and acenaphthenequinone degrading defective mutant (Poonthrigpun, 2002), was then selected for isolation and identification of intermediate in an upper pathway of acenaphthylene degradative pathway. HPLC analysis of the culture extract collected after 1 day of incubation of B1 with acenaphthylene showed the formation of a compound corresponding to acenaphthenequinone with no other intermediates. However, from 8h-culture extract, one additional peak of intermediate with a retention time of 25.7 min was detected and designated as intermediate III. The concentration of this intermediate increased during the incubation and reached the maximum at 12 h. After that, the concentration was dramatically decreased and completely disappeared after 18 h of incubation as shown in Fig. 4.12. Thus, B1 was cultured in the mineral medium supplemented with acenaphthylene for 12 h in order to get the maximum amount of this intermediate for further isolation and purification. The intermediate III was purified from the extract by HPLC as described in 3.3.4 and subjected to GC-MS analysis (3.4). The purity of the purified intermediate III was present in Fig. 4.13.

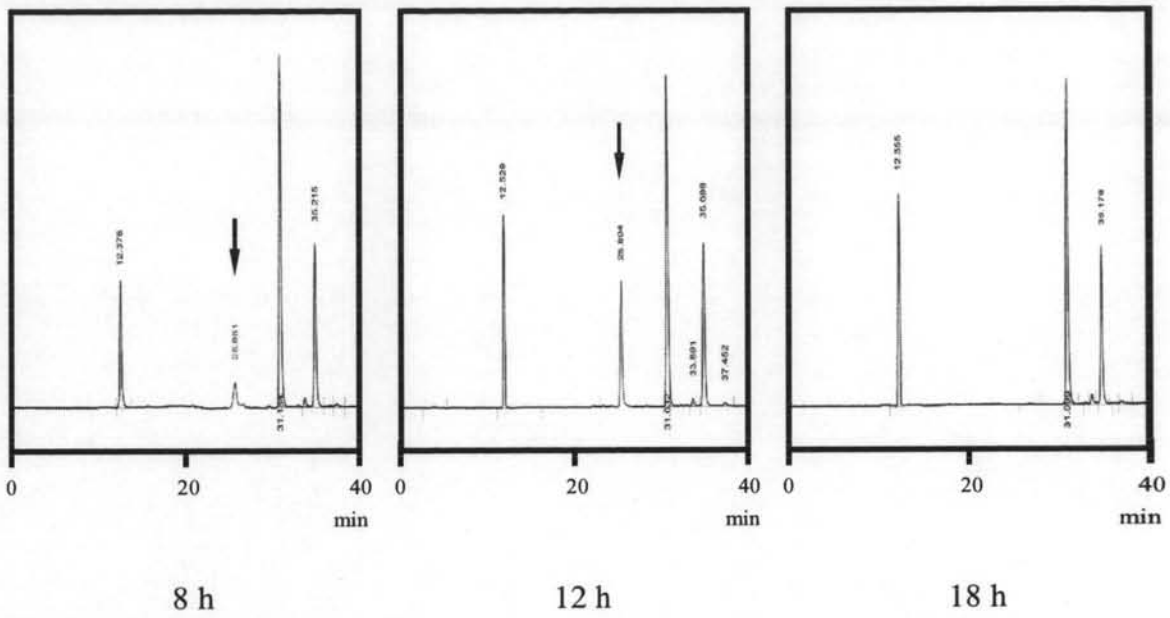

Fig. 4.12 HPLC chromatograms of intermediates produced from the degradation of acenaphthylene by B1 after 8, 12 and 18 h of incubation. The arrows indicate an intermediate with retention time of 25.7 min to be identified

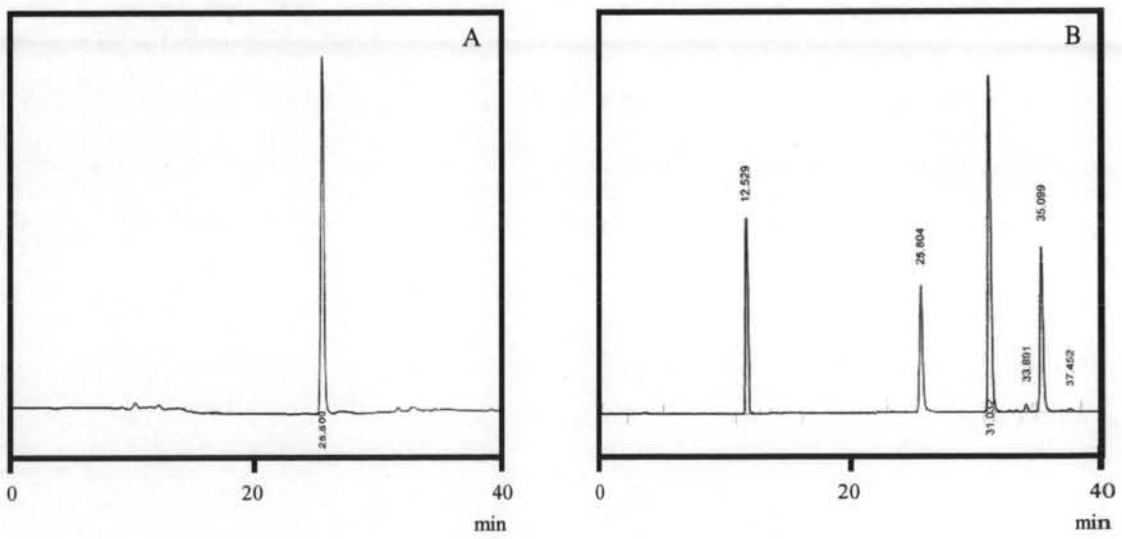

Fig. 4.13 HPLC chromatograms of purified intermediate III (A) compared with the culture extract of B1 (B)

Intermediate III exhibited a mass spectrum with a molecular ion at m/z value of 186 and a fragmentation pattern at m/z 168, 154 and 126 as shown in Fig. 4.14. This mass spectrum was similar to those of 1,2-acenaphthenediol found in Wiley Mass Spectra database and therefore tentatively identified as acenaphthenediol which had a molecular structure as revealed in Fig. 4.15. Authentic 1,2-acenaphthenediol was not available to compare the mass spectrum with those of intermediate III.

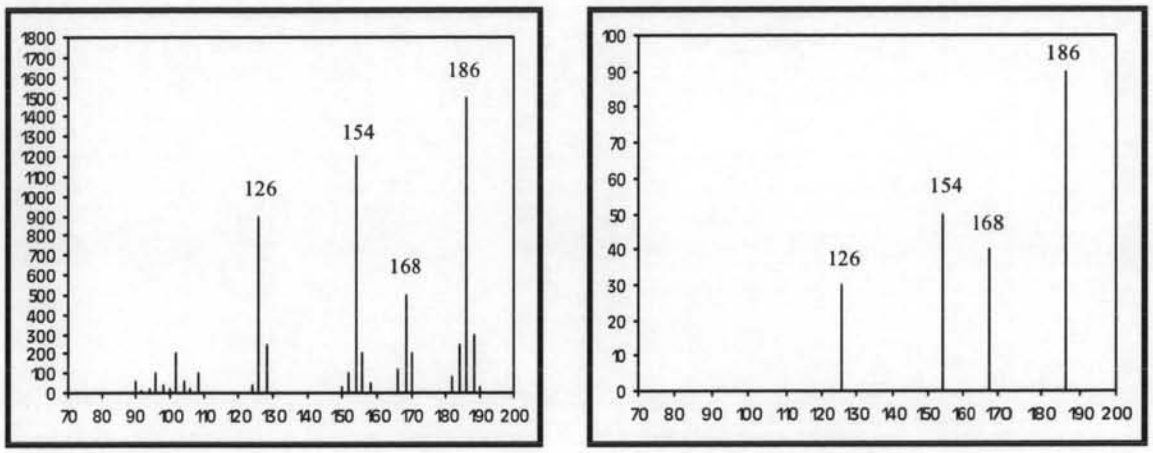

Fig. 4.14 Mass spectrum of intermediate III from B1 [A] compared with those of 1,2-acenaphthenediol found in MS database [B]

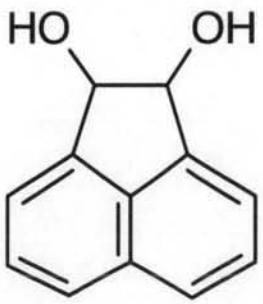

Fig. 4.15 Molecular structure of 1,2-acenaphthenediol

4.1.5 Identification of acenaphthylene intermediates from a wild type *Rhizobium* sp. CU-A1

HPLC chromatogram of the extract of the culture from *Rhizobium* sp. CU-A1 cultivated in mineral medium for 48 h in the presence of acenaphthylene as a sole carbon source showed the formation of a number of intermediates (Fig. 4.16). The HPLC elution profile revealed several major peaks of intermediates with five of them corresponded to acenaphthenequinone, naphthalene-1,8-dicarboxylic acid, 1-naphthoic acid, 1,2-dihydroxynaphthalene, and gentisic acid identified previously (Poonthrigpun, 2002) and including in the present work. However, another compound eluted at the retention time of 19.784 was observed. Therefore, this intermediate, designated as intermediate IV, was preliminary purified by HPLC and identified by GC-MS after methylation. Intermediate IV showed a mass spectrum (Fig. 4.17, A) identical to 3-hydroxybenzoic acid and salicylic acid (2-hydroxybenzoic acid, Fig. 4.17, B). These two compounds had almost similar structure with the difference only in the substitution position of the hydroxyl group at position 2 or 3 as shown in Fig. 4.19.

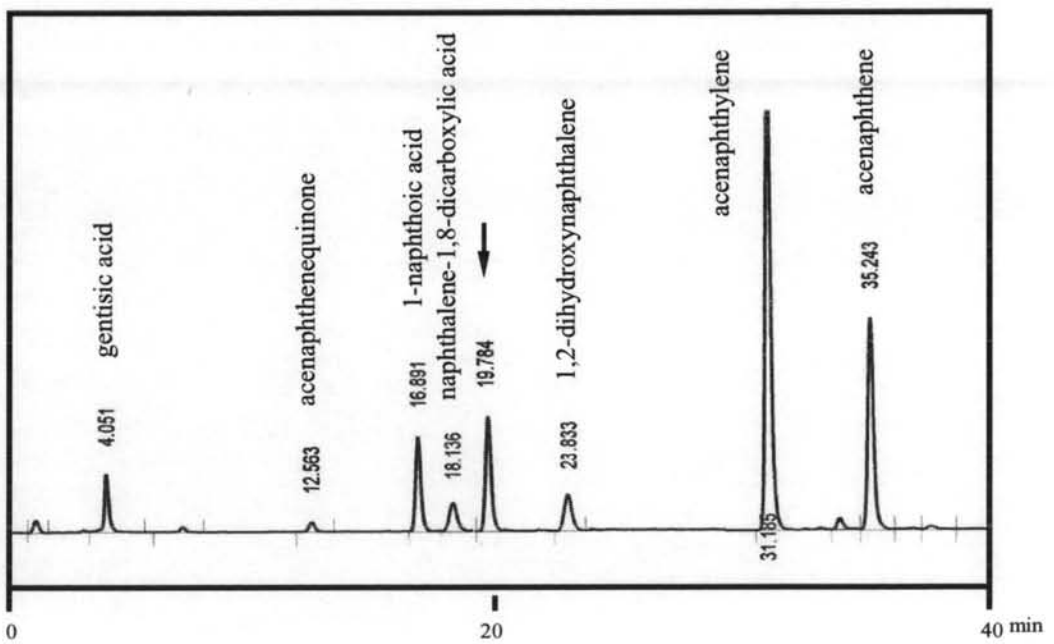

Fig. 4.16 HPLC elution profile of the extract from the culture of *Rhizobium* sp. CU-A1 cultivated in mineral medium for 48 h in the presence of acenaphthylene. The arrow indicates an intermediate with retention time of 19.784 min to be identified.

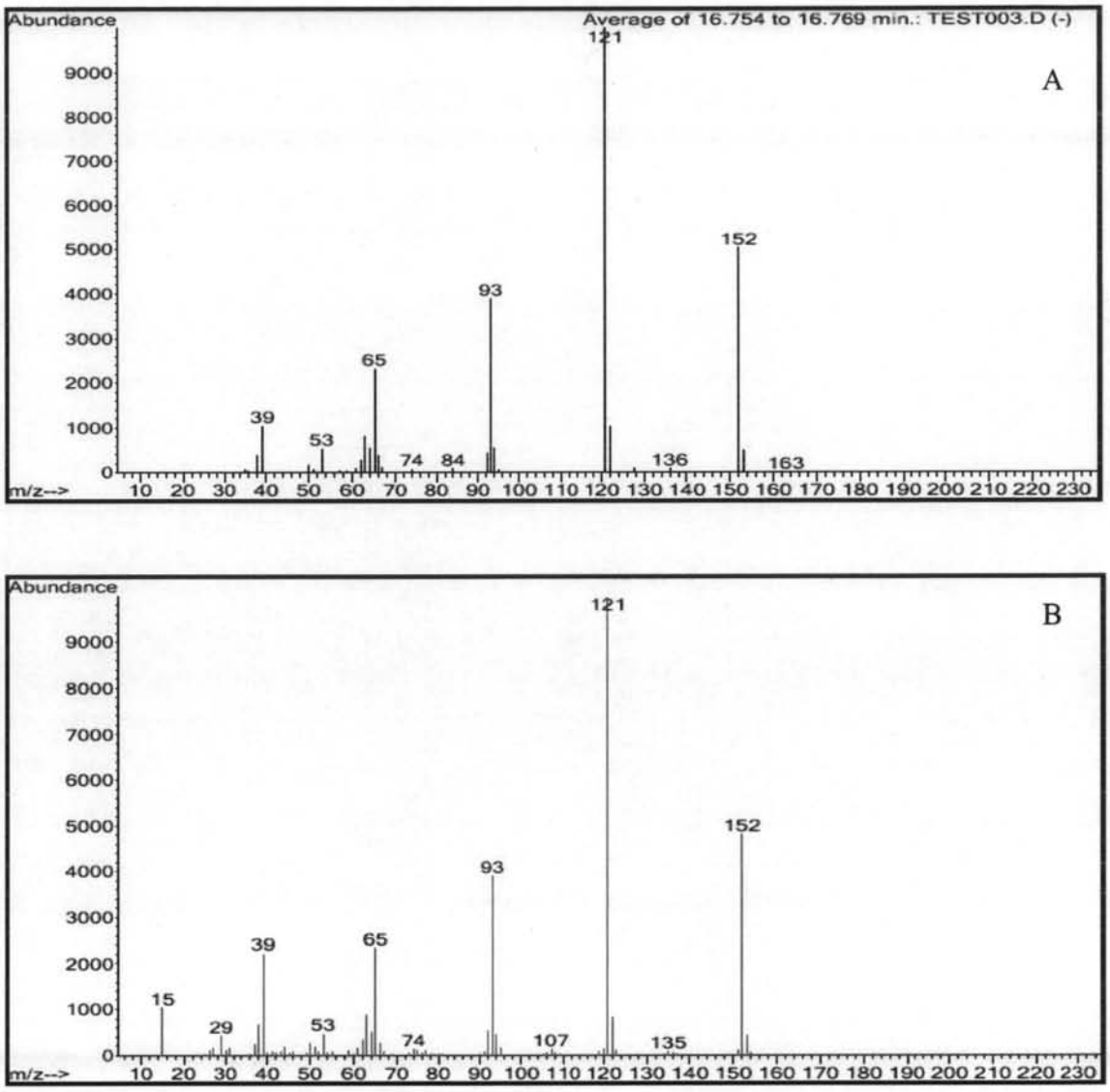

Fig. 4.17 Mass spectrum of intermediate IV from *Rhizobium* sp. CU-A1 [A] compared with those of 3-hydroxybenzoic acid and salicylic acid found in MS database and those of authentic standard salicylic acid and 3-hydroxybenzoic acid [B]

To specify whether intermediate IV is 3-hydroxybenzoic acid or salicylic acid, Nuclear Magnetic Resonance (NMR) analysis is required. But due to the impurity and the limited amount of this intermediate preparation, it could not be subjected to NMR analysis. However, by testing the growth of *Rhizobium* sp. CU-A1 on salicylic acid or 3-hydroxybenzoic acid as a sole source of carbon, the result shown in Fig. 4.18 indicated that *Rhizobium* sp. CU-A1 could grow on salicylic acid not on 3-hydroxybenzoic acid. Therefore, intermediate IV was identified as salicylic acid.

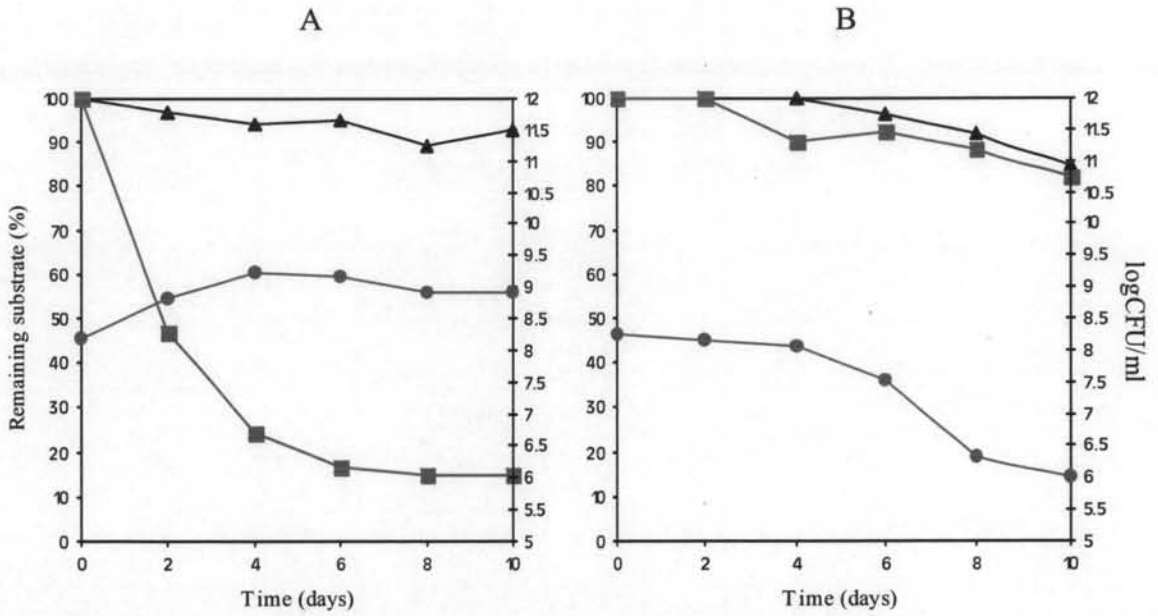

Fig. 4.18 Growth profiles of *Rhizobium* sp. CU-A1 on salicylic acid (A) and 3-hydroxybenzoic acid (B)

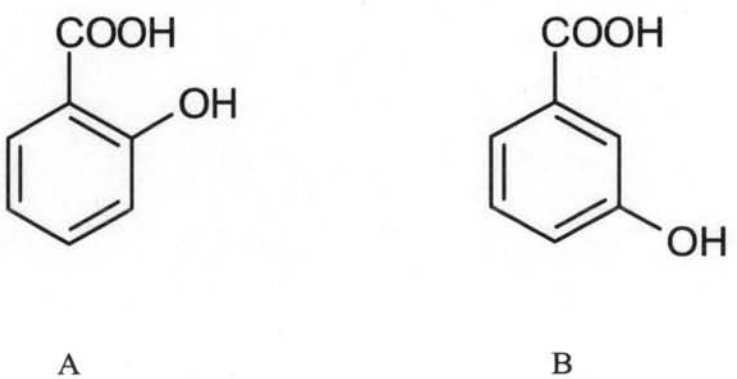

Fig. 4.19 Molecular structure of salicylic acid (A) and 3-hydroxybenzoic acid (B)

In addition, GC-MS analysis of the extract from the culture of *Rhizobium* sp. CU-A1 grown on acenaphthylene for 24 h revealed the presence of low molecular weight intermediate with molecular weight of 91 as shown in Fig. 4.20. The result suggested that maleylpyruvate and/or fumarylpyruvate (Fig. 4.21), which had a similar molecular weight, might be one or both metabolites in acenaphthylene degradative pathway. Both compounds were reported to be the intermediates in gentisate pathway of *Ralstonia* U2 (Ning et al., 2001 and 2002).

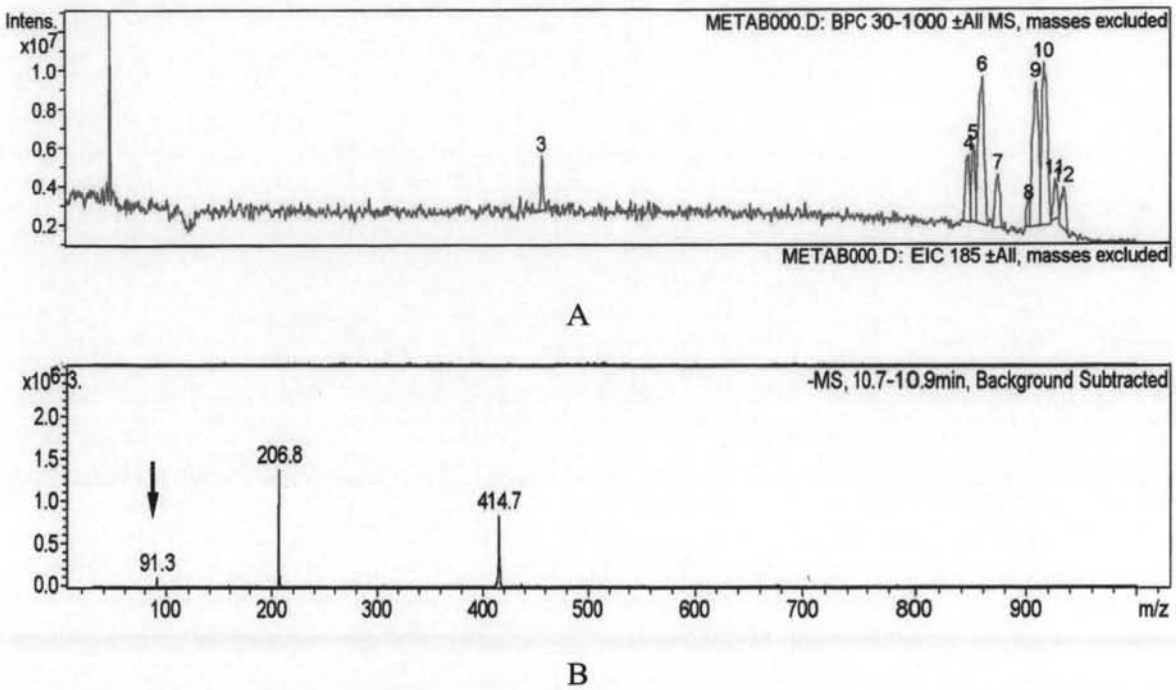

Fig. 4.20 GC chromatogram of the culture extract of *Rhizobium* sp. CU-A1. [A] and mass spectrum of the compounds, eluted at retention time between 10.7-10.9 min [B]

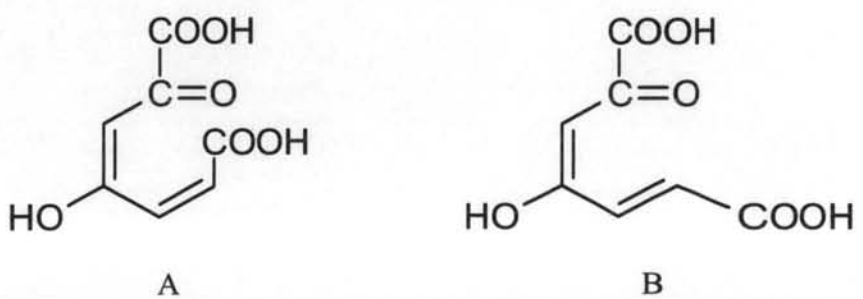

Fig. 4.21 Molecular structure of maleylpyruvate [A] and fumarylpyruvate [B]

4.1.6 Growth of *Rhizobium* sp. CU-A1 and its transposon mutants on the identified intermediates

Eight intermediates produced from the degradation of acenaphthylene were summarized in Table 4.1. The abilities of mutant strains A53, B1 and E11 to grow on these compounds as a sole carbon source compared with those of the wild type CU-A1 were determined in a similar manner to that with acenaphthylene. Each intermediate at 300 mg/L was substituted for acenaphthylene and the samples were taken for analysis every 2 day intervals for 10 days as described in 3.2. The products formed during cultivation were tentatively identified by comparison of their HPLC retention times with those of authentic standards.

Table 4.1 Summary of the acenaphthylene intermediates

Compounds	HPLC R_t (min) 40-80% methanol	Sources	References
Gentisic acid	4.1	A53	Poonthrigpun, 2002
Acenaphthenequinone	12.4	B1	Poonthrigpun, 2002
Naphthalene-1,8-dicarboxylic acid	18.1	B5	Poonthrigpun, 2002
1-Naphthoic acid	16.9	A53	This experiment
1,2-Dihydroxynaphthalene	23.5	E11	This experiment
Acenaphthenediol	25.7	B1	This experiment
Salicylic acid	19.7	CU-A1	This experiment
Fumarylpyruvate	Not detected	CU-A1	This experiment
Maleylpyruvate	Not detected	CU-A1	This experiment

4.1.6.1 The growth of *Rhizobium* sp. CU-A1

From the results shown in Fig. 4.22, the wild type *Rhizobium* sp. CU-A1 was able to grow on all given compounds including acenaphthenequinone,

naphthalene-1,8-dicarboxylic acid, 1-naphthoic acid, 1,2-dihydroxynaphthalene, salicylic acid and gentisic acid as a sole source of carbon and energy, which was similar to that of acenaphthylene as a sole carbon source. The identified intermediates produced during the degradation of acenaphthenequinone, naphthalene-1,8-dicarboxylic acid and other given intermediates summarized in Table 4.2 were corresponding to those of acenaphthylene degradation.

4.1.6.2 The growth of A53

A transposon mutant A53 grew moderately on acenaphthenequinone, naphthalene-1,8-dicarboxylic acid, 1-naphthoic acid and 1,2-dihydroxynaphthalene as shown in Fig. 4.23 and gave the corresponding intermediates with the accumulation of gentisic acid as shown in Table 4.2. No growth was observed with salicylic acid and gentisic acid. However, gentisic acid was also accumulated during the incubation with salicylic acid. A53 was confirmed to be an acenaphthylene and gentisic acid degrading defective mutant which gentisic acid was identified to be an accumulated intermediate from the degradation of acenaphthylene (Poonthrigpun, 2002). According to the previous result shown in 4.1.2, this strain accumulated not only gentisic acid but also 1-naphthoic acid from acenaphthylene degradation. The result suggested that the accumulation of gentisic acid may cause slow degradation of upper intermediates resulting in the presence of 1-naphthoic acid. Gentisic acid was reported to be an intermediate in the lower pathway of many aromatic compounds such as naphthalene (Starovoitov, 1975) and phenanthrene (Moody et al., 2001) which would describe the ability of moderate growth of this strain on acenaphthylene (Fig. 4.1) as well as on the other intermediates (Fig. 4.23) including acenaphthenequinone, naphthalene-1,8-dicarboxylic acid, 1-naphthoic acid and 1,2-dihydroxynaphthalene, the intermediates with higher molecular weight than that of gentisic acid as it could obtain a limited amount of energy from carbon atoms removed from one aromatic ring of these compounds.

4.1.6.3 The growth of B1

B1 could not utilize acenaphthylene as its sole source of carbon and energy for growth as shown in Fig. 4.1 and acenaphthenequinone was also found as

an accumulated intermediate. However, when this strain was grown on acenaphthenequinone, a slightly increasing in cell number and a number of intermediates were detected as shown in Fig. 4.24 and Table 4.2. These results were similar to those of the previous report (Poonthrigpun, 2002), which revealed that B1 present moderate growth on its accumulated intermediate, acenaphthenequinone. This might be due to some spontaneous conversion of acenaphthenequinone to naphthalene-1,8-dicarboxylic acid as reported in the literature (Selifenov et al., 1996). Furthermore, in a control experiment without bacteria spontaneous degradative product of acenaphthenequinone, identified as naphthalene-1,8-dicarboxylic acid, could be detected. However, as this strain had much lower growth efficiency on acenaphthenequinone (Fig. 4.24, 1) than on naphthalene-1,8-dicarboxylic acid (Fig. 4.24, 2), the conversion between these two compounds may not be just by spontaneous reaction alone, but an enzyme-catalyzed conversion may also be involved. This strain also had ability to grow on 1-naphthoic acid, 1,2-dihydroxynaphthalene, salicylic acid and gentisic acid. The intermediates produced from the degradation of the given intermediates were identical to those for the acenaphthylene intermediates occurred during the degradation of acenaphthylene (Table 4.2).

4.1.6.4 The growth of E11

E11 could not grow on all tested compounds with exception for salicylic acid and gentisic acid as shown in Fig. 4.25. However, the substrates were transformed to various intermediates as shown in Table 4.2. Intermediates detected in the transformation of acenaphthenequinone were identified as naphthalene-1,8-dicarboxylic acid, 1-naphthoic acid and 1,2-dihydroxynaphthalene. In the same way, intermediates detected in the naphthalene-1,8-dicarboxylic acid transformation were identified as 1-naphthoic acid and 1,2-dihydroxynaphthalene. Although the concentration of 1,2-dihydroxynaphthalene was slightly reduced when incubating with this strain, no products were observed in the transformation of this compound. This result suggested that 1,2-dihydroxynaphthalene might not be an accumulated intermediate in E11.

Table 4.2 Products formation from the transformation of various compounds by *Rhizobium* sp. CU-A1 and its transposon mutants

	Substrates	Growth	Products					
			AQ	NDA	NA	DHN	SAL	GEN
CU-A1	AE	+	+	+	+	+	+	+
	AQ	+	-	+	+	+	+	+
	NDA	+	-	-	+	+	+	+
	NA	+	-	-	-	+	+	+
	DHN	+	-	-	-	-	+	+
	SAL	+	-	-	-	-	-	+
	GEN	+	-	-	-	-	-	-
A53	AE	+	+	+	+	+	+	+
	AQ	+	-	+	+	+	+	+
	NDA	+	-	-	+	+	+	+
	NA	+	-	-	-	+	+	+
	DHN	+	-	-	-	-	+	+
	SAL	-	-	-	-	-	-	+
	GEN	-	-	-	-	-	-	-
B1	AE	-	+	-	-	-	-	-
	AQ	+	-	+	+	+	-	-
	NDA	+	-	-	+	+	+	+
	NA	+	-	-	-	+	+	+
	DHN	+	-	-	-	-	+	+
	SAL	+	-	-	-	-	-	+
	GEN	+	-	-	-	-	-	-
E11	AE	-	+	+	+	+	-	-
	AQ	-	-	+	+	+	-	-
	NDA	-	-	-	+	+	-	-
	NA	-	-	-	-	+	-	-
	DHN	-	-	-	-	-	-	-
	SAL	+	-	-	-	-	-	+
	GEN	+	-	-	-	-	-	-

AE, acenaphthylene; AQ, acenaphthenequinone; NDA, naphthalene-1,8-dicarboxylic acid; NA, 1-naphthoic acid; DHN, 1,2-dihydroxynaphthalene; SAL, salicylic acid; GEN, gentisic acid; +, detected; -, not detected

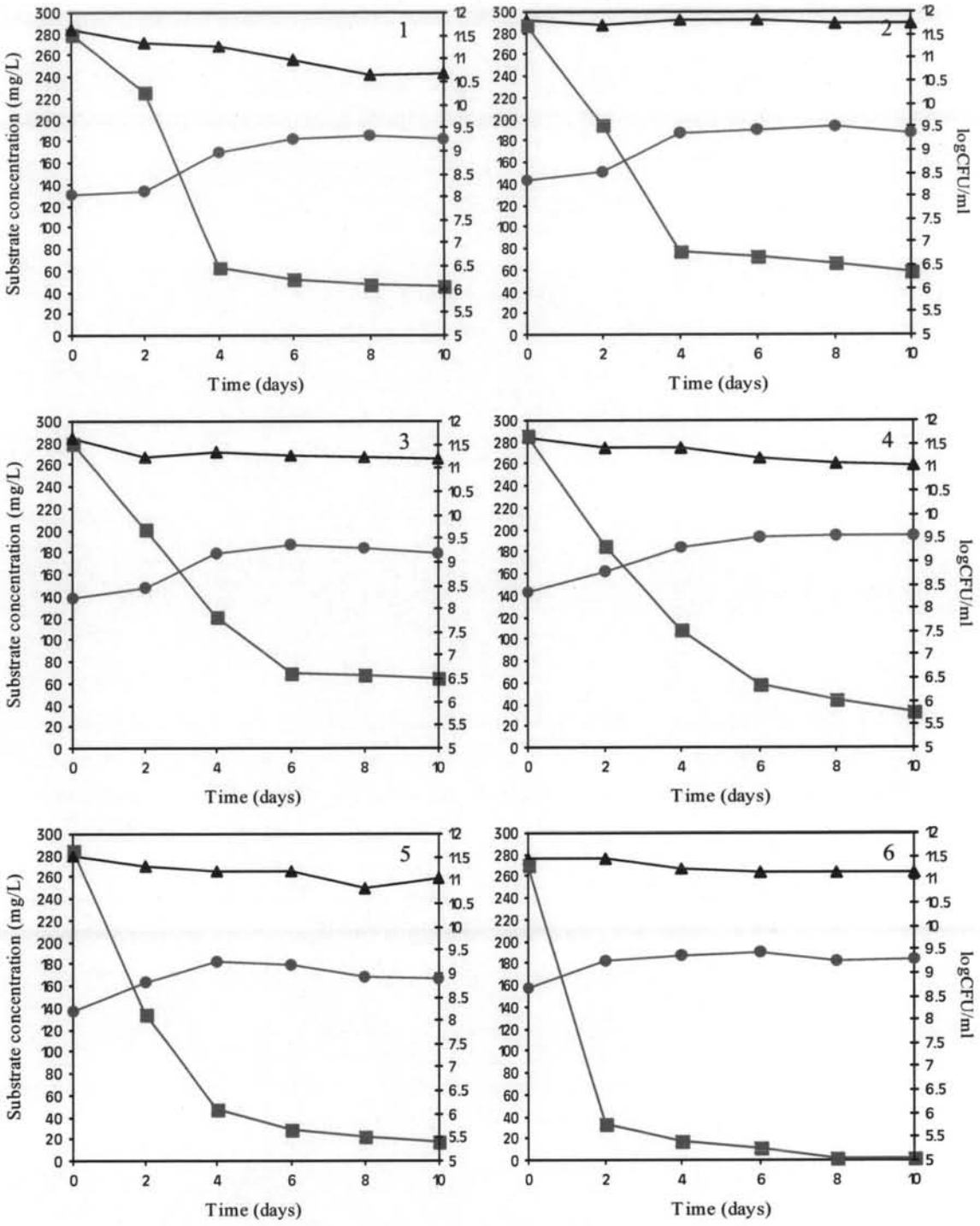

Fig. 4.22 Growth profiles of *Rhizobium* sp. CU-A1 in mineral medium containing 300 mg/L acenaphthenequinone (1), naphthalene-1,8-dicarboxylic acid (2), 1-naphthoic acid (3), 1,2-dihydroxynaphthalene (4), salicylic acid (5) and gentisic acid (6)

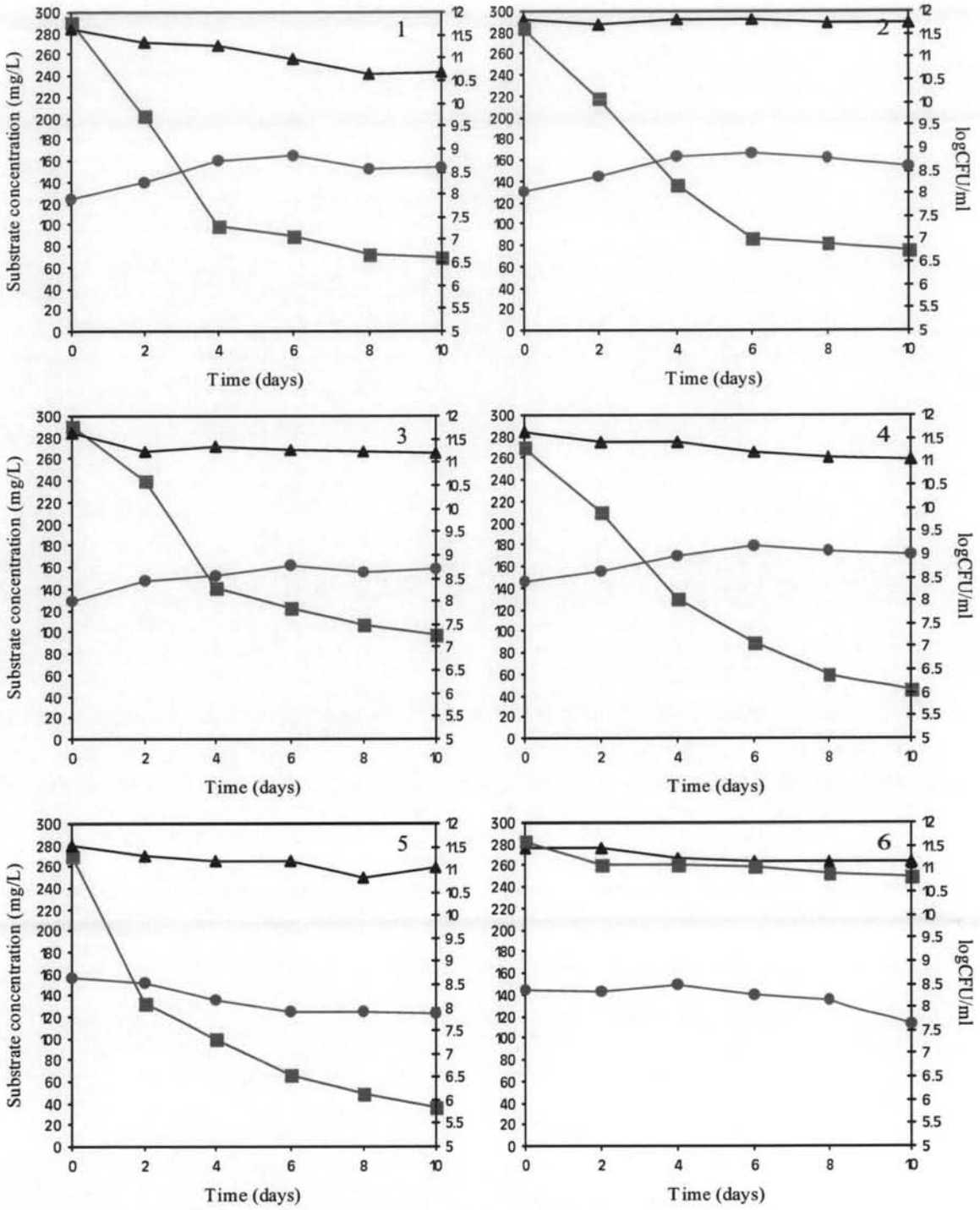

Fig. 4.23 Growth profiles of A53 in mineral medium containing 300 mg/L acenaphthenequinone (1), naphthalene-1,8-dicarboxylic acid (2), 1-naphthoic acid (3), 1,2-dihydroxynaphthalene (4), salicylic acid (5) and gentisic acid (6)

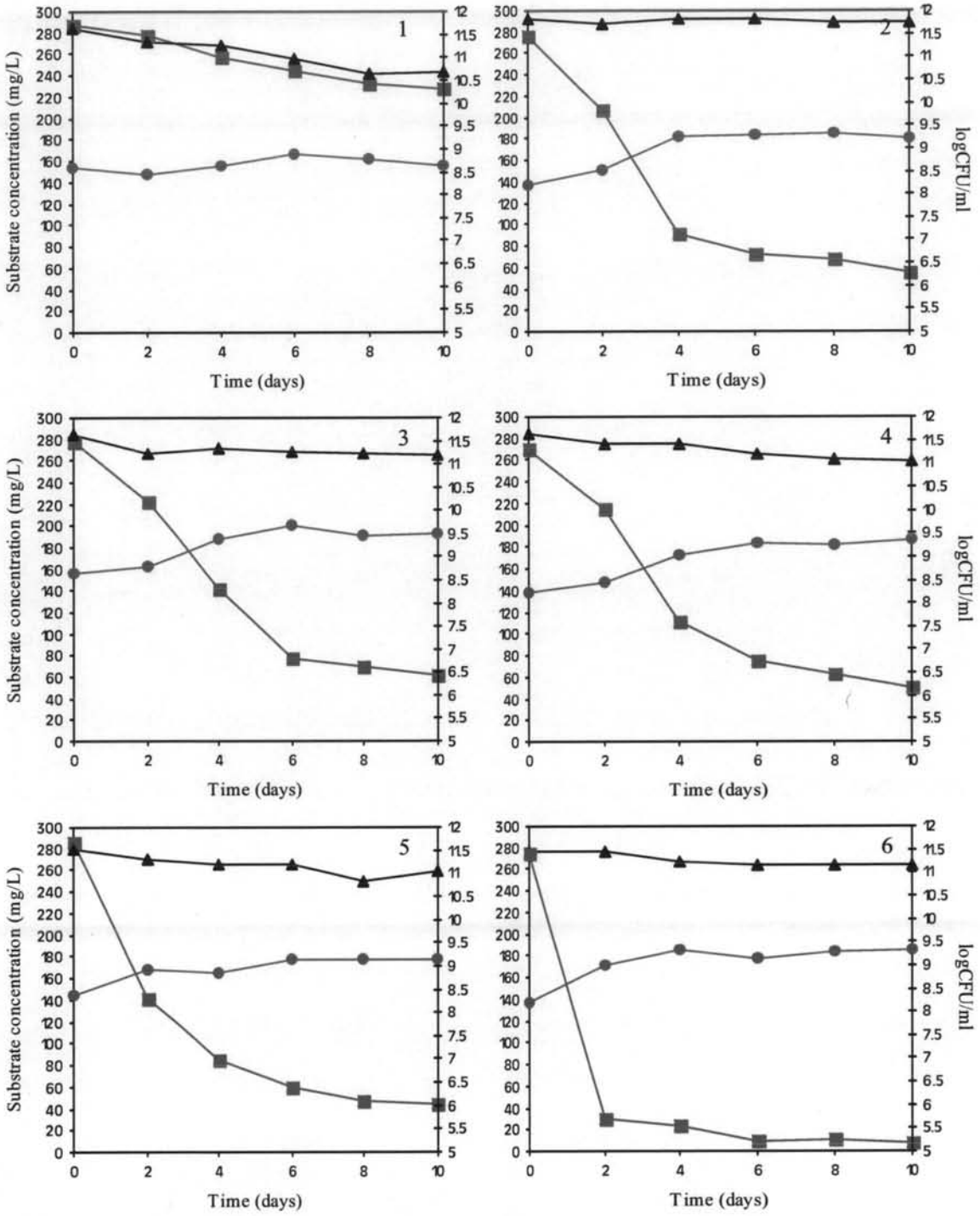

Fig. 4.24 Growth profiles of B1 in mineral medium containing 300 mg/L acenaphthenequinone (1), naphthalene-1,8-dicarboxylic acid (2), 1-naphthoic acid (3), 1,2-dihydroxynaphthalene (4), salicylic acid (5) and gentisic acid (6)

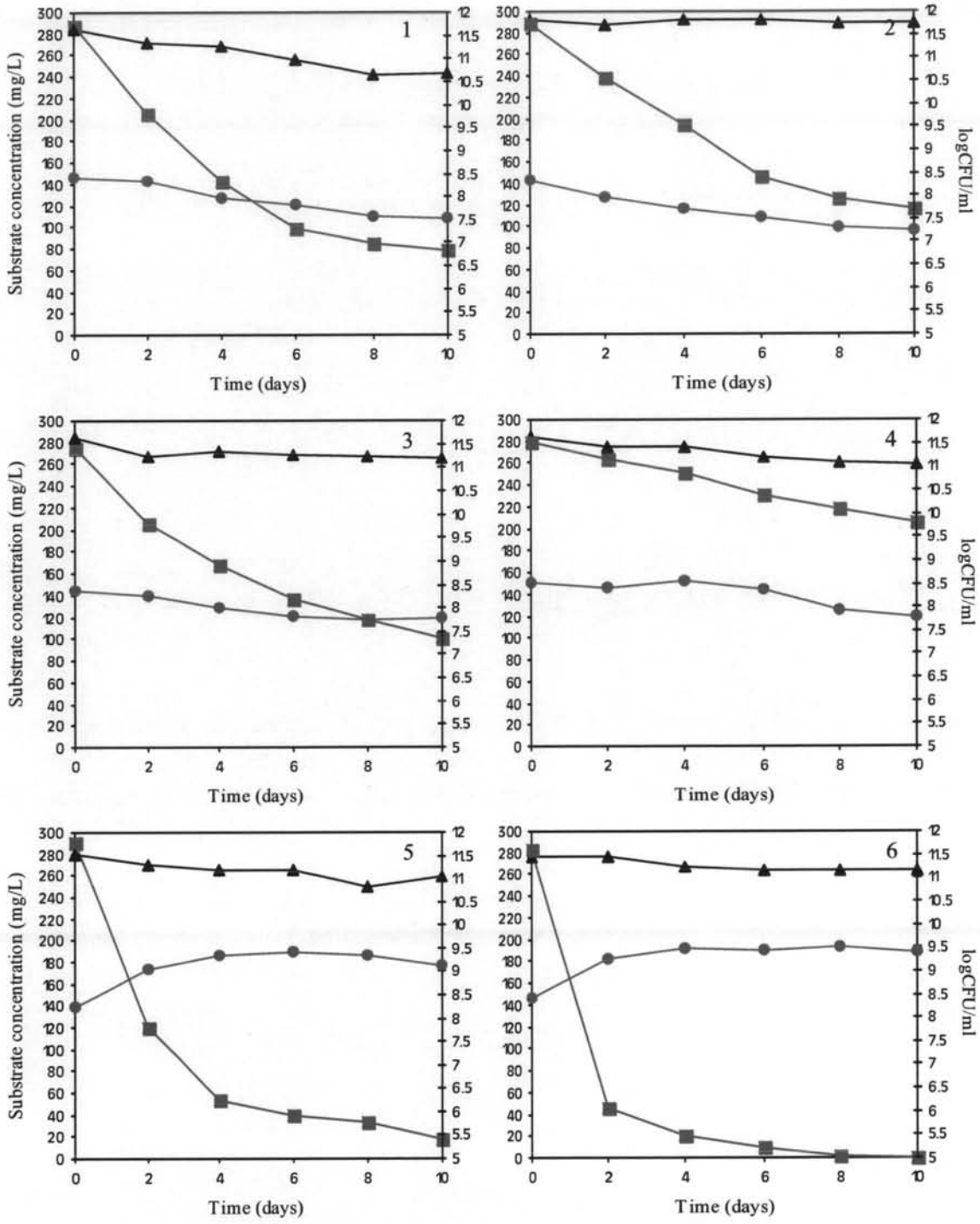

Fig. 4.25 Growth profiles of E11 in mineral medium containing 300 mg/L acenaphthenequinone (1), naphthalene-1,8-dicarboxylic acid (2), 1-naphthoic acid (3), 1,2-dihydroxynaphthalene (4), salicylic acid (5) and gentisic acid (6)

4.1.7 Catabolic pathway of acenaphthylene degradation in *Rhizobium* sp. CU-A1

In order to confirm that all identified intermediates isolated from culture of *Rhizobium* sp. CU-A1 and its transposon mutants growing on acenaphthylene were the intermediates from the degradation of acenaphthylene by *Rhizobium* sp. CU-A1, the disappearance of acenaphthylene and the appearance of intermediates were measured in the culture extract of *Rhizobium* sp. CU-A1 growing on acenaphthylene as a sole carbon source for 96 h. The result, shown in Fig. 4.26, revealed the correlation between the decreasing of substrate and the occurrence of the intermediates. The substrate, acenaphthylene, and its intermediates produced during the degradation of acenaphthylene were utilized corresponding to the growth of bacteria.

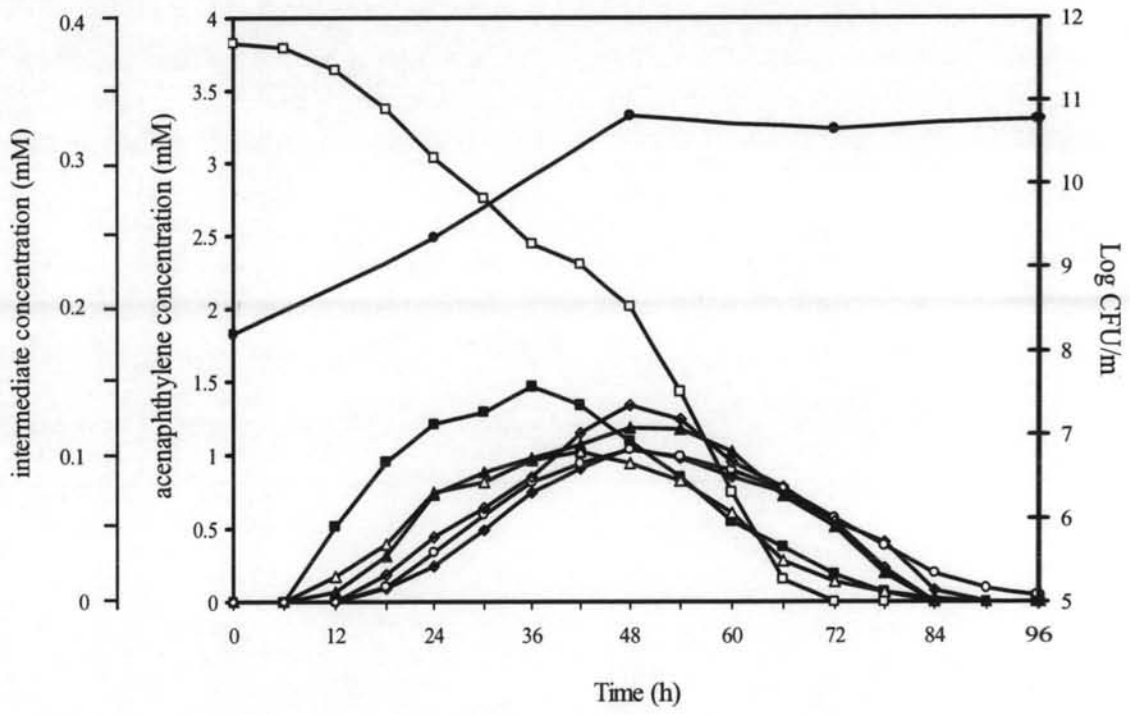

Fig. 4.26 The disappearance of acenaphthylene and the appearance of intermediates during the growth of *Rhizobium* sp. CU-A1 in mineral medium containing acenaphthylene; ●: number of cell, □: acenaphthylene, ■: acenaphthenequinone, △: naphthalene-1,8-dicarboxylic acid, ▲: 1-naphthoic acid, ◇: 1,2-dihydroxy naphthalene, ◆: salicylic acid, ○: gentisic acid

HPLC elution profile of the extract of acenaphthylene-grown *Rhizobium* sp. CU-A1 for 36 h showed the occurrence of all identified intermediates except for acenaphthenediol, maleylpyruvate and fumarylpyruvate (Fig. 4.27). The intermediates were identified by comparison of their HPLC retention times with those of authentic standards and by cochromatography with authentic standards. Although the commercially available acenaphthylene have been found to contaminate with acenaphthene, an experiment using acenaphthene as a carbon source for *Rhizobium* sp. CU-A1 revealed that acenaphthene could not be utilized by this strain and no intermediate after 36 h of incubation was detected. The result confirmed that acenaphthenequinone, naphthalene-1,8-dicarboxylic acid, 1-naphthoic acid, 1,2-dihydroxynaphthalene, salicylic acid and gentisic acid were the intermediates from acenaphthylene degradation.

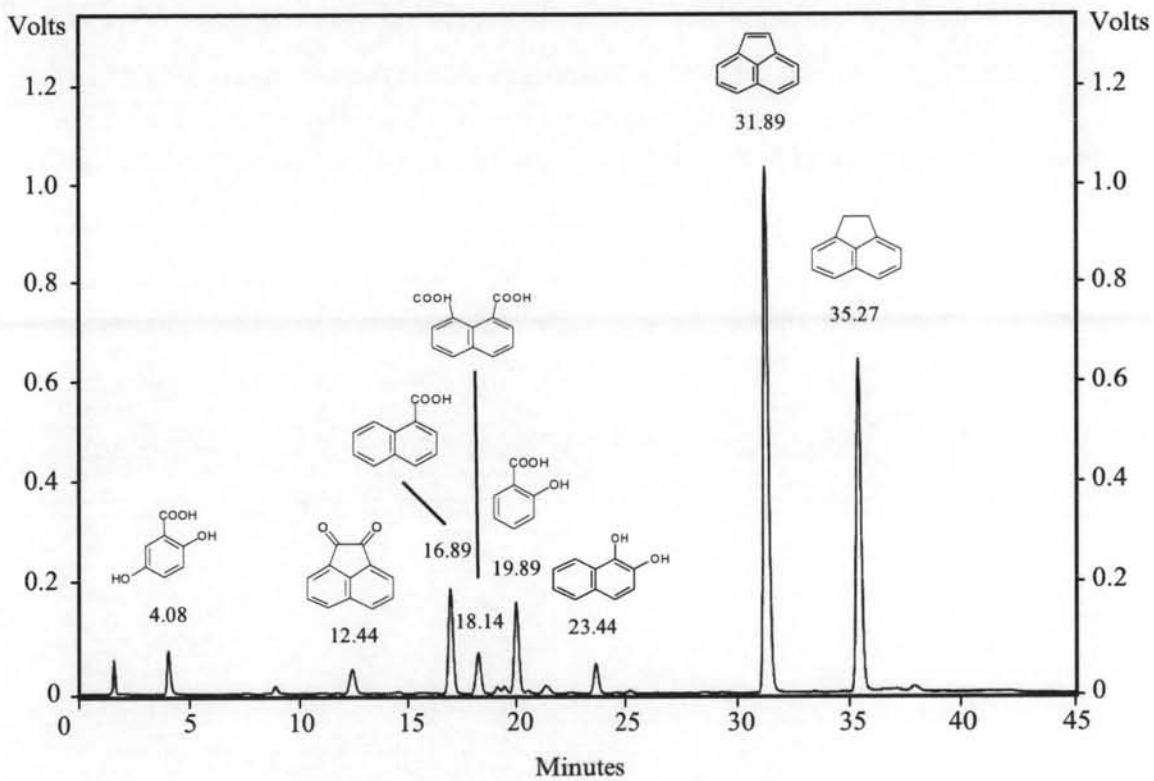

Fig. 4.27 HPLC elution profile of intermediates formed from the degradation of acenaphthylene by *Rhizobium* sp. CU-A1 after 36 h of cultivation

Evidence present in this work demonstrates that *Rhizobium* sp. CU-A1 is capable of metabolizing acenaphthylene to acenaphthenediol, acenaphthenequinone and naphthalene-1,8-dicarboxylic acid. Thus, the early oxidation processes may occur in the same manner as that reported for *Beijerinckia* sp. (Shocken and Gibson, 1984) and *Pseudomonas aeruginosa* PA01, a recombinant strain harboring plasmid pRE695 containing naphthalene dioxygenase gene, *nahA* (Selifenov et al., 1996) as shown in Fig. 4.28.

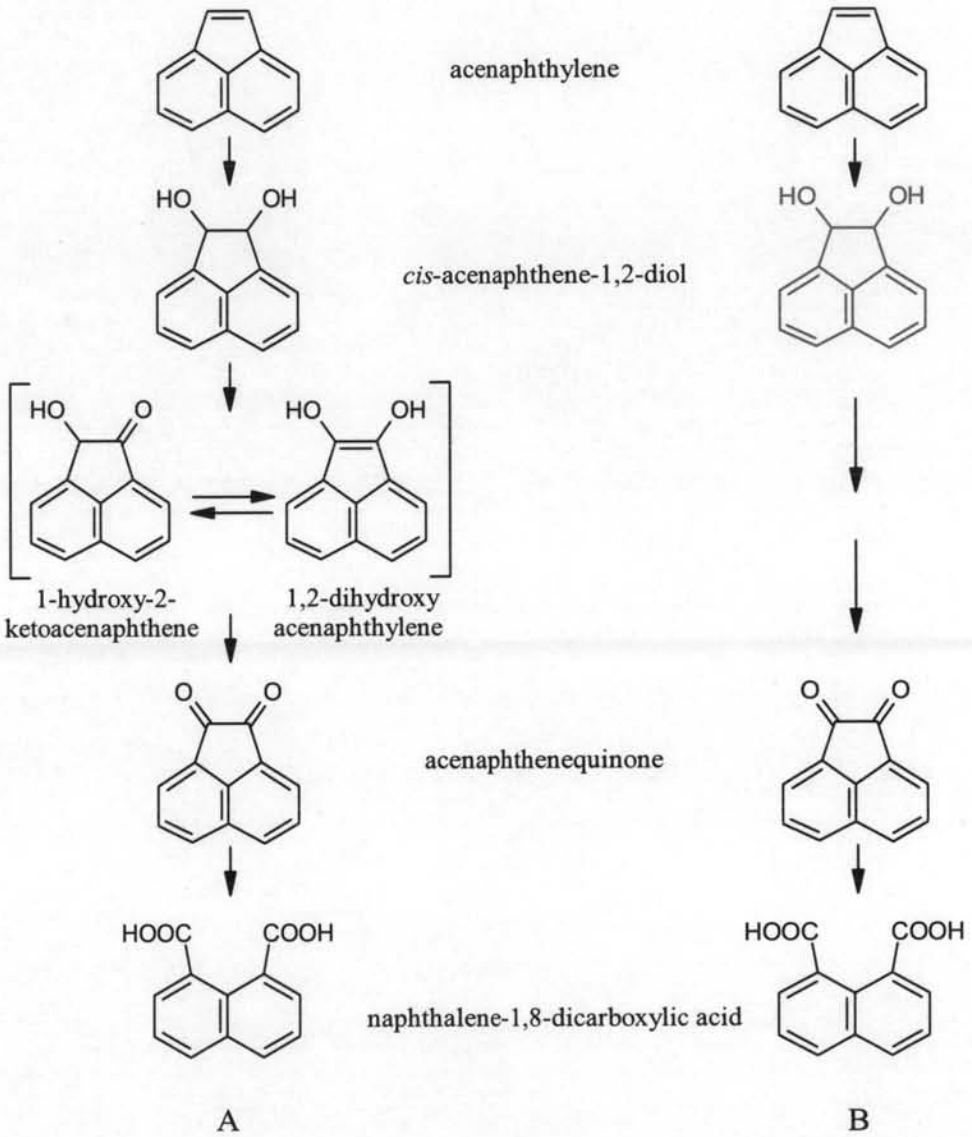

Fig. 4.28 Acenaphthylene catabolic pathway in *Beijerinckia* sp. (Shocken and Gibson, 1984) and *Pseudomonas aeruginosa* PA01 (Selifenov et al., 1996) (A) and a proposed acenaphthylene catabolic upper pathway in *Rhizobium* sp. CU-A1 (B), (The red color represents the isolated and identified intermediate from this work)

Poonthrigpun (2002) showed for the first time the ability of bacterium strain *Rhizobium* sp. CU-A1 to degrade naphthalene-1,8-dicarboxylic acid, previously reported to be a dead end product of acenaphthylene oxidation by *Pseudomonas cepacia* F297 (Grifoll et al., 1995) and *Pseudomonas aeruginosa* PA01 (Selifenov et al., 1996), to gentisic acid. The result suggested that naphthalene-1,8-dicarboxylic acid could be further oxidized to the intermediates in the lower pathway and eventually to CO_2. In this study, 1-naphthoic acid was identified as an intermediate of acenaphthylene degradation by *Rhizobium* sp. CU-A1. The formation of 1-naphthoic acid may occur from the degradation of naphthalene-1,8-dicarboxylic acid. This result suggested that decarboxylation at one carboxyl group of naphthalene-1,8-dicarboxylic acid occurred similar to that reported in the oxidation of pyrene by *Mycobacterium* sp. PYR-1 (Young et al., 1995) *Mycobacterium* sp. KR2 (Rehmann et al., 1998) and *Mycobacterium* sp. AP1 (Vila et al., 2001) in which phenanthrene-4,5-dicarboxylic acid, an intermediate having two carboxyl groups on one aromatic ring, was decarboxylated to phenanthrene-4-carboxylic acid as shown in Fig. 4.29.

The resulting 1-naphthoic acid would then be dioxygenated at C-1 and C-2 positions on the ring containing carboxyl group following by decarboxylation resulting in the formation of 1,2-dihydroxynaphthalene, one of the identified intermediates. This compound could be further oxidized to salicylic acid similar to that reported in naphthalene catabolic pathway by *Sphingomonas yanoikuyae* B1 and *Pseudomonas putida* G7 (Kim et al., 1997; Yen and Gunsulas, 1982). This might not be similar to Phale et al. (1995) who reported that 1-naphthoic acid was dioxygenated at the aromatic ring adjacent to the one bearing the carboxyl group resulting in the formation of 1,2-dihydroxy-8-carboxynaphthalene. Then, it was further oxidized to salicylic acid via 3-formylsalicylic acid and 2-hydroxyisophthalic acid as shown in Fig. 4.30. However, more intermediates in 1-naphthoic acid catabolic pathway of *Rhizobium* sp. CU-A1 are still needed to be identified to specify its precise metabolic route.

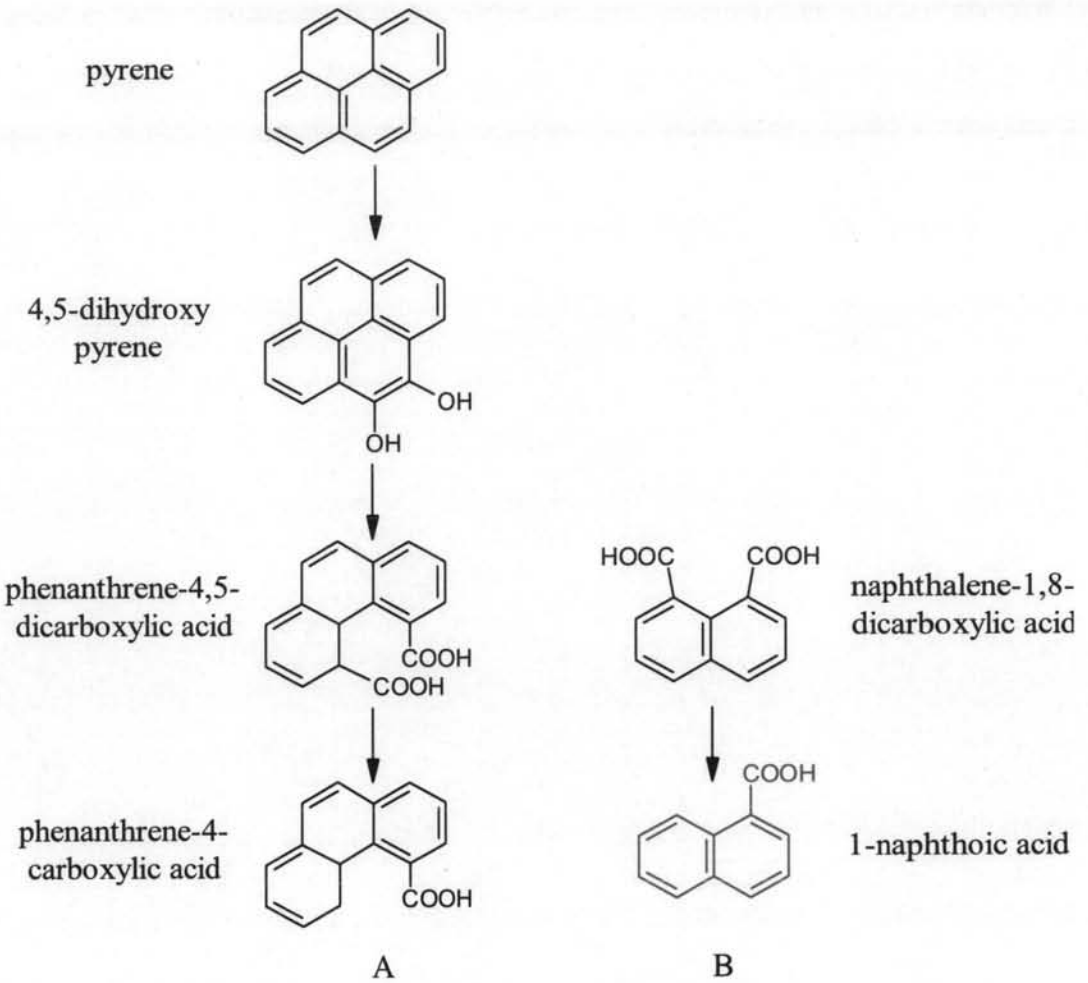

Fig. 4.29 Pyrene catabolic pathway in *Mycobacterium* sp. PYR-1 (Young et al., 1995) *Mycobacterium* sp. KR2 (Rehmann et al., 1998) and *Mycobacterium* sp. AP1 (Vila et al., 2001) (A) and a proposed naphthalene-1,8-dicarboxylic acid decarboxylation to 1-naphthoic acid in *Rhizobium* sp. CU-A1 (B), (The red color represents the isolated and identified intermediate from this work)

To our knowledge, catechol is a common intermediate found in most PAHs lower catabolic pathways. However, catechol was not detected as an intermediate from the degradation of acenaphthylene by CU-A1 and it was also found that this compound could not serve as a substrate for the growth of this strain (Paengthai, 2000). Moreover, gentisic acid was found as an intermediate from acenaphthylene oxidation. Therefore, the results suggested that salicylic acid was further oxidized to gentisic acid, which was further oxidized to maleylpyruvate or fumarylpyruvate and then to central intermediates in the TCA cycle as reported in *Ralstonia* sp. (Ning et al., 2001 and 2002), as shown in Fig. 4.31.

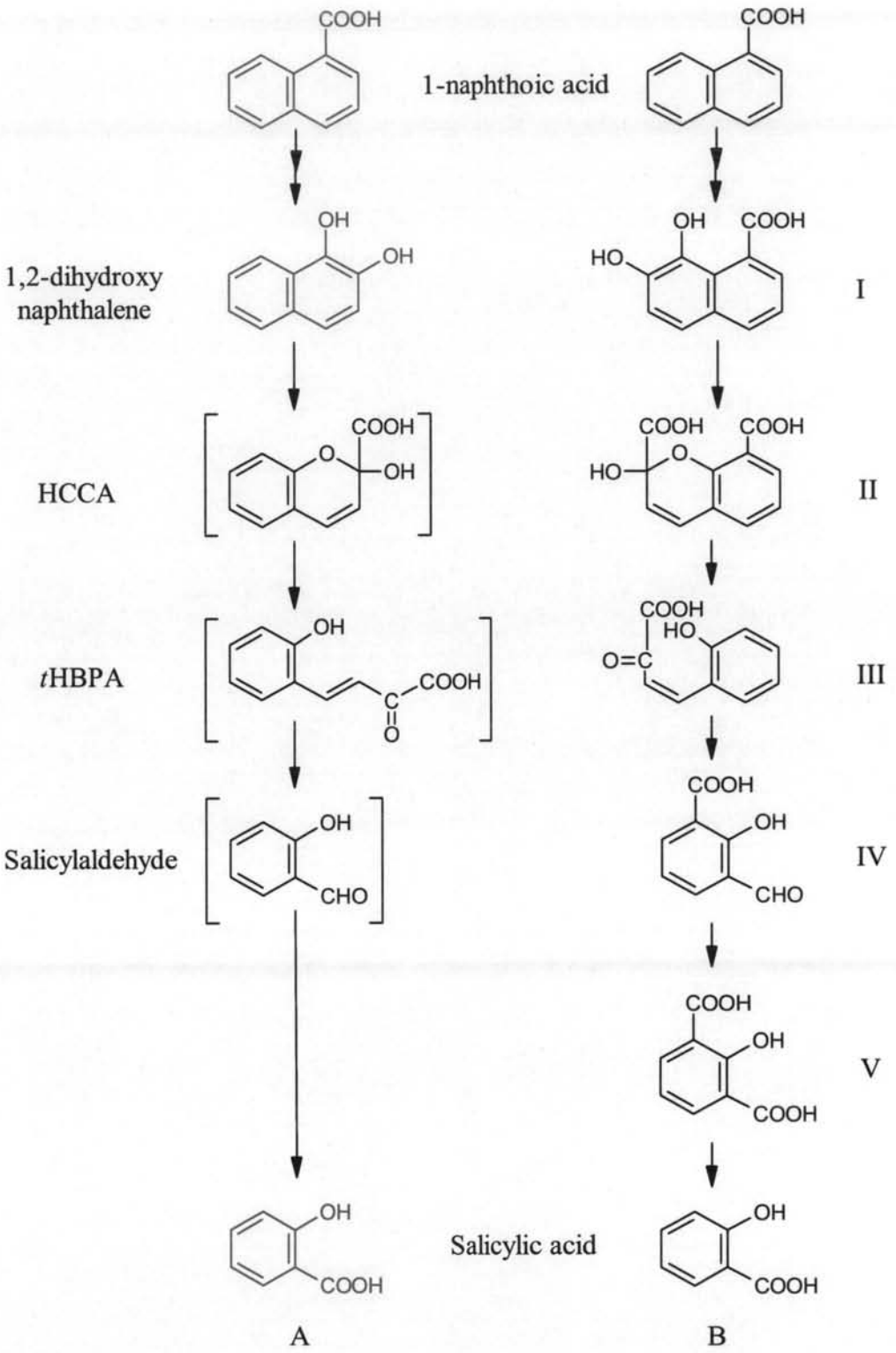

Fig. 4.30 Proposed 1-naphthoic acid catabolic pathway in *Rhizobium* sp. CU-A1 (A) and 1-naphthoic acid catabolic pathway in *Pseudomonas maltophilia* CSV89 (Phale et al.,1995) (B), (The red color represents the isolated and identified intermediates from this work; I, 1,2-dihydroxy-8-carboxynaphthalene; II, 2-carboxy-2-hydroxy-8-carboxychromene; III, 2-hydroxy-3-carboxybenzylpyruvate; IV, 3-formyl-salicylic acid; V, 2-hydroxyisophthalic acid)

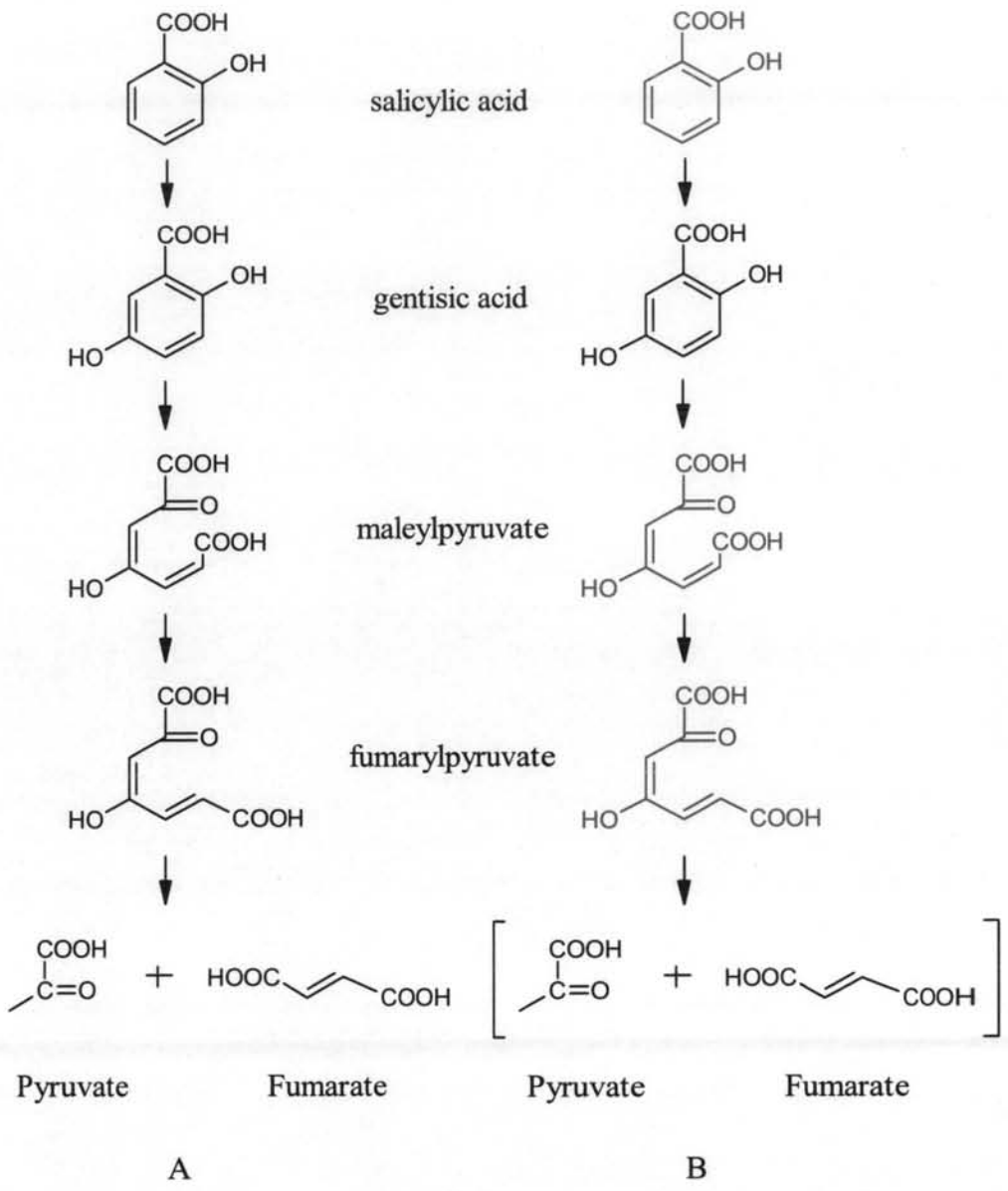

Fig. 4.31 Salicylic acid catabolic pathway via gentisic acid in *Ralstonia* U2 (Ning et al., 2001 and 2002) (A) and proposed salicylic acid catabolic pathway in *Rhizobium* sp. CU-A1 (B), (The red color represents the isolated and identified intermediates from this work)

From the $^{18}O_2$ incorporation experiment, it suggested that the initial reaction in the degradation of acenaphthylene by *Rhizobium* sp. CU-A1 was the incorporation of two oxygen atoms into cyclopentene ring of acenaphthylene (position C-1 and C-2) to form acenaphthenediol. This reaction was catalyzed by an enzyme termed

acenaphthylene dioxygenase. Subsequent dehydrogenation by acenaphthenediol dehydrogenase would then result in the formation of 1,2-dihydroxyacenapthylene which would be further oxidized to acenaphthenequinone. Although acenaphthenequinone could be spontaneously oxidized to naphthalene-1,8-dicarboxylic acid as reported by Selifenov et al. (1996), the result as described in 4.1.6.3 indicated that enzyme-catalyzed conversion was also involved. A possible second dioxygenation of acenaphthenequinone would result in the cleavage of the oxidation product to naphthalene-1,8-dicarboxylic acid. Further decarboxylation of naphthalene-1,8-dicarboxylic acid would give 1-naphthoic acid. The results also showed that CU-A1 can dioxygenate an aromatic ring of 1-naphthoic acid and form 1,2-dihydroxynaphthalene. The resulting 1,2-dihydroxynaphthalene would then be oxidized to salicylic acid and undergo enzymatic hydroxylation to form gentisic acid. Then, dioxygenation of gentisic acid following by ring fission would result in the formation of central intermediates in the TCA cycle such as pyruvate and fumarate via maleylpyruvate or fumarylpyruvate. The proposed complete acenaphthylene catabolic pathway in *Rhizobium* sp. CU-A1 was shown in Fig. 4.32.

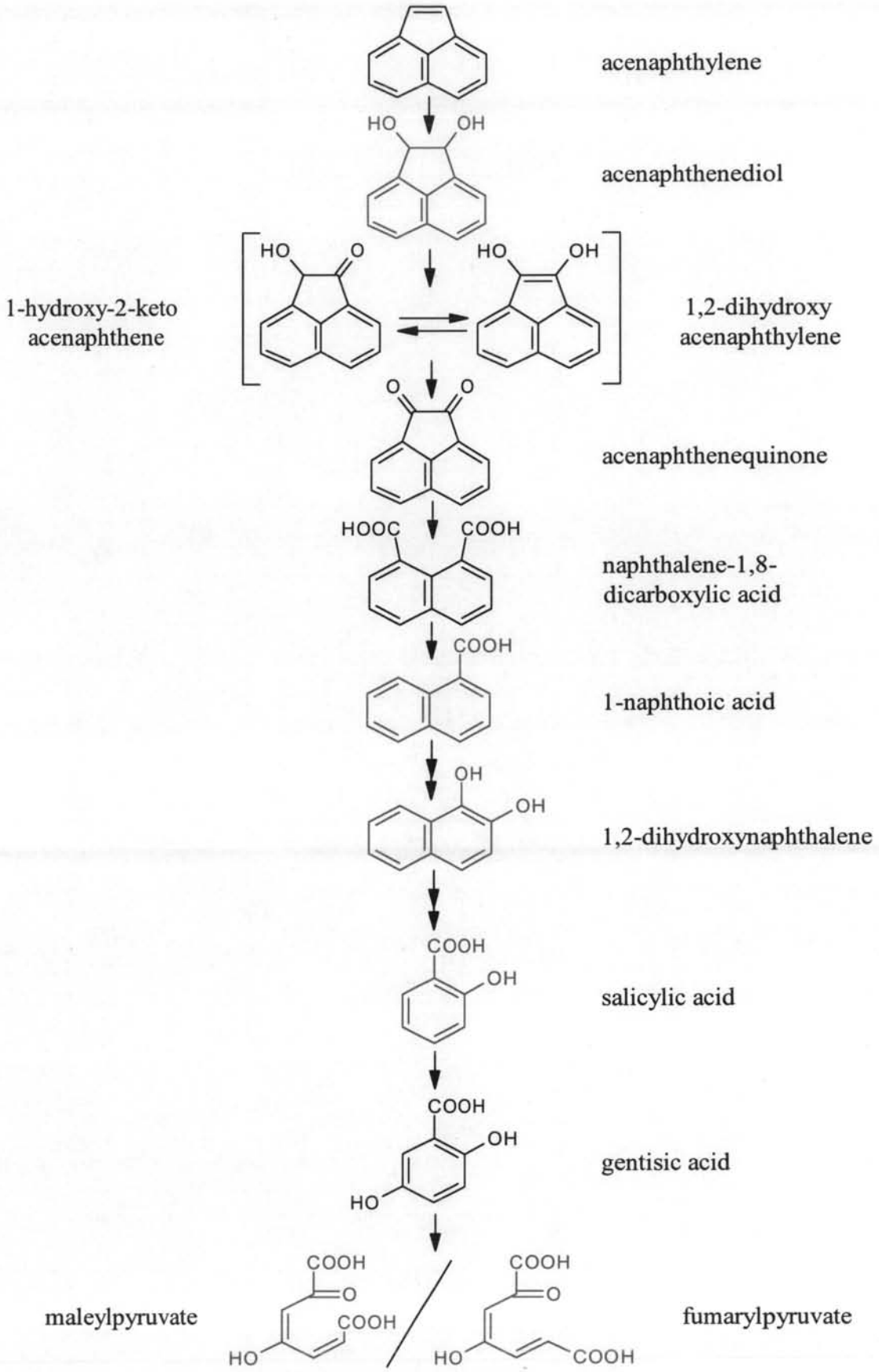

Fig. 4.32 Proposed acenaphthylene catabolic pathway in *Rhizobium* sp. CU-A1

4.2 Characterization of acenaphthylene dioxygenase from *Rhizobium* sp. CU-A1

4.2.1 Oxidation of acenaphthylene by the crude cell free extract and preliminary identification of the oxidizing products

The ability of the crude cell free extract, prepared from *Rhizobium* sp. CU-A1, grown in protocatechuic acid and induced by acenaphthylene as described in 3.7.1 to oxidize acenaphthylene was shown in Fig. 4.33. When acenaphthylene was incubated with crude cell extract, reduction of the substrate was observed. The remaining acenaphthylene was approximately 73.28% of the initial concentration after 3 h of incubation. In the control experiment without crude cell extract or with boiled cell free extract, the loss of acenaphthylene was not found after 3 h under the same condition.

Beside acenaphthylene, the crude cell free extract also had ability to oxidize acenaphthylene intermediates as shown in Fig. 4.34. The results revealed that after 3 h of incubation, the remaining acenaphthenequinone, naphthalene-1,8-dicarboxylic acid, 1-naphthoic acid, 1,2-dihydroxynaphthalene, salicylic acid and gentisic acid were approximately 76.42, 87.45, 82.28, 87.36, 87.43 and 78.32% of the initial concentration, respectively.

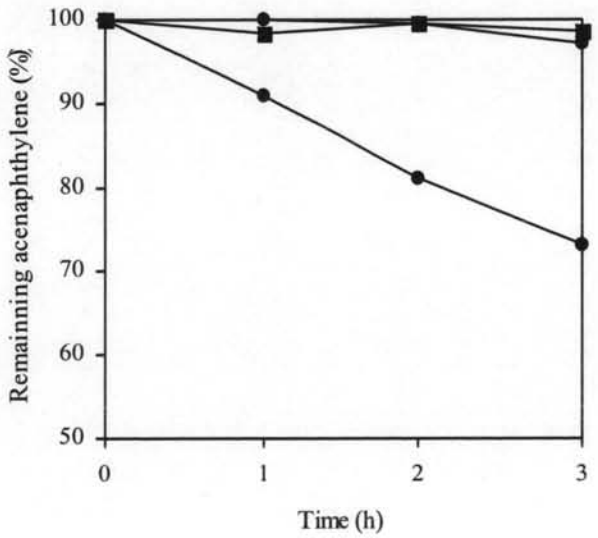

Fig. 4.33 Oxidation profiles of acenaphthylene by crude cell free extract (●), boiled cell free extract(◆) and without crude cell free extract (■)

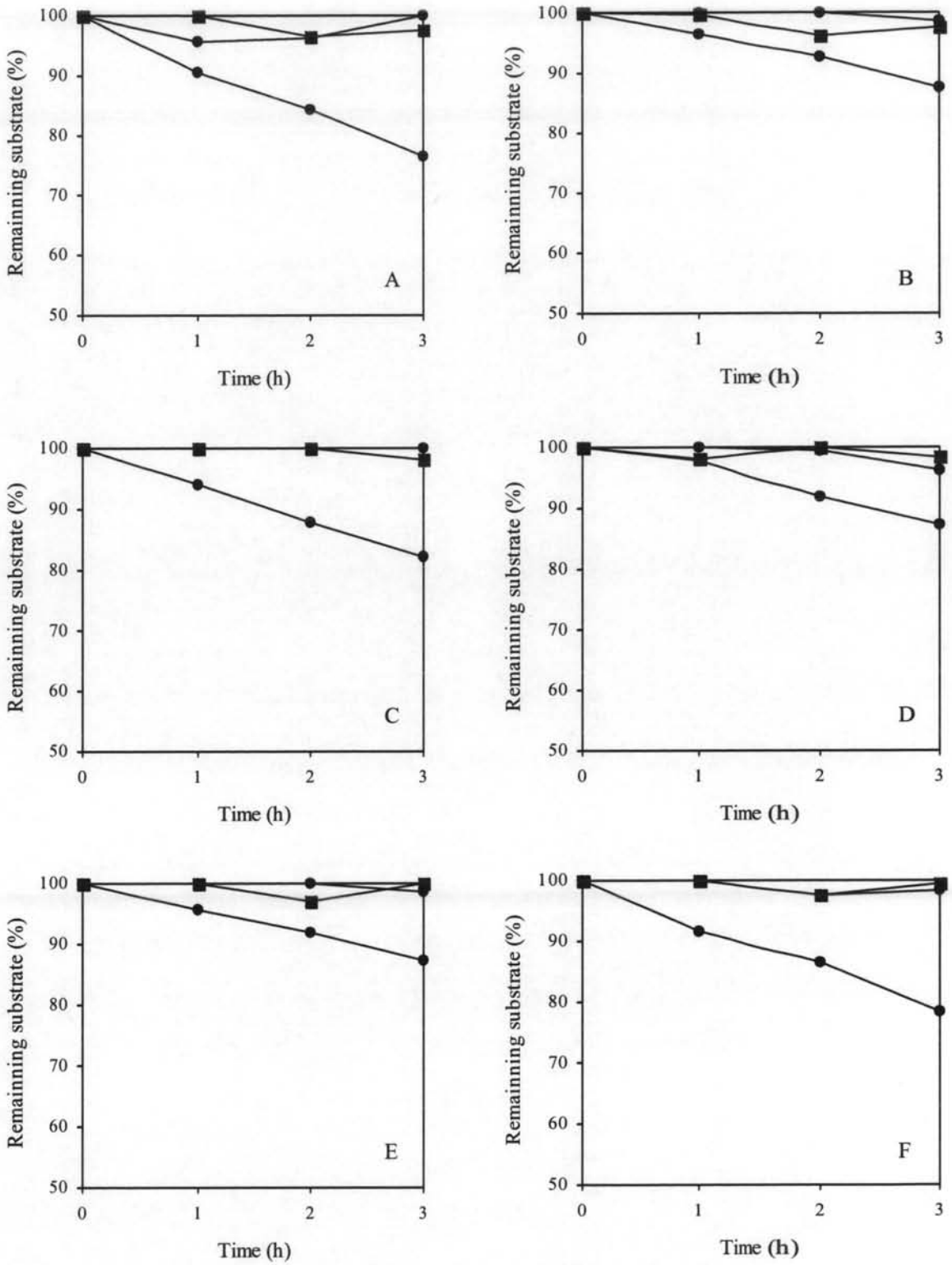

Fig. 4.34 Oxidation profiles of acenaphthenequinone (A), naphthalene-1,8-dicarboxylic acid (B), 1-naphthoic acid (C), 1,2-dihydroxynaphthalene (D), salicylic acid (E), and gentisic acid (F) by crude cell free extract (●), boiled cell free extract(◆) and without crude cell free extract (■)

The HPLC analysis of the oxidation products of acenaphthylene were shown in Fig. 4.35. After 2 h of incubation, several peaks, designated as compounds I, II, III, IV, V and VI were observed (Fig. 4.35, C). All of these compounds were preliminary purified by HPLC using ODS column as described in 3.3.4 and identified by gas chromatography-electron impact mass spectral analysis as described in 3.4. HPLC retention times and mass spectral characteristics of these compounds were shown in Table 4.3.

Table 4.3 HPLC retention times and electron impact mass spectral properties of the intermediates from acenaphthylene degradation by crude cell free extract of *Rhizobium* sp. CU-A1

Compounds	R_t (min)	m/z of fragment ions (% relative intensity)	Identification
I	12.26	182(M^+,17), 154(M^+-CO, 66), 126(100), 99(10), 98(12), 87(22), 75(11), 74(26), 63(15)	Acenaphthenequinone
II	18.22	198(M^+,66), 154(M^+-CO_2, 100), 127(10), 126(79), 99(8), 98(6), 87(7), 77(10), 76(11), 74(15), 63(21)	Naphthalene-1,8-dicarboxylic acid
III	4.04	154 (M^+,60), 136 (H^+-H_2O, 100), 108(17), 80(22)	2,5-Dihydroxybenzoic acid (Gentisic acid)
IV	16.91	172(M^+,100), 155(M^+-OH, 53), 127(M^+-COOH, 72), 115(18), 101(8), 98(5), 89(4), 87(6), 86(5), 77(12), 75(11), 74(12), 63(14)	1-Naphthoic acid
V	19.74	138(M^+,15), 121(10), 120(M^+-H_2O, 12), 92(M^+-HCOOH, 81), 81(11), 66(16), 65(48), 64(71), 63(100), 62(36), 61(13), 53(53)	2-Hydroxybenzoic acid (Salicylic acid)
VI	23.56	160(M+, 100), 131(49), 114(12), 103(7), 77(12), 51(12)	1,2-Dihydroxy naphthalene

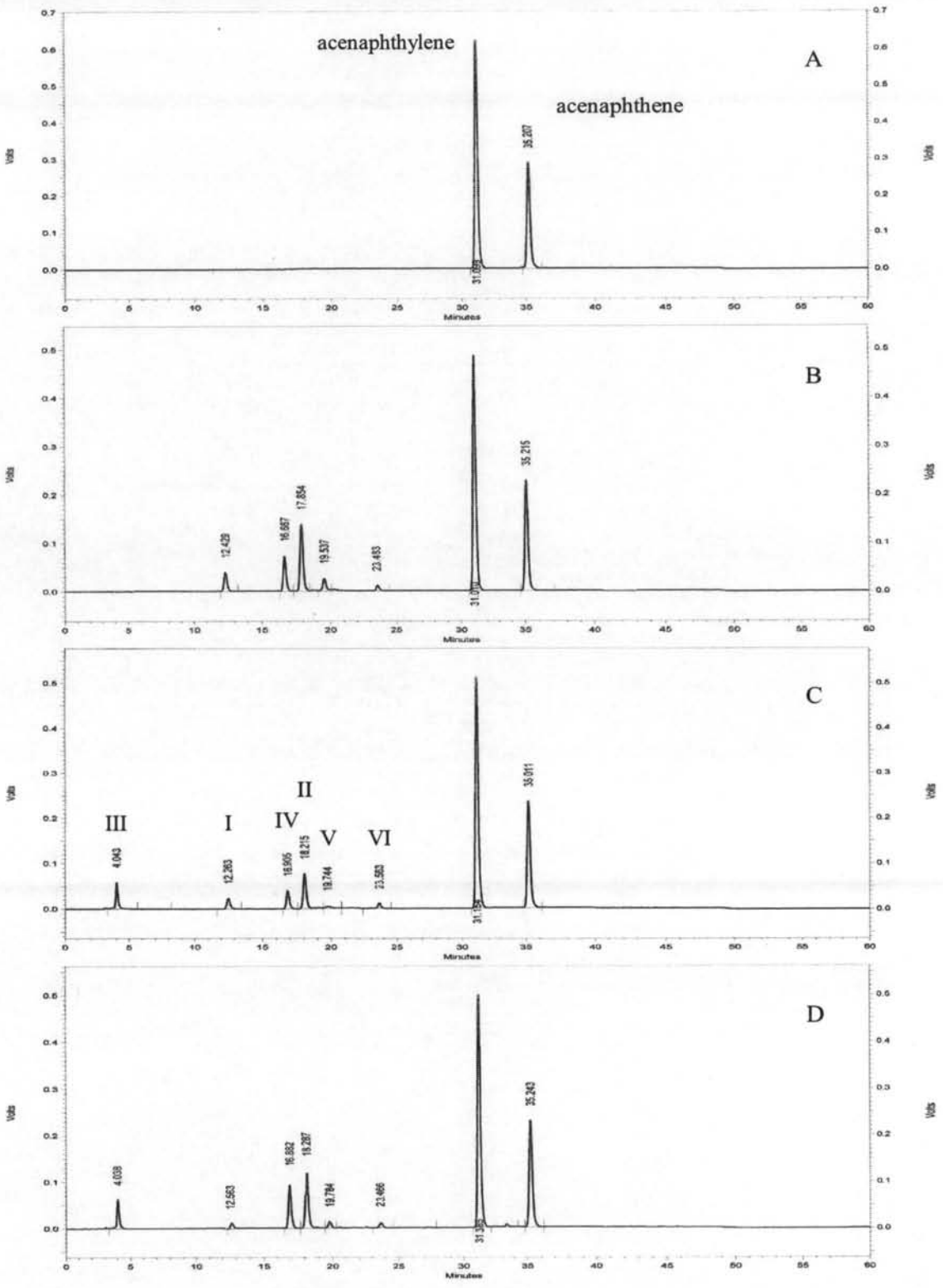

Fig. 4.35 HPLC elution profiles of acenaphthylene oxidation products produced from the reaction with the crude cell free extract from *Rhizobium* sp. CU-A1 when incubated at 35°C for 0 h (A), 1 h (B), 2 h (C), and 3 h (D). I to VI are oxidation products after 2 h of incubation.

Mass spectra of compounds I, II, III, IV, V and VI showed similarity to those of the authentic compounds and therefore identified as acenaphthenequinone, naphthalene-1,8-dicarboxylic acid, gentisic acid, 1-naphthoic acid, salicylic acid and 1,2-dihydroxynaphthalene, respectively.

The crude cell extract catalyzed the oxidation of not only acenaphthylene but also six other aromatic compounds tested, the intermediates from the degradation of acenaphthylene, to the corresponding products as summarized in Table 4.4. These products were identified by comparing their HPLC retention times with those of the authentics as well as cochromatography with the authentic compounds.

Table 4.4 Catalytic activity of the crude cell free extract on the intermediates from acenaphthylene degradation. Products formed were identified by cochromatography with authentic compounds.

Substrates	%remaining substrate	Products formed
Acenaphthenequinone	76.42	Naphthalene-1,8-dicarboxylic acid 1-Naphthoic acid 1,2-Dihydroxynaphthalene Salicylic acid Gentisic acid
Naphthalene-1,8-dicarboxylic acid	87.45	1-Naphthoic acid 1,2-Dihydroxynaphthalene Salicylic acid Gentisic acid
1-Naphthoic acid	82.23	1,2-Dihydroxynaphthalene Salicylic acid Gentisic acid
1,2-Dihydroxynaphthalene	87.36	Salicylic acid Gentisic acid
Salicylic acid	87.43	Gentisic acid
Gentisic acid	78.32	Not detected

4.2.2 Effect of N-ethylmaleimide (NEM) on the enzyme activity

Most dioxygenase enzymes are generally highly sensitive to oxygen and completely inactivated in the presence of NEM indicating the enzymes might have thiol groups at catalytic site. Due to the extremely unstable of the acenaphthylene dioxygenase activity in the crude cell extract during preliminary study, the catalytic site of this enzyme might consist of the thiol groups.

The effect of N-ethylmaleimide on the crude cell free extract of *Rhizobium* sp. CU-A1 was carried out as described in 3.7.1.1. The results shown in Fig. 4.36 revealed that NEM inactivated the acenaphthylene dioxygenase activity within 15 min of incubation at 4°C. With 0.2 mM NEM, 82% of its activity was lost, and its activity was almost completely lost at 0.4 mM NEM.

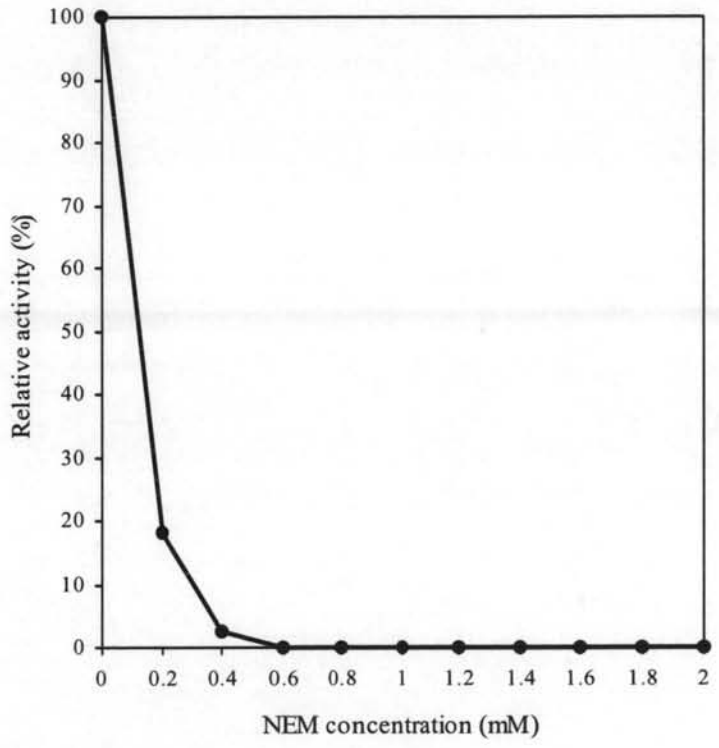

Fig. 4.36 Effect of N-ethylmaleimide, a sulfhydryl agent, on the enzyme activity using acenaphthylene as a substrate

4.2.3 Effect of dithiothreitol (DTT)

Effect of DTT, a thiol reducing agent, to restore the activity of enzyme after the incubation with NEM was determined. The cell free extract was pre-incubated with NEM at the final concentration of 0.2 mM at 4°C for 15 min and DTT was then introduced to the extract to the final concentration of 0.5 to 5 mM and incubated at 4°C for another 15 min. The results shown in Fig. 4.37 revealed that DTT could restore activity of the enzyme exposed to NEM. Treatment of the enzyme with 0.2 mM NEM caused nearly complete loss of activity while subsequent treatment with 1 mM DTT restored 76% of the activity.

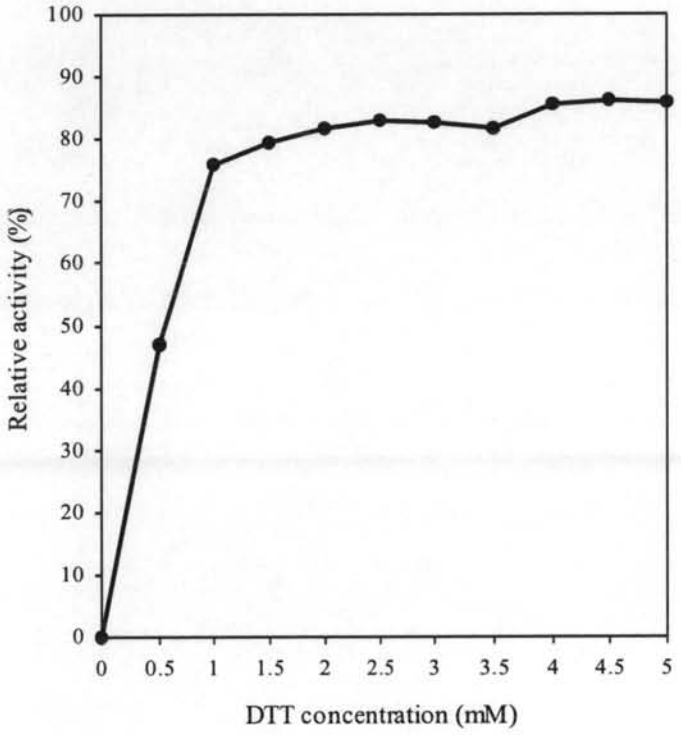

Fig. 4.37 Effect of dithiothreitol to restore an enzyme activity after treatment with 0.2 mM N-ethylmaleimide

The inactivation of the dioxygenase enzyme was generally due to oxidation by oxygen in the atmosphere. To determine whether DTT can prevent the inactivation of the enzyme, the cell free extract from 3.7.1 was added with DTT at a final concentration of 0.5 to 2 mM and incubated in the atmosphere at 4°C for 48 h.

The samples were collected at every 6 h and determined for their remaining activities as described in 3.7.1.2. The results shown in Fig. 4.38 indicated that in the absence of DTT, the enzyme completely lost its activity after 48 h of incubation whereas in the presence of 1 mM more than 80% and 60% of the original activity were still remained after 30 h and 48 h of incubation, respectively.

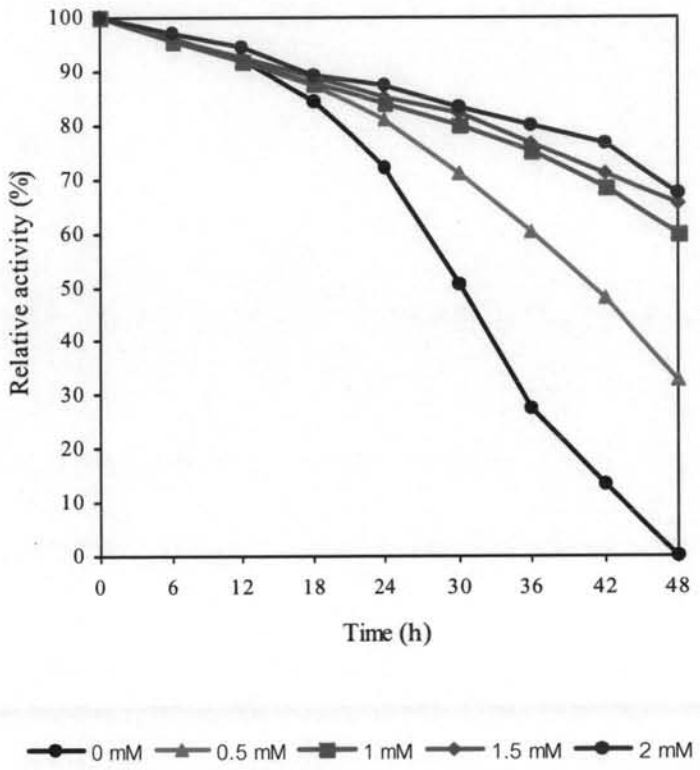

Fig. 4.38 Effect of dithiothreitol concentrations on stabilization of the enzyme activity

According to these results, thiol group, an oxygen labile group, may play an important role in the catalytic activity of this enzyme. DTT, a thiol reducer, could be used to stabilize the enzyme activity. In order to obtain the suitable concentration of DTT to be used as a stabilizer for this enzyme, various concentrations ranging from 0.2 to 2 mM of DTT were added to the reaction mixture as described in 3.7.1.2. The result showed that 1 mM DTT increased the activity of enzyme to 136% (Fig. 4.39). Therefore, DTT was routinely added to the enzyme buffer at the final concentration of 1 mM.

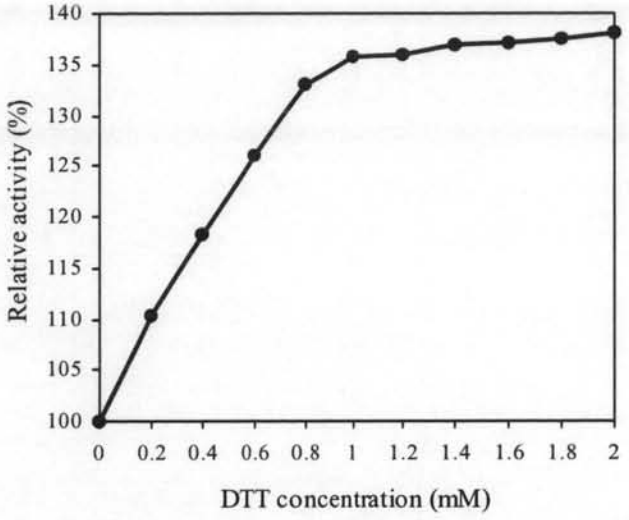

Fig. 4.39 Effect of dithiothreitol concentrations on the enzyme activity

4.2.4 Preliminary study for optimum pH, temperature and co-factors requirement for the enzyme activity

Crude cell free extract was prepared from the frozen cell of *Rhizobium* sp. CU-A1 in 50 mM sodium phosphate buffer pH 7.5 containing 1 mM DTT. Optimization of the assay conditions for acenaphthylene oxidizing activity in the cell free extract was determined according to the methods 3.5.2.1 to 3.5.2.3. The pH and temperature optima for acenaphthylene conversion were shown in Fig. 4.40. The maximum activity of the enzyme was achieved at 35°C and pH 7.5 in 50 mM phosphate buffer.

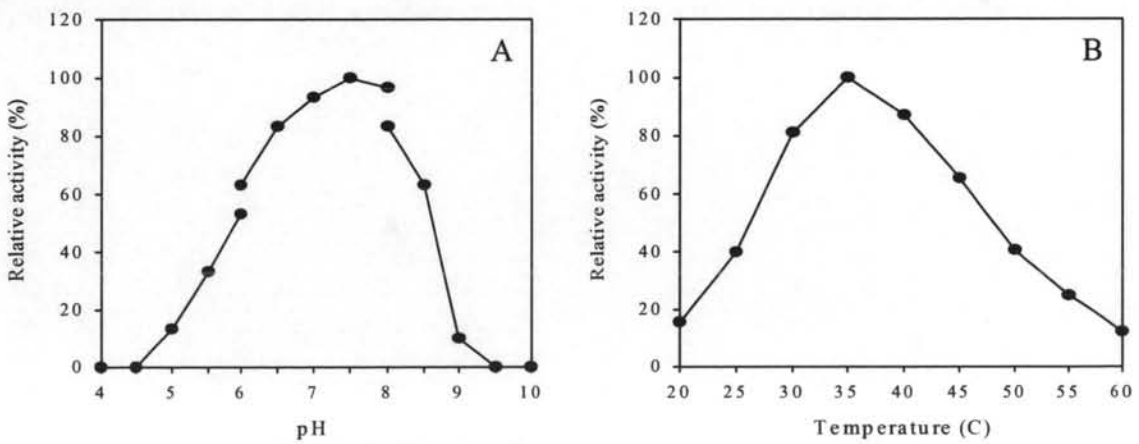

Fig. 4.40 Effect of pH [A] and termperature [B] on the enzyme activity in the cell free extract

Acenaphthylene was found to be oxidized by the cell free extract in the absence of any supplement. However, stimulation of the enzyme activity was observed in the presence of reduced pyridine nucleotides, flavin nucleotides and metal ion. Table 4.5 summarizes the effect of NADH, NADPH, FAD, FMN and Fe^{2+} on the enzyme activity. The enzyme activity was significantly stimulated by NADH and NADPH, in which NADH was more effective than NADPH. Fe^{2+} also increased the enzyme activity in the presence of NADH. Furthermore, in addition of NADH and Fe^{2+}, supplementation with either FAD or FMN also increased the enzyme activity. The reaction mixture containing 50mM sodium phosphate buffer pH 7.5, 2 mM of NADH, 2 μM of FAD, 200 μM of $FeSO_4$ and 10 mM of acenaphthylene resulted in the highest specific activity of 0.68 U/mg. Therefore, the acenaphthylene oxidizing activity was routinely determined under this conditions.

Table 4.5 Effect of various supplements on acenaphthylene dioxygenase activity in the cell extract

Presence of the following components						Specific Activity (U/mg)
Cell free extract	NADH	NADPH	Fe^{2+}	FAD	FMN	
+	-	-	-	-	-	0.32 ± 0.01
+	+	-	-	-	-	0.57 ± 0.03
+	-	+	-	-	-	0.43 ± 0.01
+	+	-	+	-	-	0.62 ± 0.02
+	+	-	+	+	-	0.68 ± 0.01
+	+	-	+	-	+	0.64 ± 0.01
-	+	-	+	+	-	0.02 ± 0.02

Final concentration were as follows: cell free extract, 0.38 mg protein/ml; acenaphthylene, 10 mM: NADH or NADPH, 2 mM; $FeSO_4 7H_2O$, 200 μM; FAD or FMN, 2 μM. Assay conditions were as follows: 50 mM phosphate buffer containing 1 mM DTT pH 7.5; temperature 35 °C.

In addition, it was observed that the conversion of acenaphthylene as a function of protein concentration in the cell free extract was not linear (Fig. 4.41) suggesting that this enzyme may be a multi-component enzyme system (Ensley and Gibson, 1983).

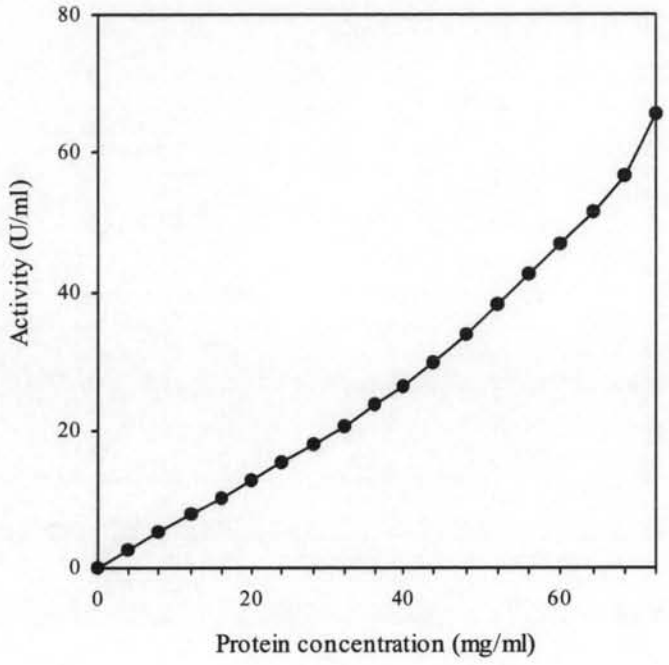

Fig. 4.41 Dependence of the enzyme activity on protein concentration in the crude cell free extract

4.2.5 Effect of NaCl or KCl on enzyme activity

Ion exchange chromatography is one of the most effective techniques for protein purification. However, it requires elution of the protein by salt containing solution. Therefore, the effect of salt concentration on the acenaphthylene oxidizing activity was determined by adding NaCl or KCl to the reaction mixture in a various final concentration. The addition of either NaCl or KCl affected the enzyme activity as shown in Fig. 4.42. The activity was reduced to 84 and 66% in the presence of 500 mM NaCl or KCl, respectively. The result suggested that KCl had higher inhibition effect than NaCl therefore, NaCl was selected to use in the further enzyme purification step.

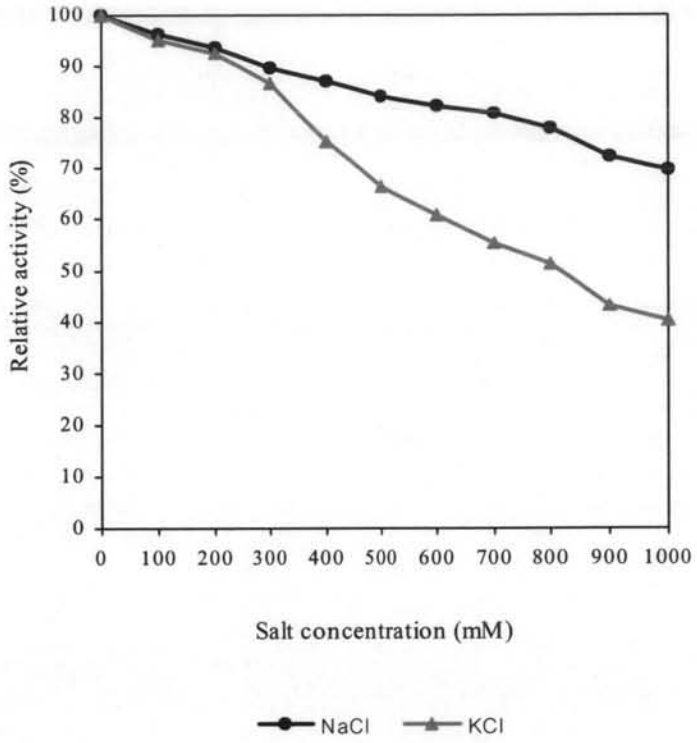

Fig. 4.42 Effect of NaCl and KCl on acenaphthylene oxidizing activity of the crude cell free extract

4.2.6 Ammonium sulfate fractionation

Fractionation of acenaphthylene dioxygenase activity from the crude cell free extract by ammonium sulfate precipitation was preliminary studied. First, the salt was added slowly to the extract while mixing gently to 40% salt saturation. After stirring for 1 h, precipitate was separated by centrifugation. The pellets were washed twice with equivalent saturated salt solution (40%) and then resuspended in phosphate buffer. The supernatant was then subsequently saturated to 60, 80, 100% salt concentration. The fractions were then desalted by dialysis in phosphate buffer and assayed for the enzyme activity. According to the results shown in Table 4.6, high amount of protein was precipitated in 0-40% salt saturated fraction. However, the enzyme activity was only found in significant level in the fraction of 40-60% salt saturation. The specific activity of the enzyme in this fraction was 4.64 U/mg with 34.67% recovery. Therefore, for the purification of acenaphthylene dioxygenase, 40-60% ammonium sulfate saturation was chosen to precipitate this enzyme.

Table 4.6 Fractionation of acenaphthylene dioxygenase by ammonium sulfate precipitation

Salt fraction (%)	Volume (ml)	Protein (mg/ml)	Total Protein (mg)	Activity (U/ml)	Total activity (U)	Specific activity (U/mg)	Yield
Crude enzyme	5.0	16.24	81.20	10.5	52.50	0.65	100
0-40	2.1	15.02	31.54	1.1	2.31	0.07	4.4
40-60	2.0	1.96	3.92	9.1	18.20	4.64	34.67
60-80	2.2	1.24	2.73	0.2	4.40	0.16	8.38
80-100	4.8	0.94	4.51	1.6	7.68	1.70	14.63

4.2.7 Enzyme purification

4.2.7.1 Ammonium sulfate precipitation

In order to obtain large amount of bacterial cell, *Rhizobium* sp. CU-A1 was cultivated in mineral medium supplemented with protocatechuic acid and induced with acenaphthylene in a total volume of 40 L. The crude cell free extract was prepared according to the method 3.7.1. The acenaphthylene oxidizing activity was determined as described in 3.5.3. The total activity, protein concentration and specific activity of the crude extract were 3,090.0 units, 5,139.0 mg protein and 0.60 U/mg, respectively (Table 4.10). Acenaphthylene dioxygenase was fractionated by 40-60% saturation of ammonium sulfate. The protein precipitate was resuspended in phosphate buffer pH 7.5, dialyzed against the same buffer and the activity was determined. The specific activity was 3.66 U/mg with the purity increased to about 6 folds comparing with that of the crude cell free extract with the recovery yield of 49.71%. This enzyme fraction was further purified by column chromatography techniques.

4.2.7.2 Q Sepharose fast flow column

The 40-60% salt saturated fraction with the total protein of 419.2 mg from step 4.2.7.1 was applied to Q Sepharose fast flow, an anion exchanger column. Unbound proteins were eluted by washing with the starting buffer. The result shown in Fig. 4.43 indicated that the acenaphthylene dioxygenase was bound to the column and then eluted from the column with 0.45-0.60 M NaCl while running a linear gradient from 0 to 1.0 M NaCl in phosphate buffer containing 1 mM DTT. The fractions with activity were pooled, concentrated and desalted by ultrafiltration for the following purification steps. From this step, the purity was increased to about 26 folds with recovery yield of about 21% as shown in Table 4.10.

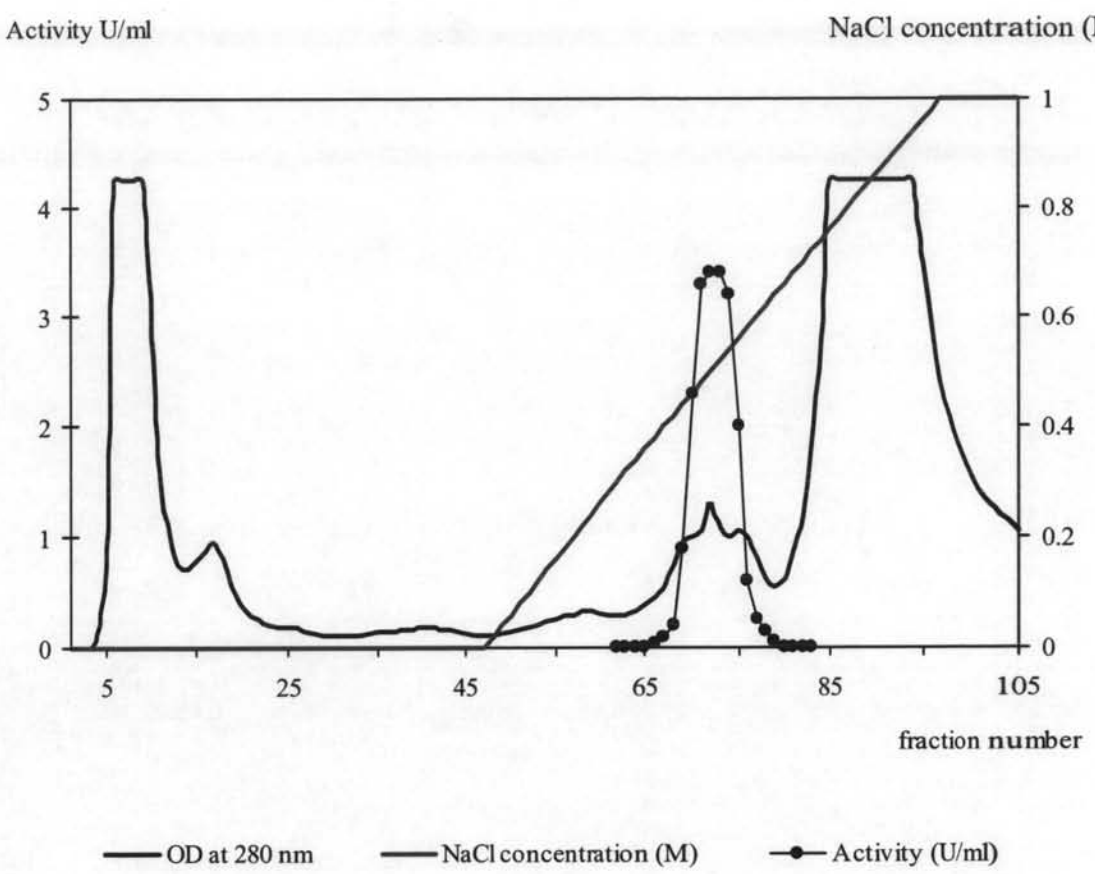

Fig. 4.43 Anion exchange chromatography using Q Sepharose fast flow column of 40-60% salt saturated fraction. Protein as determined by optical density at 280 nm

4.2.7.3 Superdex G200 column

The enzyme with total protein of 41.0 mg from the anion exchange chromatography (4.2.7.2) was loaded onto a hiload Superdex G200 preparative gel filtration column, subsequently eluted with 50 mM sodium phosphate buffer pH 7.5 containing 1 mM DTT. Acenaphthylene dioxygenase activity was not detected in any of the single fractions eluted from Superdex G200 column. From the earlier result using crude cell free extract suggested that the enzyme may be a multi-component enzyme system (Fig. 4.41), pooled different fractions were then assayed in various combinations. It was found that three fractions were needed to restore the enzyme activity : designated as component A (brown) eluted between 207-234 ml of elution volume, B (yellow) eluted between 240-261 ml of elution volume, C (light brown) eluted between 279-303 ml of elution volume. The resolution of this enzyme components were shown in Fig. 4.44 and Table 4.7.

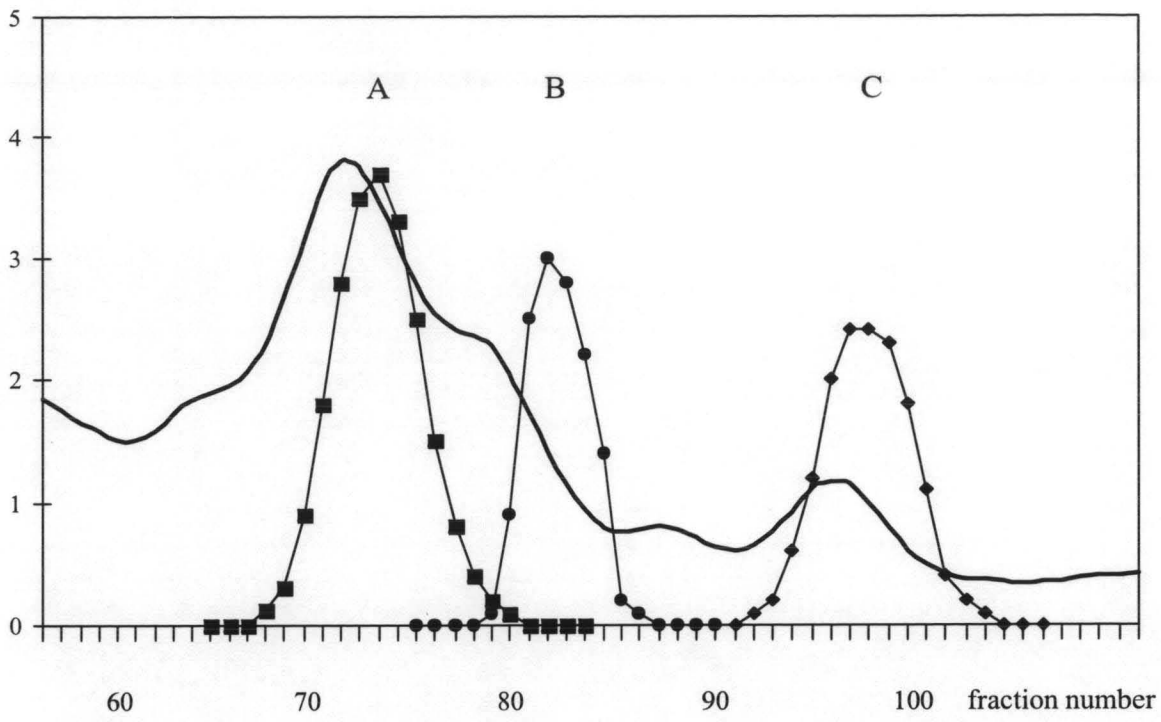

Fig. 4.44 Superdex G200 chromatography of acenaphthylene oxidizing protein from ion exchange chromatography represents resolution of the enzyme into three protein components, A (brown), B (yellow) and C (light brown). Protein was determined by optical density at 280 nm and enzyme activity was assayed as described in 3.5.3 using 100 µl of the fraction to be determined in the presence of 25 µg/ml each of the other two components.

Table 4.7 Resolution of acenaphthylene dioxygenase into three protein components by gel filtration on Superdex G200

Component	Volume (ml)	Protein (mg/ml)	Total Protein (mg)
A (brown)	4.5	2.55	11.45
B (yellow)	4.7	0.89	4.14
C (light brown)	4.5	0.51	2.30

The requirement of these three protein components for the enzyme activity was tested by determining the enzyme activity of each component or of the reconstitution of two or three components in various combinations. The result shown in Table 4.8 indicated that the enzyme system absolutely required the presence of all three components for its full activity. In addition, these components were also reconstituted in various ratios (w/w/w) in order to obtain the optimal enzyme activity. From the result shown in Table 4.8, combination of A, B and C in the ratio 2:1:1 resulted in the highest activity and specific activity. Therefore, this ratio was used to determine the activity for any further purification steps.

Table 4.8 Reconstitution of components A, B and C for acenaphthylene dioxygenase activity

Ratio A:B:C (w)	Protein (mg/ml)	Activity (U/ml)	Specific activity (U/mg)
1:0:0	0.24	0	0
0:1:0	0.27	0	0
0:0:1	0.26	0	0
1:1:0	0.49	0	0
1:0:1	0.51	0.7 ± 0.01	1.37
0:1:1	0.52	0	0
1:1:1	0.75	11.2 ± 0.04	14.93
1:2:1	1.02	12.0 ± 0.02	11.71
1:1:2	1.11	12.8 ± 0.02	11.64
1:2:2	1.25	13.3 ± 0.03	10.64
2:1:1	1.08	16.4 ± 0.01	15.26
2:2:1	1.26	16.5 ± 0.02	13.20
2:1:2	1.23	16.4 ± 0.01	13.39

The oxidation product of acenaphthylene by partially purified component A after gel filtration step in the presence of components B and C was identified by GC-MS. The product gave a mass spectrum as shown in Fig. 4.45 identical to that of acenaphthenediol, found in the instrumental library (Wiley Mass Spectra database). Therefore, this product was identified as acenaphthenediol. The result suggested that reconstituted partially purified components A, B and C after gel filtration did not contain dehydrogenase activity, which interfered the identification of the initial reaction product when the cell free extract was used.

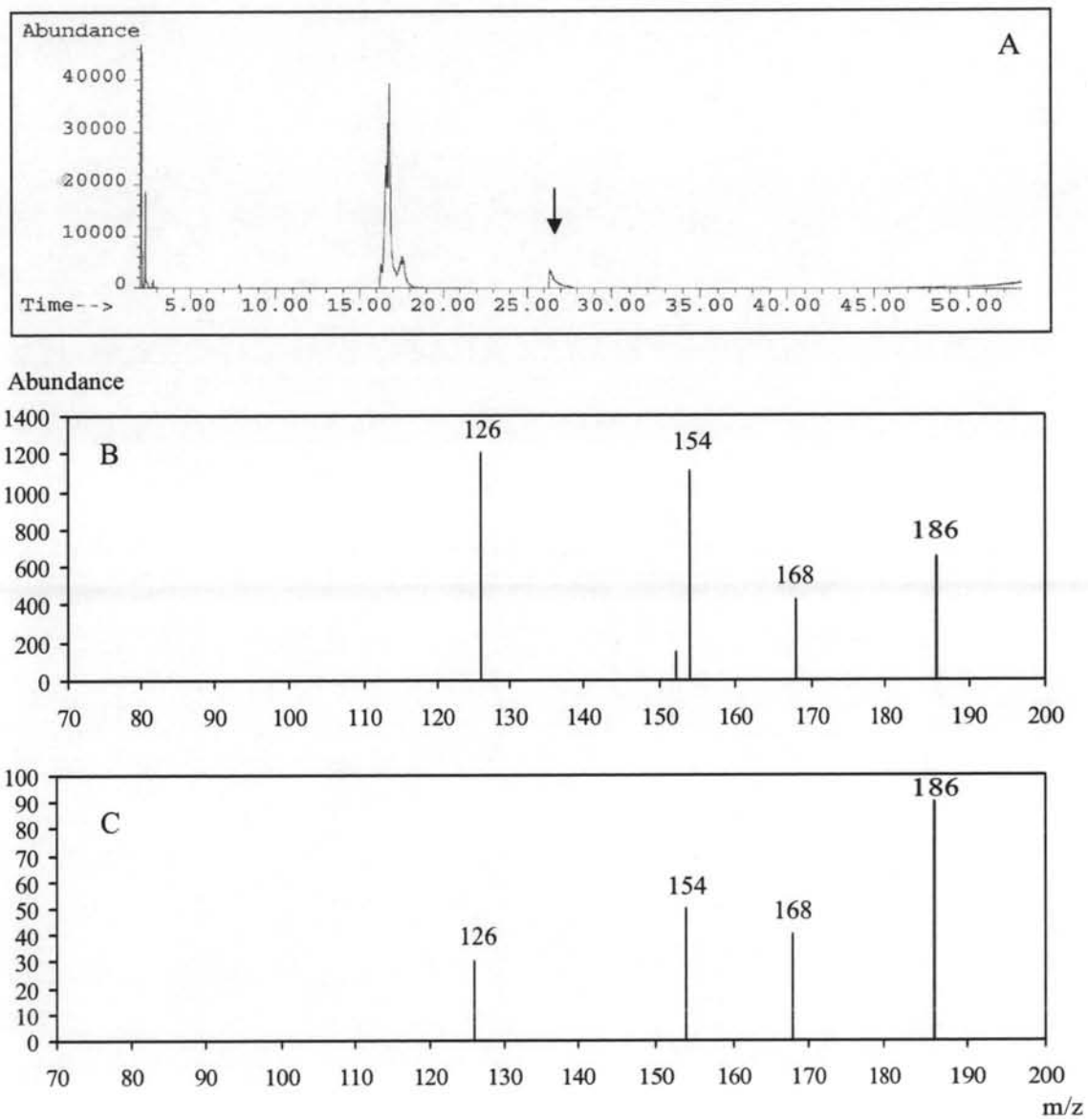

Fig. 4.45 GC chromatogram (A) and mass spectrum (B) of the oxidation product (indicated by an arrow in A) of acenaphthylene compared with the mass spectrum of 1,2-acenaphthenediol (C)

According to the results in Table 4.5, the stimulation of enzyme activity by flavin nucleotides suggested that a flavoprotein may be involved in the acenaphthylene oxidation. Thus, all three components were assayed for cytochrome *c* reductase activity as described in 3.5.4 as this enzyme contains flavoprotein as its prosthetic group (Haigler and Gibson, 1990) and furthermore as mentioned early, several ferredoxin reductases also posses cytochrome *c* reductase activity (Ensley and Gibson, 1983). The results summarized in Table 4.9 indicated that only component B, a yellow solution, not A or C strongly reduced cytochrome *c* in the presence of NADH and FAD with the rate 0.28 μmole/min/mg. The activity was stimulated by the addition of brown solution, component C to 1.92 μmole/min/mg. This activity was not observed in the reaction mixture without the addition of FAD suggested that most FAD content in the protein preparation might be lost during the purification. For acenaphthylene oxidation, it is presumably component B would catalyze the transfer of electrons from NADH to component C and further to acenaphthylene concomitant with the incorporation of two oxygen atoms into its molecule which is catalyzed by component A, presumably a terminal oxidase. This speculation was proven in the later experiments. The purification of acenaphthylene dioxygenase was summarized in Table 4.10.

Table 4.9 Cytochrome *c* reductase activity of components A, B and C

Presence of the following components						Cytochrome *c* reductase activity (μmole/min/mg)
A	B	C	NADH	FAD	FMN	
+	-	-	+	+	-	0.06 ± 0.02
-	+	-	+	+	-	0.28 ± 0.01
-	-	+	+	+	-	0.05 ± 0.01
+	+	-	+	+	-	0.39 ± 0.04
+	-	+	+	+	-	0.09 ± 0.02
-	+	+	+	+	-	1.92 ± 0.02
-	+	+	+	-	+	1.47 ± 0.03
-	+	+	+	-	-	0.02 ± 0.01

Final concentration were as follows: each protein component, 50 μg; cytochrome *c*, 87 nmole; NADH, 0.3 mM; FAD and FMN, 1 μM. Assay conditions

were as follows: 50 mM Tris-HCl buffer pH 7.5; temperature 25 °C; molar extinction coefficient, 21,000 M^{-1} cm^{-1}.

Table 4.10 Summary of the purification of acenaphthylene dioxygenase

Step	Volume (ml)	Protein (mg)	Activity (U)	Specific activity (U/mg)	Yield	Fold
Crude enzyme	300.0	5139.0	3090.0	0.60	100	1
40-60% $(NH_4)_2SO_4$ precipitation	80.0	419.2	1536.0	3.66	49.71	6.1
Q Sepharose	36.0	41.0	651.6	15.88	21.09	26.47
Superdex G200*	4.5	11.5	307.8	26.77	9.96	44.62

* The components of acenaphthylene dioxygenase enzyme complex were separated at this point of the purification procedure. The values represent only for the component A. The activity was assayed in the presence of components B and C described in 3.3.4.1.

4.2.8 Purification of components A, B and C

4.2.8.1 Component A purification

4.2.8.1.1 Hydroxyapatite column

Hydroxyapatite, a calcium phosphate complex which separates proteins due to the differences in non-specific adsorption to this medium, was used for further purification of component A. The concentrated component A with the total protein of 11.5 mg and total activity of 307.8 U from 4.2.7.3 was applied to a hydroxyapatite column preequilibrated with 20 mM sodium phosphate buffer pH 7.5 containing 1 mM DTT. After the column was eluted with a linear gradient of 20-200 mM sodium phosphate buffer, pH 7.5 at a flow rate of 1 ml/min. Component A was eluted from the column between 80-140 mM sodium phosphate. Three protein peaks

with relatively low resolution were obtaind as shown in Fig. 4.46. However, component A activity was found in the second peak and its purity was increased to approximately 1.28-fold with 69.82% recovery compared with that of the fraction from gel filtration step as summarized in Table 4.11. Pooled active fractions were dialyzed, concentrated by ultrafiltration and subjected for further purification.

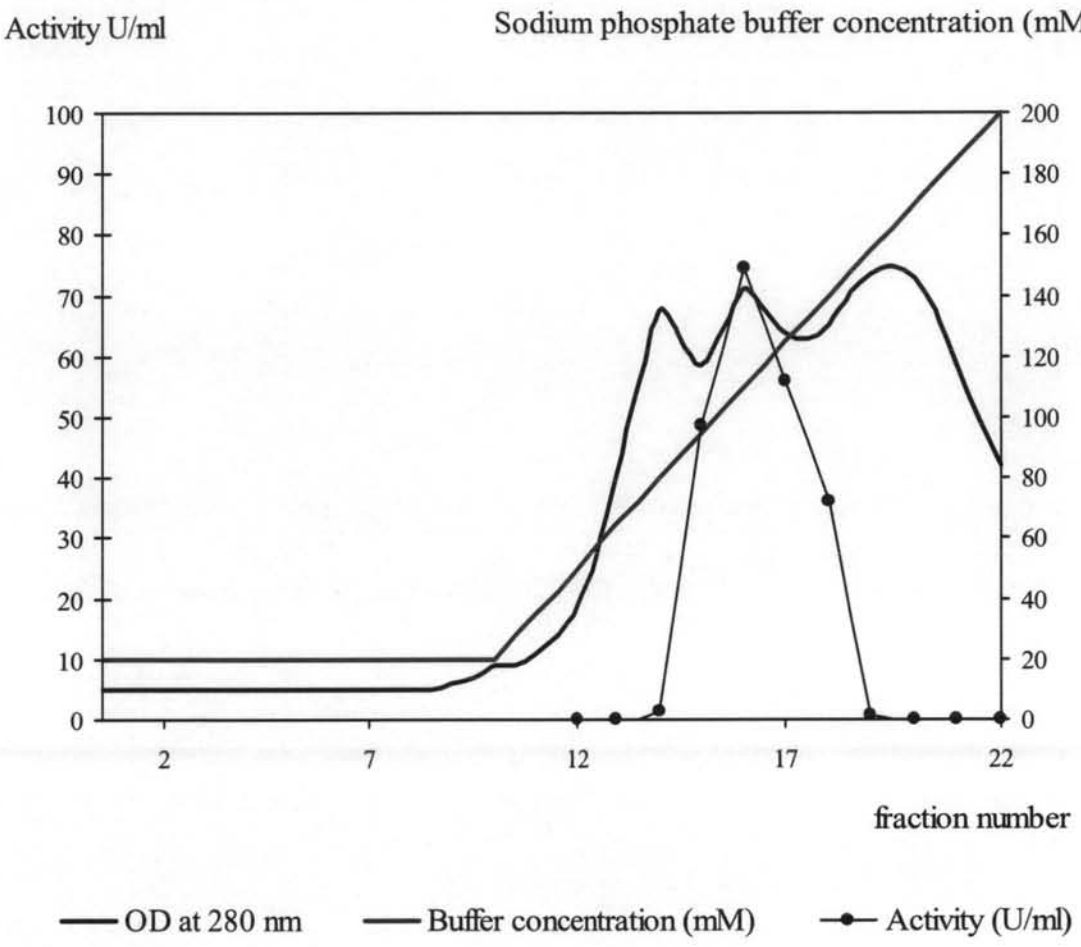

Fig. 4.46 Hydroxyapatite chromatography of the component A

4.2.8.2.2 Phenyl Sepharose column

Hydrophobic interaction which separates proteins due to their hydrophobic properties, was chosen for further purification of component A after hydroxyapatite step by using phenyl Sepharose column. The active fraction from hydroxyapatite column was adjusted to 1.0 M salt concentration by adding

ammonium sulfate powder and applied onto a phenyl Sepharose column previously equilibrated with 50 mM sodium phosphate buffer pH 7.5 containing 1.0 M ammonium sulfate. The majority of proteins with no acenaphthylene dioxygenase activity did not bind to the column and were eluted during washing. After washing, the bound proteins were eluted with a linear 1.0-0 M-descending gradient of ammonium sulfate in the same buffer. Fractions possessing activity eluted between 0.6-0.8 M salt concentration as shown in Fig. 4.47 were pooled, dialyzed and concentrated by ultrafiltration. The total activity, specific activity, purification fold and recovery yield of component A after this step were 166.7 U, 36.23 U/mg protein, 1.35 and 54.16%, respectively, as shown in Table 4.11.

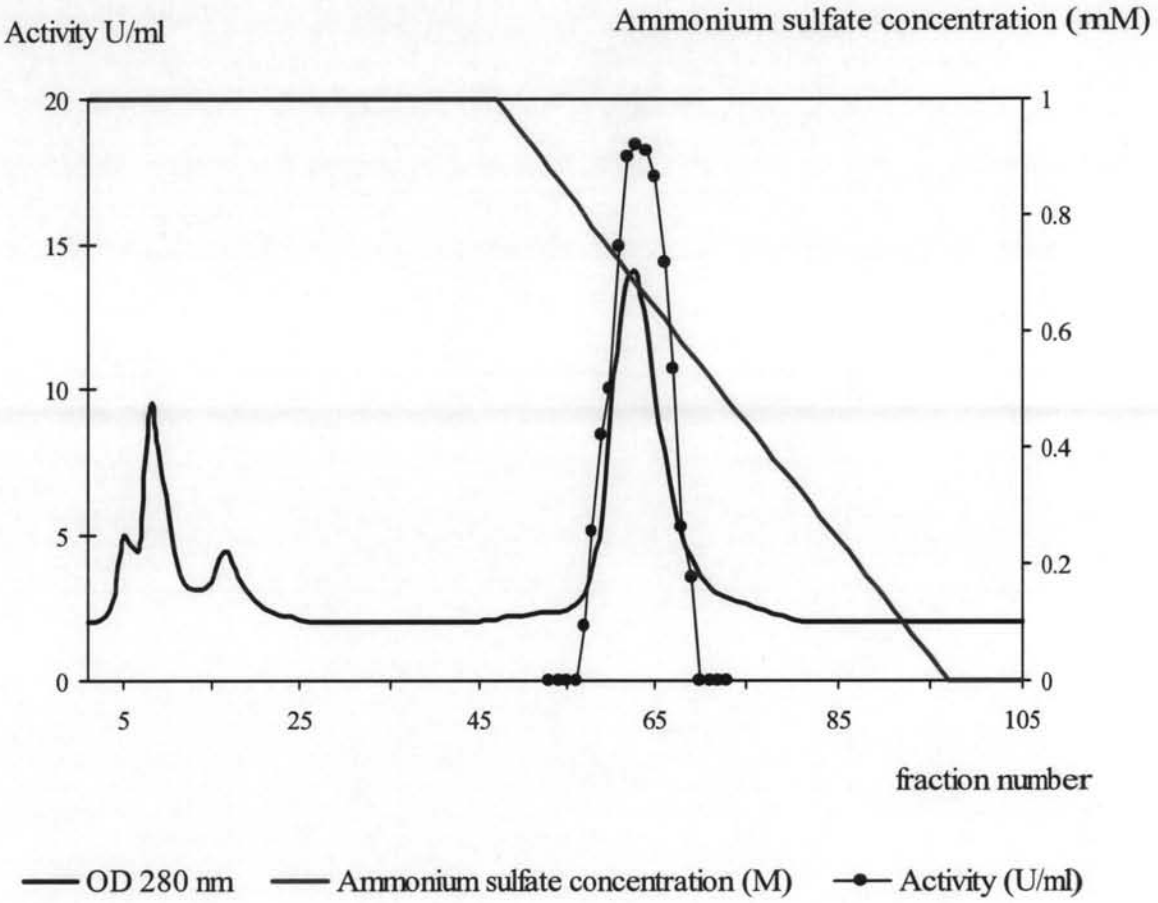

Fig. 4.47 Chromatography of component A on phenyl Sepharose column

Table 4.11. Purification table of component A

Step	Volume (ml)	Protein (mg)	Activity (U)	Specific activity (U/mg)	Yield	Fold
Gel filtration	4.5	11.5	307.8	26.77	100	1
Hydroxyapatite	4.0	6.3	214.9	34.12	69.82	1.28
Hydrophobic interaction	4.0	4.6	166.7	36.23	54.16	1.35

4.2.8.2 Component B purification

Component B with the total protein and total activity of 4.14 mg and 1.31 U, respectively, was loaded onto Blue Sepharose column, suitable for purification of NAD^+ or $NADP^+$ dependent enzyme as described in 3.7.7. After washing the unbound proteins with 50 mM sodium phosphate buffer pH 7.5, the column was eluted with a linear gradient of 0-2 M NaCl in the same buffer for 60 min and then with 2 M NaCl for another 10 min at the flow rate of 1 ml/min. The activity of component B was measured by detecting the cytochrome *c* reductase activity as described in 3.5.4. The result shown in Fig. 4.48 indicated that component B was eluted from the column between 0.80-1.20 M NaCl. These fractions were pooled, dialyzed, concentrated, determined for cytochrome *c* reductase activity and kept at -20°C for further study. The total activity and its specific activity were 1.12 U and 0.95 U/mg protein, respectively. Component B was purified to 3-fold purity with the yield of 85.5%, as shown in Table 4.12.

Table 4.12 Purification table of component B from gel filtration

Fraction	Volume (ml)	Protein (mg/ml)	Total protein (mg)	Activity (U/ml)	Total activity (U)	Specific activity (U/mg)	Yield	Fold
Gel filtration	4.7	0.89	4.14	0.29	1.31	0.31	100	1
Blue Sepharose	2.0	0.59	1.18	0.56	1.12	0.95	85.5	3.07

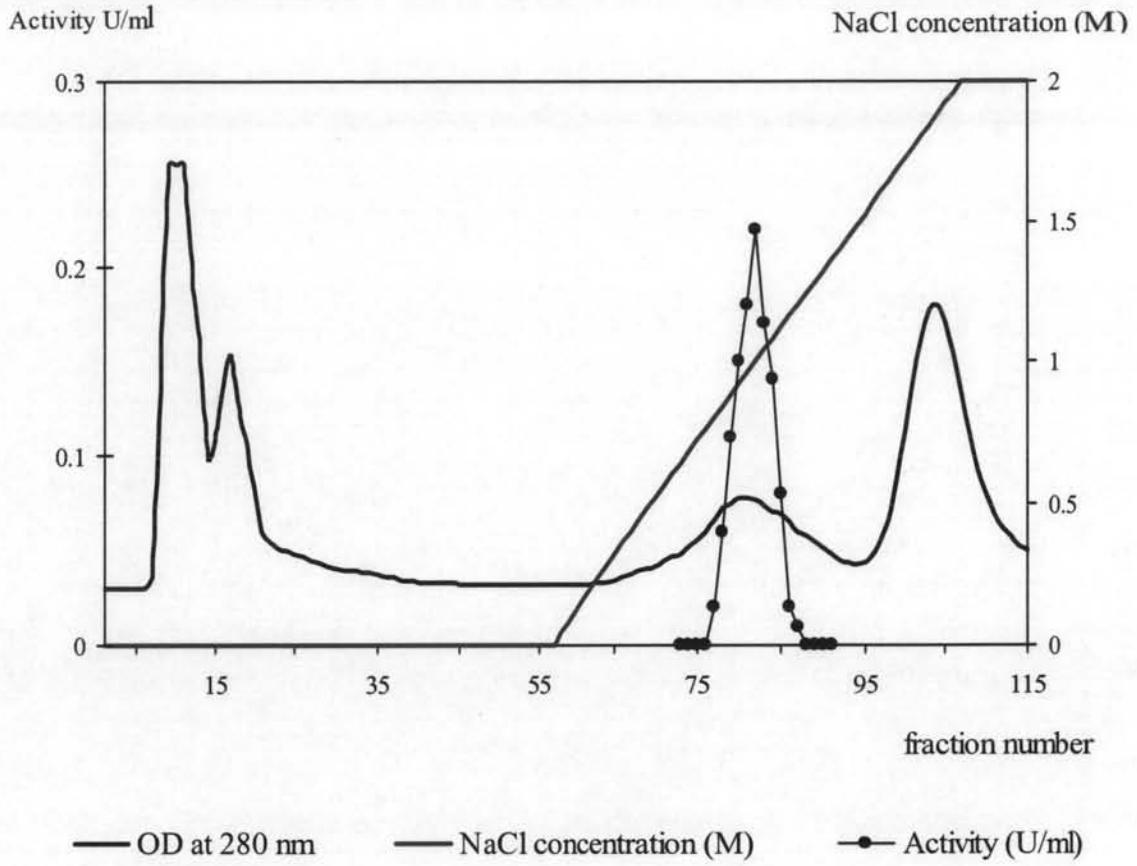

Fig. 4.48 Blue Sepharose chromatography of component B from gel filtration fraction

4.2.8.3 Component C purification

Those fractions containing component C, eluted from gel filtration column were pooled, concentrated and used for determination of acenaphthylene dioxygenase activity without further purification as it showed one major band of protein on PAGE as shown in Fig. 4.49.

4.2.9 Summary of the purification

The crude cell free extract of *Rhizobium* sp. CU-A1 showing catalytic activity on the conversion of acenaphthylene to acenaphthenequinone were purified by fractionation with 40-60% saturation of ammonium sulfate following by chromatography on Q Sepharose and Superdex G200 (Table 4.10). Three components, A, B and C were separated on Superdex G200 and shown full enzyme activity with the re-constitution of all components (Table 4.8).

Component A was further purified by chromatography on hydroxyapatite and phenyl Sepharose columns giving 1.35-fold increase in purity compared with that of the Superdex G200 step (Table 4.11).

Component B was further purified by chromatography on Blue Sepharose column giving about 3-fold increase in purity compared with that of the Superdex G200 step (Table 4.12).

Analysis of the enzyme from each purification step on PAGE shown in Fig. 4.49 indicated that component A from phenyl Sepharose column and component C from gel filtration step were purified to almost homogeneity. Component B from Blue Sepharose column showed aggregated form on PAGE, however, only a single band was observed on SDS-PAGE (Fig. 4.50) indicated that it was also purified to almost homogeneity.

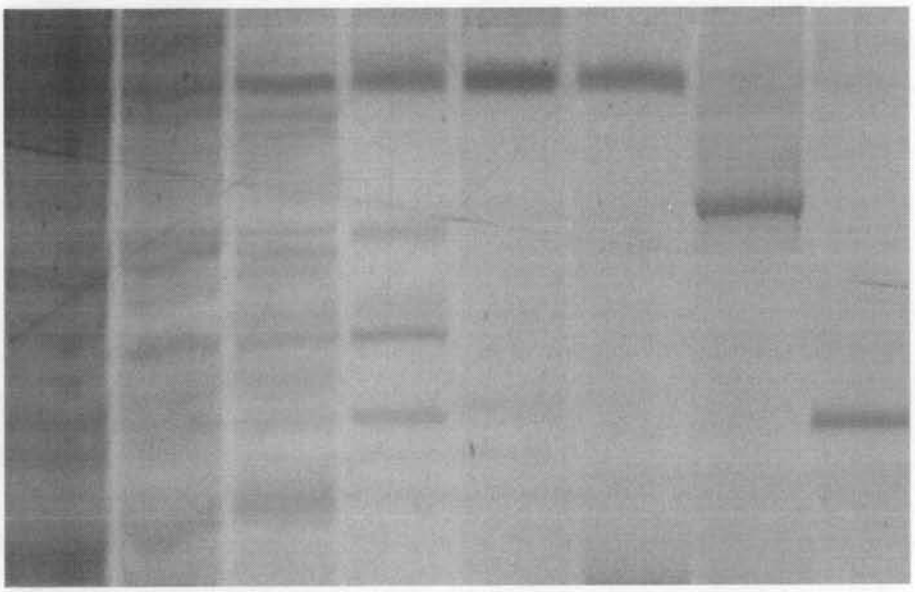

Fig. 4.49 PAGE of samples from each step of the enzyme purification taken during the purification. Lanes: 1 crude cell extract; 2, 40-60% $(NH_4)_2SO_4$ fraction; 3, Q Sepharose active fraction; 4, Component A from Superdex G200 column; 5, Component A from hydroxyapatite column; 6, Component A from phenyl Sepharose column; 7, Component B from Blue Sepharose column; 8, Component C from Superdex G200 column

4.2.10 Characterization of the purified enzyme

4.2.10.1 Molecular mass determination

The molecular masses of component A, B and C were estimated by gel filtration on Superdex G200 column under the same condition for protein purification as described in 3.7.4. The calibration curve was obtained by using protein standards with known molecular weight and K_{av} values were calculated according to the following equation:

$$K_{av} = V_e - V_0 / V_t - V_0$$

where V_e : elution volume of the protein

V_0 : elution volume of dextran (void volume)

V_t : elution volume of riboflavin (total volume)

The standard proteins, their molecular weight, elution volume and K_{av} values were shown in Appendix C, Table C.1. The molecular weights of component A, B and C were estimated to be 129.6, 42.7 and 9.3 kDa, respectively.

SDS-PAGE was performed to determine the molecular mass and subunit contents of each protein component. The calibration curve was made by plotting mobility of known low molecular weight standard proteins, shown in Appendix C, Fig. C.5. Analysis of protein component A by SDS-PAGE suggested that it comprised of two nonidentical subunits as indicated in Fig. 4.50. The estimated molecular weights of a larger protein, designated as α subunit and a smaller, designated as β subunit were 45 and 22 kDa, respectively. According to the molecular mass of native component A, estimated by gel filtration, the data suggested that the protein component A has an $\alpha_2\beta_2$ configuration.

Analysis by SDS-PAGE of component B and C revealed the presence of major single protein band with a molecular mass of 48 and 9.8 kDa, respectively, as shown in Fig. 4.50.

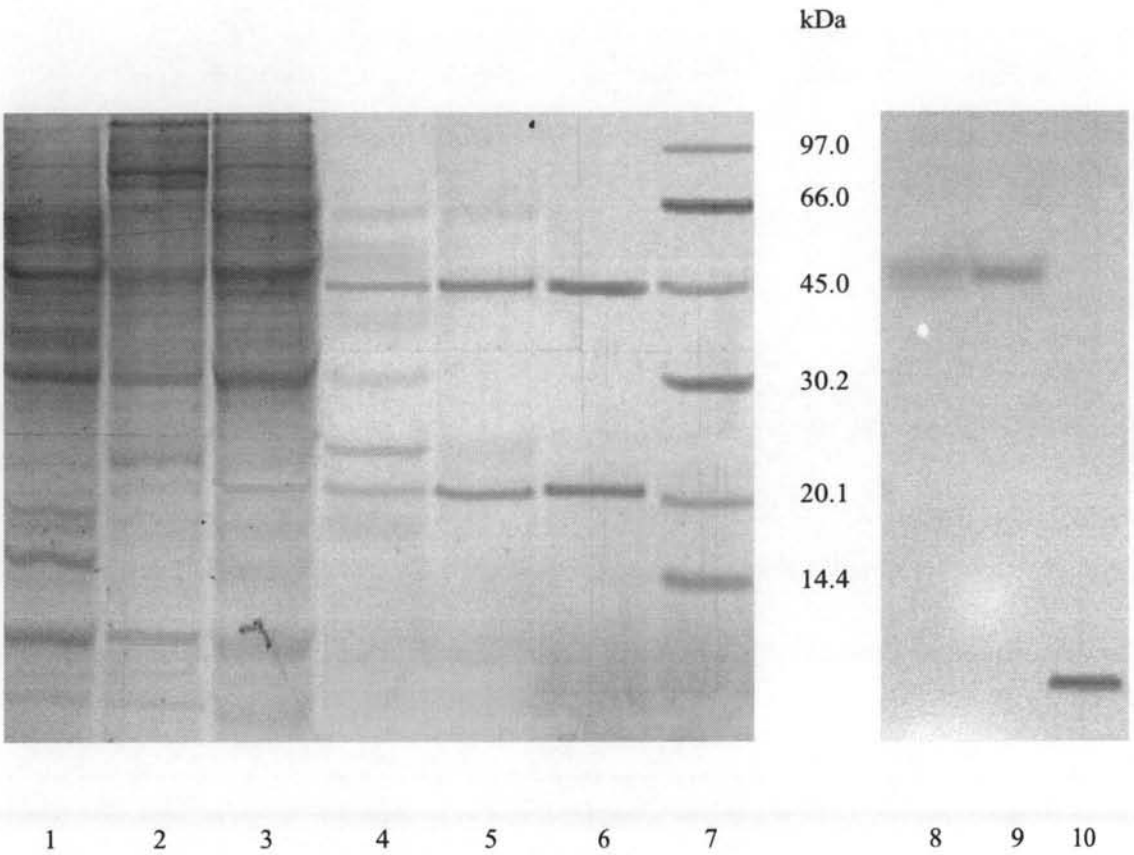

Fig. 4.50 SDS-PAGE of samples from each step of the enzyme purification. taken during the purification. Lanes: 1 crude cell extract; 2, 40-60% $(NH_4)_2SO_4$ fraction; 3, Q Sepharose active fraction; 4, Component A from Superdex G200 column; 5, Component A from hydroxyapatite column; 6, Component A from phenyl Sepharose column; 7, low molecular weight markers 8, Component B from Superdex G200 column; 9, Component B from Blue Sepharose column; 10, Component C from Superdex G200 column

4.2.10.2 Spectral properties

The UV/visible absorption spectra of components A, B and C were measured spectrophotometrically in a one-cm pathlength-cuvette using Uvikron 860 spectrometer (Switzerland). The absorbance spectrum of the purified component A showed a large peak at 320 nm and a broad peak at 465 with a shoulder at 560 (Fig. 4.51). For component B, the absorption spectrum showed maxima at 458, 355, and shoulders at 550 and 410 as shown in Fig. 4.52, which are the typical characteristics of flavoprotein (Subramanian and Gibson, 1981). Partially purified component C showed absorption maxima at 332, 470 and a shoulder at 562 nm (Fig. 4.53). The absorption spectra obtained from the oxidized components A and C indicated the characteristics of protein containing a Rieske-type [2Fe-2S] iron sulfur center (Cosper et al., 2002) which were similar to those found in dibenzofuran dioxygenase (Bunz and Cook, 1993), biphenyl-2,3-dioxygenase (Haddock and Gibson, 1995) and halobenzoate-1,2-dioxygenase (Hetzner and Lingens, 1992). Because of the insufficient amount of each enzyme component, anaerobic reduction of the enzyme could not be tested in this experiment.

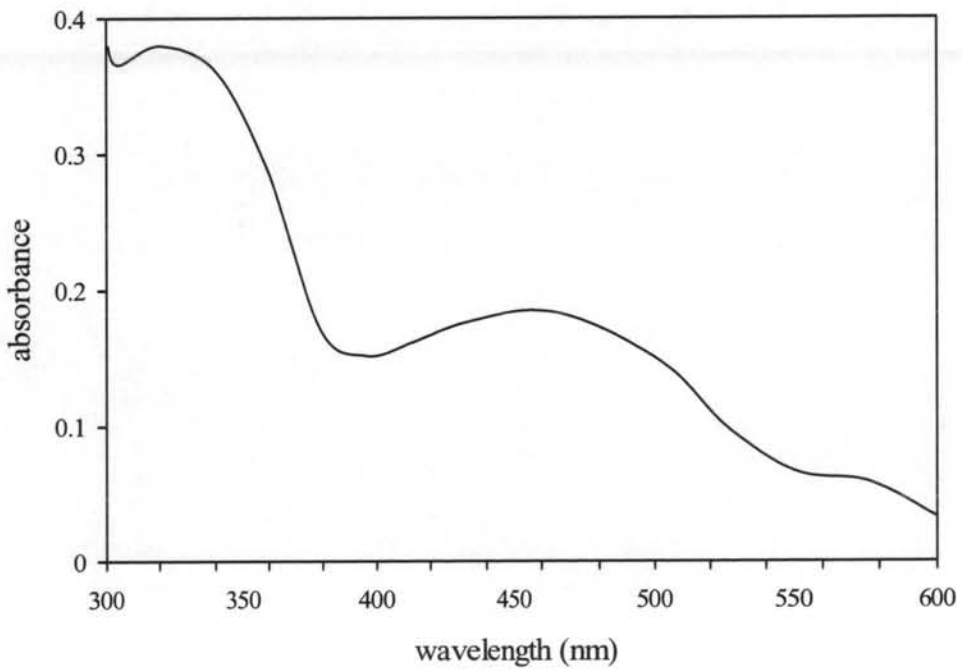

Fig. 4.51 Absorption spectrum of component A

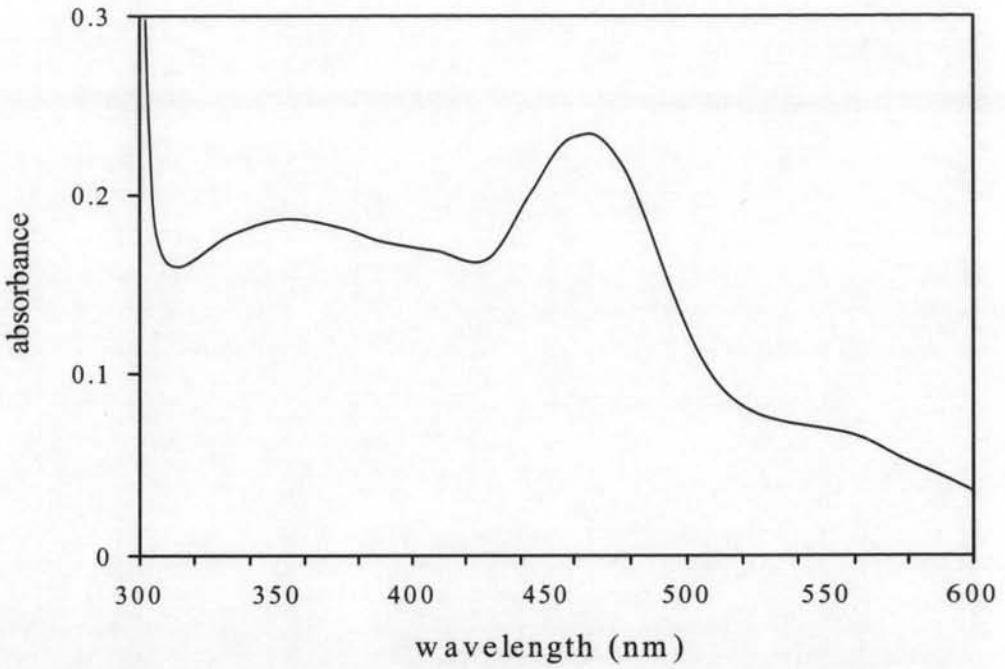

Fig. 4.52 Absorption spectrum of component B

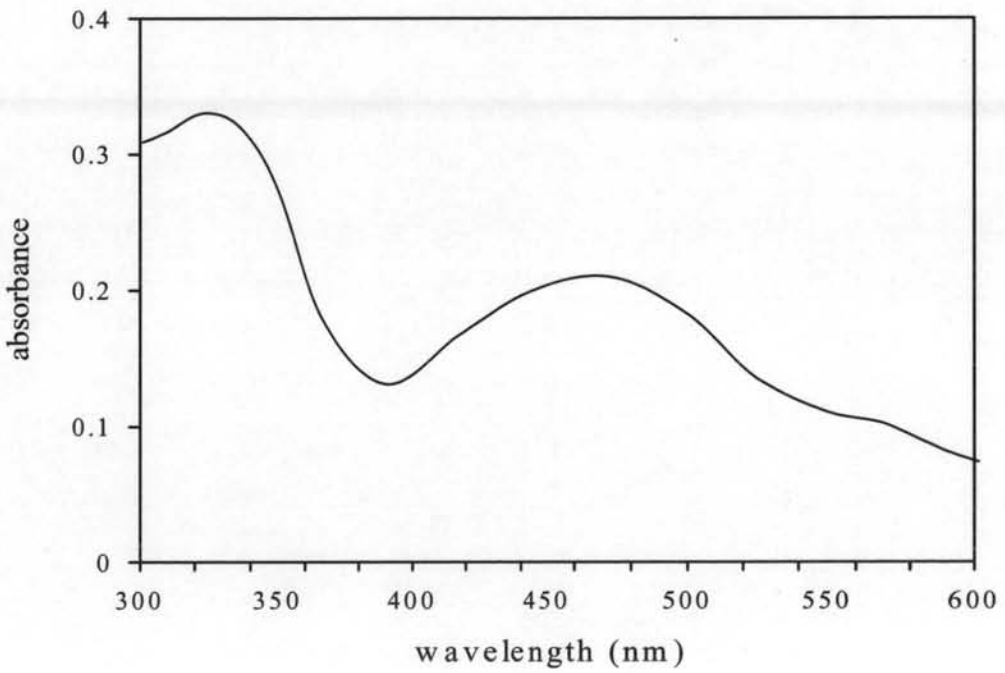

Fig. 4.53 Absorption spectrum of component C

According to properties of components A, B and C, each component was tentatively identified as follow:

Component A was identified as a terminal oxygenase as it showed some oxidation activity on acenaphthylene in the presence of component C (Table 4.8) but no reductase activity on cytochrome *c* (Table 4.9). Components B and C were identified as proteins in electron transport chain, probably a redox center of component A. The molecular mass of component A was estimated by gel filtration chromatography to be 129.6 kDa and by SDS-PAGE to be two nonidentical subunits of 45 and 22 kDa. The results indicated that component A was the largest component in the acenaphthylene dioxygenase enzyme complex which has an $\alpha_2\beta_2$ configuration similar to benzene dioxygenase and toluene dioxygenase from *Pseudomonas putida* (Zamamina and Mason, 1987 and Suramanian et al., 1985). Furthermore, in aqueous solution, it had brown color with maximal UV/visible absorption spectrum at 320 and 465 nm with a shoulder at 560 nm. These characteristics are common for iron-sulfur protein containing Rieske-type iron-sulfur center which have been reported with other terminal oxygenases such as those catalyzing benzene (Crutcher and Geary, 1979), naphthalene (Ensley and Gibson, 1983 and Larkin et al., 1999) and dibenzofuran (Bunz and Cook, 1993). The presence of Rieske-type iron-sulfur center in component A was also supported by the finding of conserved cysteine and histidine residue ($CX_1HX_{15\text{-}17}CX_2H$) in the deduced amino acid sequence of the large subunit of the enzyme at position 74-97 that are thought to be ligands of the center (Thupmongkhon, 2003). A mononuclear iron center in the terminal oxygenases of dioxygenases such as naphthalene dioxygenase (Bassan et al., 2004) and biphenyl dioxygenase (Haddock and Gibson, 1995), has been reported to be an electron acceptor of the iron-sulfur center during catalysis. In this experiment, iron content of the component A was not determined but it was found that addition of exogenous iron was required for the maximal enzyme activity. Furthermore, Thupmongkon (2003) found conserved aspartate and histidine residues ($DX_2HX_{4\text{-}5}H$) in the deduced amino acid sequence of the large subunit of this component at position 198-207, which might be ligands to coordinate with the mononuclear iron.

Component B was identified as a reductase component by its ability to directly reduce cytochrome *c* in the presence of NADH. The presence of component C enhanced the cytochrome *c* reductase activity of component B more than 5 folds whereas component A and C did not oxidize NADH. The molecular mass of component B was estimated from gel filtration to be 42.7 kDa which was closely related to the masses of the reductase component of toluene dioxygenase (Suramanian et al., 1985), biphenyl dioxygenase (Broadus and Haddock, 1998) and dibenzofuran dioxygenase (Bunz and Cook, 1993). SDS-PAGE analysis of the component B showed the presence of a single polypeptide band corresponding to a molecular mass of about 48.2 kDa. The aqueous solution of component B was yellow in color and its UV/visible absorption spectrum was similar to the characteristics of a flavoprotein. From the early results showed that acenaphthylene dioxygenase and cytochrome *c* reductase activities were stimulated by the addition of FAD, these results suggested that FAD might be a prosthetic group of component B. Typically, the reduction of cytochrome *c* by flavoprotein requires two prosthetic groups. For example in toluene dioxygenase system, ferredoxin reductase acts as initial electron acceptor which accepts electrons from NADH and shuttles them to a ferredoxin (Suramanian et al., 1985). Similarly, component B and C of acenaphthylene dioxygenase system were both required for cytochrome *c* reductase activity. However, low activity was still observed with only component B alone. This observation might be due to trace amount of component C remaining in the component B preparation although it could not be detected by SDS-PAGE. On the other hand, the second prosthetic group (iron-sulfur center) may be present on the same protein molecule similar to that found in the reductase component of naphthalene dioxygenase which could directly reduce cytochrome *c* without ferredoxin requirement (Haigler and Gibson, 1990). However, we had limited data on this part because only limited quantity of component B was available. Additional studies on the prosthetic group, iron and sulfur contents determination, and flavin co-enzyme identification will be necessary before the actual function of the component can be resolved.

Component C had no reductase activity toward NADH but it was required to enhance reductase activity of component B on cytochrome *c*. It, therefore, was identified as an intermediate electron transport protein to shuttle electrons from reductase, component B, to cytochrome *c*. Its molecular mass was estimated by gel

filtration chromatography to be 9.3 kDa. SDS-PAGE analysis revealed the presence of a single protein band with a molecular mass of approximately 9.8 kDa. These results suggested that component C was the smallest component in the acenaphthylene dioxygenase complex which similar to those of naphthalene dioxygenase (Haigler and Gibson, 1990), dibenzofuran dioxygenase (Bunz and Cook, 1993) and pyrazon dioxygenase (Sauber et al., 1977). The UV/visible spectrum of component C showed the pair of maxima at 332 and 470 nm indicating the typical Rieske-type protein which was similar to those of terminal oxygenase component. This evidence was supported by the finding of conserved motif (cysteine and histidine residue, $CX_1HX_{15-17}CX_2H$) in the deduced amino acid sequence of this component that are thought to be ligands of the Rieske-type iron-sulfur center at amino acid position 43-65 (CTHDTWSLADGALEDGIVECSLH) (Thupmongkhon, 2003). From its molecular mass and UV/visible spectral properties, therefore component C was considered as a Rieske type ferredoxin similar to the ferredoxins of other dihydroxylating dioxygenases such as those catalyzing benzene (Axcell and Geary, 1975), toluene (Subramanian, 1985), naphthalene (Haigler and Gibson, 1990) and dibenzofuran (Bunz and Cook, 1993).

Dioxygenases have been classified according to their various combination of electron transport co-factors involved in reducing the terminal oxygenase components as shown in Table 4.13. According to the above results, acenaphthylene dioxygenase system consists of three protein components, a Rieske type iron sulfur [2Fe-2S] center terminal oxygenase, a Rieske type iron sulfur [2Fe-2S] center ferredoxin, and an FAD ferredoxin reductase which could reduce cytochrome *c*. Therefore, acenaphthylene dioxygenase from *Rhizobium* sp. CU-A1 has been tentatively classified as dioxygenase group II, subgroup IIB. This finding is the first representative of US-EPA listed polycyclic aromatic hydrocarbon dioxygenase that belongs to subgroup IIB. Similarly, dioxin dioxygenase (Armanguad et al. 1998), and biphenyl dioxygenase (Haddock and Gibson, 1995) also belong to subgroup IIB. Whereas naphthalene dioxygenase was classified as dioxygenase group III (Bertini et al., 1996). The electron transport scheme for acenaphthylene dioxygenase has also been proposed in Fig. 4.54.

Table 4.13 Classification of dioxygenase

Class	Terminal oxygenase	Reductase	Ferredoxin	Examples	References
IA	Rieske [2Fe-2S], Fe^{2+}	Plant [2Fe-2S], FMN	None	Phthalate dioxygenase	Bertini et al., 1987
IB	Rieske [2Fe-2S], Fe^{2+}	Plant [2Fe-2S], FAD	None	Benzoate dioxygenase	Yamagushi and Fugisawa, 1982
IIA	Rieske [2Fe-2S], Fe^{2+}	FAD	Plant [2Fe-2S]	Dibenzofuran dioxygenase	Bunz and Cook, 1993
IIB	Rieske [2Fe-2S], Fe^{2+}	FAD	Rieske [2Fe-2S]	Dioxin dioxygenase Biphenyl dioxygenase Acenaphthylene dioxygenase	Armanguad et al., 1998 Haddock and Gibson, 1995 This experiment
III	Rieske [2Fe-2S], Fe^{2+}	Plant [2Fe-2S], FAD	Rieske [2Fe-2S]	Naphthalene dioxygenase	Bertini et al., 1996

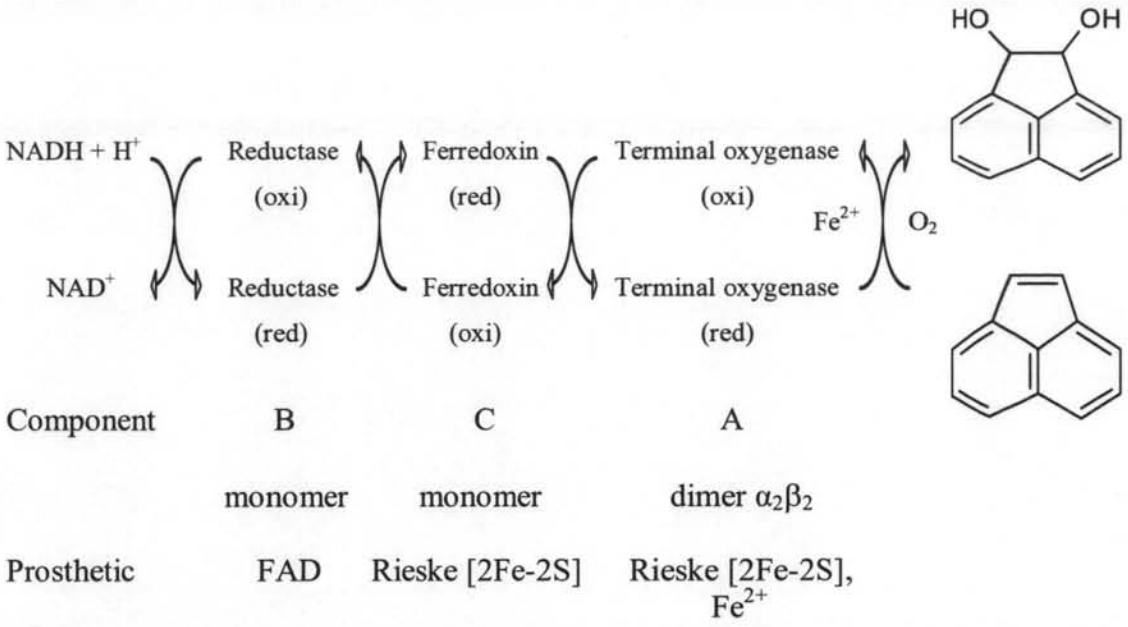

Fig. 4.54 The proposed electron transport scheme for acenaphthylene dioxygenase from *Rhizobium* sp. CU-A1

4.2.10.3 Temperature and pH optima

Temperature and pH optima for acenaphthylene dioxygenase activity of the reconstituted purified components A, B and C were determined according to the method described in 3.10.1. Fig. 4.55 revealed that the highest activity was obtained at a temperature of 35°C and pH 7.5.

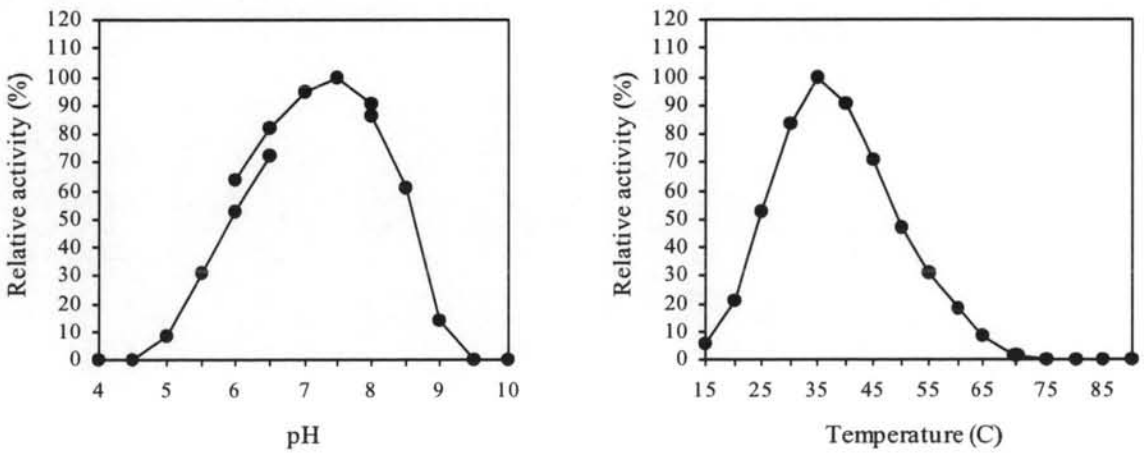

Fig. 4.55 Effect of temperature and pH on the activity of acenaphthylene dioxygenase complex protein

4.2.10.4 Temperature and pH stability

Temperature and pH stability of the reconstituted purified enzyme were determined by incubating the mixture of enzyme complex at the different desired temperature (15-90°C) and pH (4-10). At time interval, aliquots were withdrawn from the incubation mixture and the enzyme activity was determined at the optimal temperature and pH. Fig. 4.56 showed % relative activity of enzyme complex after incubation at desired temperature and pH for 30 min. The enzyme complex was stable at temperature between 15–45°C with no significant loss of activity observed. In the other way, incubation at the temperature above 50°C resulted in the inactivation of the enzyme, and it was completely inactivated at temperature above 70°C. The enzyme was stable to the pH ranging from 6.5-9.5 with less than 20% of the initial activity was lost. But at pH below 6, the activity was decreased and completely lost at pH 4.

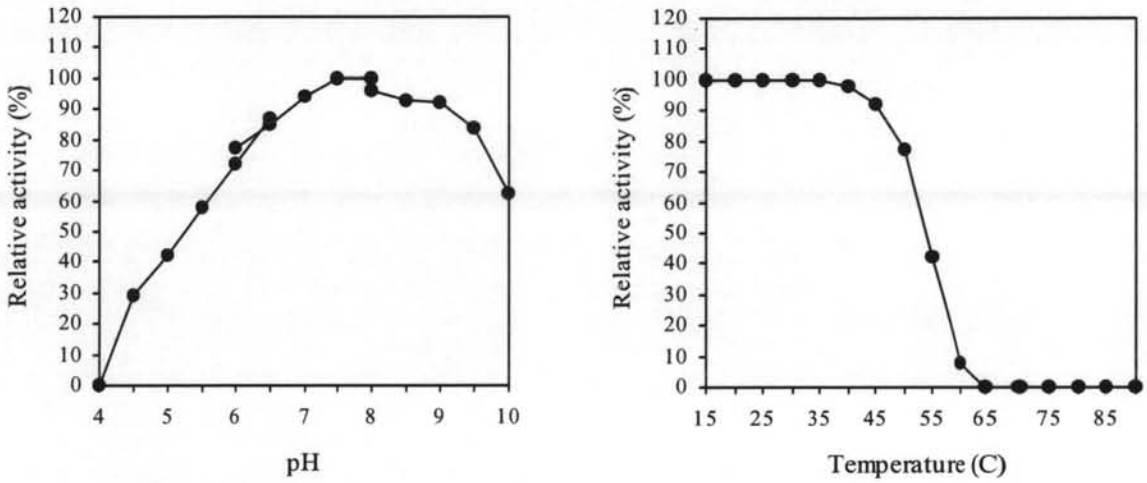

Fig. 4.56 Temperature and pH stability of acenaphthylene dioxygenase enzyme complex

For the determination of temperature and pH stability of individual component, each component was incubated in the different desired temperature and pH before assaying for the remaining activity in the presence of other two components as described in 3.10.2. The result shown in Fig. 4.57 revealed that each

individual protein component was stable in the same range of pH between 7-9. Component B was stable to temperature up to 60°C while components A and C were stable to temperature up to 45°C.

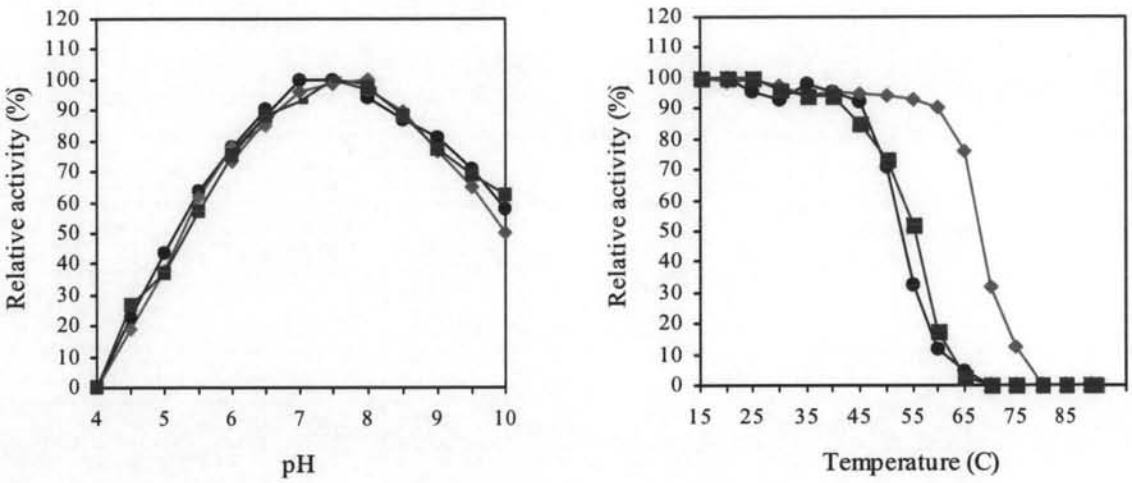

Fig. 4.57 Temperature and pH on stability of component A (●), B (◆) and C (■)

4.2.10.5 Substrate specificity

The ability of the enzyme to oxidize various aromatic compounds was examined by incubating the reconstituted purified enzyme with a different substrate which include naphthalene, acenaphthene, phenanthrene, fluorene, anthracene, fluoranthene, pyrene, acenaphthenequinone, naphthalene-1,8-dicarboxylic acid, 1-naphthoic acid, 1,2-dihydroxynaphthalene, salicylic acid and gentisic acid. The activity was measured by monitoring substrate disappearance and one unit activity represents the amount of enzyme required for catalyzing the conversion of 1.0 nmole substrate in 1 min under the assay conditions. The enzyme showed a broad specificity to substrates as shown in Table 4.14. PAHs like naphthalene, acenaphthene, phenanthrene, fluorene, and anthracene also serve as substrate with relative activity in the range between 30-80%. Pyrene and fluoranthene were very poor substrates, with only 2.3 and 7.6% relative activity of that of acenaphthylene, respectively. Many intermediates of acenaphthylene oxidation were also acted as the substrates of this enzyme, except for the naphthalene-1,8-dicarboxylic acid and salicylic acid.

Table 4.14 Activities of acenaphthylene dioxygenase on different compounds

Substrates	Relative activity (%)
Acenaphthylene	100.0
Naphthalene	54.2
Acenaphthene	78.5
Phenanthrene	41.7
Fluorene	45.5
Anthracene	35.0
Fluoranthene	7.6
Pyrene	2.3
Acenaphthenequinone	62.4
Naphthalene-1,8-dicarboxylic acid	0
1,2-Dihydroxynaphthalene	31.8
1-Naphthoic acid	79.8
Salicylic acid	0
Gentisic acid	24.2

Kinetic characterization of the enzyme for acenaphthylene, acenaphthenequinone, 1-naphthoic acid and naphthalene were determined. From Lineweaver-Burk plot shown in Fig. 4.58, the K_m and V_{max} values of the enzyme for acenaphthylene were 0.59 mM and 4.5×10^{-2} μmol/min/mg, respectively. The K_m values for acenaphthene, acenaphthenequinone, 1-naphthoic acid and naphthalene were also calculated from Lineweaver-Burk plots to be 0.75, 0.96, 0.70, and 1.27, respectively. Although, this enzyme has broad spectrum of substrates but from the K_m values, they suggested that the enzyme is more specific to acenaphthylene than 1-naphthoic acid, acenaphthene, acenaphthenequinone, and naphthalene.

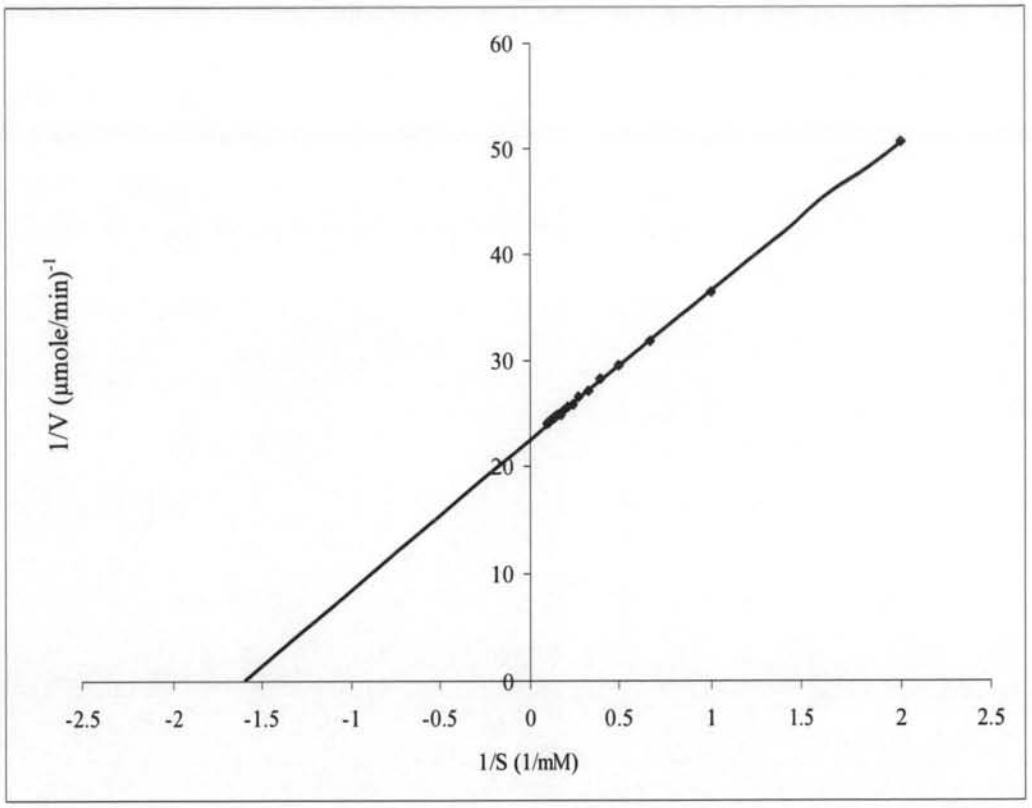

Fig. 4.58 Lineweaver-Burk plot of acenaphthylene dioxygenase for acenaphthylene

4.2.10.6 $^{18}O_2$ incorporation experiment

$^{18}O_2$ incorporation into acenaphthylene and acenaphthenequinone molecules catalyzed by the purified enzyme were examined as described in 3.10.6. The mass spectrum chromatograms of the products formed from the oxidation of acenaphthylene and acenaphthenequinone by the reconstituted enzyme were present in Fig. 4.59 and 4.60, respectively. A representative fragment, at m/z equal to M^+, of the electron impact mass spectrum of acenaphthenediol produced from acenaphthylene oxidation in the air was seen at m/z 186 (Fig. 4.59, A) whereas the value of m/z at 190 was obtained in the presence of $^{18}O_2$ as shown in Fig. 4.59 (B). Similarly, the m/z of naphthalene-1,8-dicarboxylic acid formed from oxidation of acenaphthenequinone by this enzyme in the presence of air only (Fig. 4.60, A) or air containing $^{18}O_2$ were 198 (Fig. 4.60, A) and 198 and 202 (Fig. 4.60, B), respectively. The results indicated that both atoms of molecular oxygen were incorporated into acenaphthylene and acenaphthenequinone molecules.

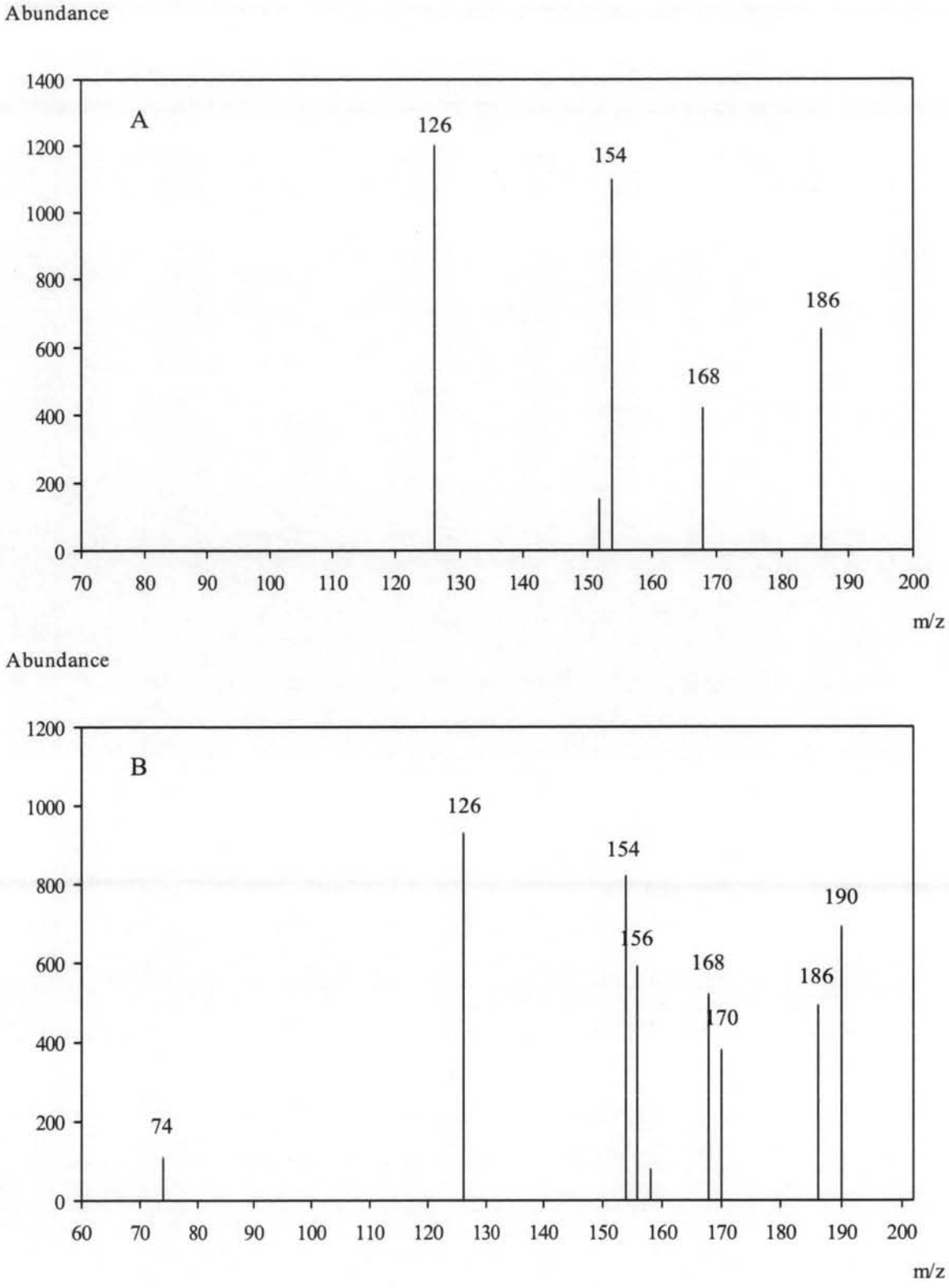

Fig. 4.59 Mass spectra of acenaphthenediol, the product produced from the oxidation of acenaphthylene by acenaphthylene dioxygenase enzyme system in the presence of only $^{16}O_2$ (A) and in the presence of both $^{16}O_2$ and $^{18}O_2$ (B)

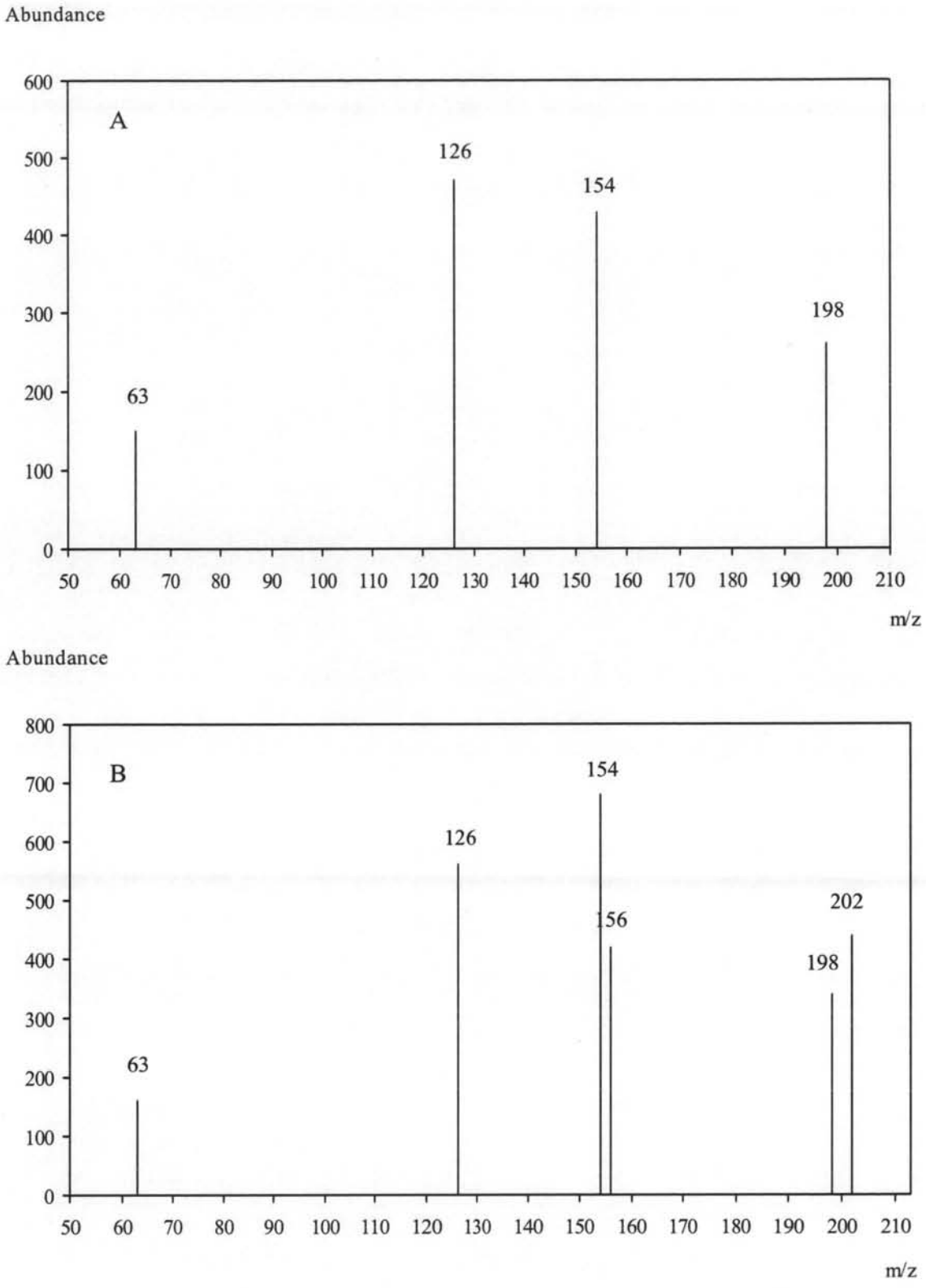

Fig. 4.60 Mass spectra of naphthalic anhydride (naphthalene-1,8-dicarboxylic acid), the product produced from the oxidation of acenaphthenequinone by acenaphthylene dioxygenase enzyme system in the presence of only $^{16}O_2$ (A) and in the presence of both $^{16}O_2$ and $^{18}O_2$ (B)

Beside acenaphthylene, acenaphthylene dioxygenase is capable of oxidizing a wide variety of aromatic compound as shown in Table 4.14. Moreover, the acenaphthylene dioxygenase is also capable of oxidizing acenaphthenequinone, 1,2-dihydroxynaphthalene and gentisic acid. Typically, 1,2-dihydroxynaphthalene and gentisic acid were oxidized by ring cleavage dioxygenases, 1,2-dihydroxynaphthalene dioxygenase (Patel and Barnsly, 1980) and gentisate-1,2-dioxygenase (Utkin et al., 1990), respectively. Unlike naphthalene dioxygenase, they are able to initiate the degradation by catalyzing the ring-fission reaction and by hydroxylating the ring in preparation for ring-cleavage while naphthalene dioxygenase catalyzed only dihydroxylation reaction resulting in the formation of dihydrodiol product. The formation of naphthalene-1,8-dicarboxylic acid from acenaphthenequinone catalyzed by this enzyme was of interest as it had been reported earlier that this reaction occurred spontaneously (Selifenov et al., 1996). A similar ring cleavage activity of the enzyme was probably responsible for the oxidation of acenaphthenequinone to naphthalene-1,8-dicarboxylic acid which has never been reported before in acenaphthylene catabolic pathway by bacteria. Although, naphthalene dioxygenase was reported to catalyze dioxygenation, monooxygenation and desaturation of some aromatic compounds (Lee and Gibson, 1996; Torok et al., 1995; Lee et al., 1997), no evidence on ring fission reaction of this enzyme has been reported. Although, to date, the occurrence of many aromatic compound dioxygenases has been reported, acenaphthylene dioxygenase is the only polycyclic aromatic hydrocarbon dioxygenase which can catalyze dihydroxylation of acenaphthylene to form diol product and also catalyzes ring fission of acenaphthenequinone to naphthalene-1,8-dicarboxylic acid as shown in Fig. 4.61.

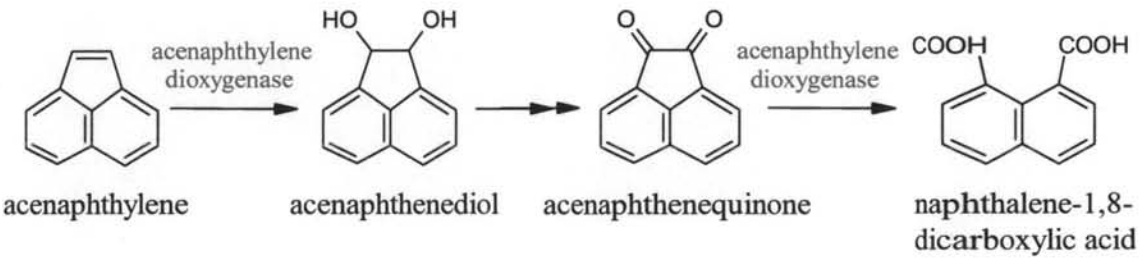

Fig. 4.61 The catalytic activities of acenaphthylene dioxygenase on the oxidation of acenaphthylene to acenaphthenediol and acenaphthenequinone to naphthalene-1,8-dicarboxylic acid in the acenaphthylene catabolic pathway

4.2.10.7 Effects of metal ions and some chemicals on enzyme activity

The effects of various metal ions and chemicals on the purified reconstituted enzyme were shown in Table 4.15.

Table 4.15 Effects of metal ions and chemicals on acenaphthylene dioxygenase activity

Ions/Chemicals	Relative activity (%)			
	Metal ions concentration (mM)			
	0.1	0.5	1	5
$CoCl_2$	58.4	39.2	22.3	0
$CuSO_4$	9.8	2.5	0	0
$FeSO_4$	101.6	105.2	109.5	112.0
$MgSO_4$	98.3	99.6	101.3	101.5
$MnSO_4$	100	99.3	101.4	99.5
$NiCl_2$	26.5	17.5	8.1	0
$ZnSO_4$	7.3	0	0	0
	Chemicals concentration (mM)			
	0.5	1	5	10
Diphenyliodonium	23.8	0	0	0
Phenylhydrazine	100	97.5	98.0	94.4
Aminobenzotriazole	99.6	98.3	98.0	96.9
EDTA	10.6	0	0	0
Iodoacetate	72.0	44.7	0	0

Ferrous ion showed slight stimulation effect on the enzyme activity at the concentration above 1 mM whereas Ni^{2+}, Zn^{2+}, $Co^{2+}$and Cu^{2+} strongly inactivated the enzyme activity in which $Zn^{2+}$and Cu^{2+} were the most potent inhibitors.

The result shown in Table 4.15 indicated that 1 mM diphenyliodonium, an NADH oxidase and flavoprotein inhibitor, completely inactivated the enzyme activity. In contrast, phenylhydrazine and aminobenzotriazole, known to be cytochrome P_{450} inhibitors, had no effect on the enzyme within the concentration tested. EDTA had strong inhibition effect on the enzyme activity in which 90% of the activity was inhibited at 0.5 mM final concentration. Sulfhydryl agent such as

iodoacetate inhibited the activity similar to N-ethylmaleimide, as already shown in 4.2.2.